NASA Technical Memorandum 87120

Lubrication of Nonconformal Contacts

Yeau-Ren Jeng
Lewis Research Center
Cleveland, Ohio

September 1985

NASA

TABLE OF CONTENTS

NOMENCLATURE

a	semimajor axis of contact ellipse, m
B	basic speed ratio, δ/S
b	semiminor axis of contact ellipse, m
D	influence coefficient matrix
D	percentage difference, $[(H_o - H_o)/H_o]*100$
d	elastic deformation, m
d_ℓ	ball diameter, m
d_m	pitch diameter, m
E	modulus of elasticity, N/m
E'	effective elastic modulus, $2/[(1 - \nu_a^2)/E_a + (1 - \nu_b^2)E_b]$, N/m
f	shear force per unit length, N/m
G	dimensionless materials parameter, $E'/p_{iv,as}$
H	dimensionless film thickness, h/R_x
H_o	dimensionless central film thickness, h_o/R_x
H_o	calculated dimensionless central film thickness from least-square analysis
h	film thickness, m
h_o	central film thickness (minimum film thickness as well in piezoviscous-rigid regime of lubrication), m
h_{min}	minimum film thickness, m
H_{min}	dimensionless minimum film thickness, h_o/R_x
k	ellipticity parameter, b/a
P	dimensionless pressure, p/E'
p	pressure, N/m^2

$p_{iv,as}$	asymptotic isoviscous pressure, N/m^2
p_s	pressure spike, N/m^2
R	effective radius, m
r	radius of curvature, m
S	geometrical distance, m
s,t	constants defining fluid used in equation (2.7)
U	dimensionless entrainment velocity, $n_o u/E'R_x$
u_x	mean entrainment velocity in x direction, m/s
u_{ax}	surface velocity of solid a in x direction, m/s
v	slip velocity, m/s
v_x	slip velocity in x direction, m/s
W	dimensionless load parameter, $w/E'R^2$
w	load, N
X,Y	dimensionless coordinate, x/R_x, y/R_x
X,Y	dimensionless coordinate, x/b,y/a
Z	viscosity pressure index, a dimensionless constant
z	height of surface a, m
z_a	mean height, $(z_a + z_b)/2$
α	radius ratio, R_y/R_x
γ	roughness anisotropy index
δ_a	random roughness height of surface a, $z_a - z_a^*$, m
η	lubricant viscosity, $(N\ s)/m^2$
$\bar{\eta}$	dimensionless viscosity, η/η^0
η_o	lubricant viscosity at atmospheric pressure, $(N\ s)/m^2$
θ	angle between lubricant entrainment vector and the x direction

μ	coefficient of rolling friction
ν	Poisson's ratio
ρ	lubricant density, kg/m^2
ρ	dimensionless density, ρ/ρ_0
ρ_0	lubricant density at atmospheric pressure, kg/m^2
σ	standard deviation of $(\delta_b - \delta_a)$, m
ϕ	$p_H 3/2$
ϕ^p	pressure flow factors
ϕ^s	shear flow factors
Λ	dimensionless film parameter, h^*/a

Subscripts

a	solid a
b	solid b
x,y	coordinates in plane of lubricating film

Superscripts

*	ensemble average (expectation) operator for stochastic quantity
	vector quantity

Chapter 1

INTRODUCTION

1.1 Conformal and Nonconformal Contacts

In many contacts between machine elements, forces are transmitted through thin, but continuous, fluid film. The fluid film lubrication is generally considered the ideal form of lubrication since the absence of asperity interaction of the surfaces provides low friction and high resistance to wear. The fluid film lubrication as related to hydrodynamic lubrication in journal and thrust bearings exhibits conformal surfaces, i.e., the surfaces snugly fit into each other with a high degree of geometrical conformity, as shown in figure 1.1. and the load is carried over a relatively large area. The load-carrying surface area remains essentially constant while the load is increased. The minimum film thickness in a hydrodynamically lubricated bearing is a function of applied load, speed, lubricant viscosity, and geometry.

Many machine elements have contacting surfaces that do not conform to each other, as shown in figure 1.2 for a rolling-element bearing. The full burden of the load is carried by a small contact area, the contact area between nonconformal surfaces enlarges with increasing load, but it remains small compared with the contact area between conformal surfaces. The form of lubrication normally found in nonconformal contacts is elastohydrodynamic lubrication.

The load per unit area in conformal bearings is relatively low, typically only 1 MN/m^2 and seldom over 7 MN/m^2. The load per unit area in nonconformal contacts generally exceeds 700 MN/m^2 even at modest applied load. These high pressures result in elastic deformation of the bearing materials such that elliptical contact areas are formed for oil film generation and load support. High contact pressures can produce considerable increases in fluid viscosity. Inasmuch as viscosity is a measure of a fluid's resistance to flow, this increase greatly enhances the lubricant's ability to support load without being squeezed out of the contact zone. The high contact pressures between nonconformal surfaces result in an elastic deformation of the surfaces and large increases in the fluid's viscosity. The resulting minimum film thickness is a function of the parameters found for hydrodynamic lubrication with the addition of an effective modulus-of-elasticity parameter and a pressure-viscosity coefficient.

1.2 Lubrication Regimes

Since the lubrication of nonconformal contacts is influenced by two major physical effects, the elastic deformation of the solids under an applied load and the increase in fluid viscosity with pressure, four main regimes of fluid film lubrication have been delineated depending on the relative magnitude of these effects, (Hamrock and Dowson, 1981):

Isoviscous-rigid. - In this regime, the magnitude of the elastic deformation of the surface is an insignificant part of the fluid film thickness and the maximum pressure in the contact is too low to increase fluid viscosity significantly. This form of lubrication is typically encountered in circular-arc thrust bearing pads; and in industrial coating processes.

Piezoviscous-rigid. - In this regime, the pressure within the contact is sufficiently high to increase the fluid viscosity within the conjunction significantly, while the deformation of the surfaces remains an insignificant part of the fluid film thickness. This form of lubrication encountered on roller flanges, in contacts in moderately loaded cylindrical tapered rollers, and between some piston rings and cylinder liners.

Isoviscous-elastic. - In this regime, the elastic deformation of the solid is a significant part of the fluid film thickness, but the pressure within the contact is quite low and insufficient to cause any substantial increase in viscosity. This situation arises with materials of low elastic modulus, and it is a form of lubrication that may be encountered in seals, human joints, tires, and elastomeric-material machine elements. This lubrication regime is sometimes referred to as soft EHL.

Piezoviscous-elastic. - In fully developed elastohydrodynamic lubrication, the elastic deformation of the solids is often a significant parts of the fluid film thickness, and the pressure within the contact is high enough to cause a significant increase

in the viscosity of the lubricant. This form of lubrication is typically encountered in ball and roller bearings, gears and cams. This lubrication regimes is also referred to as hard EHL.

1.3 Historical Developments

The theory of fluid film lubrication developed by Osborne Reynolds (1886) was first applied to nonconformal contacts by Martin (1916). This study represented an early attempt to explain the mechanism of spur gear lubrication and Martin's celebrated solution considered the lubrication of rigid cylindrical solids by means of an isoviscous, incompressible fluid. Martin's solution greatly underestimates the film thickness; however, it was a useful beginning to the theoretical study of elastohydrodynamic lubrication of line contacts. Some 30 years transpired before any significant accomplishments were made in solving the EHL line-contact problem. Ertel (1984) (who used to be referred to as Grubin (1949), now the record is straight after a 40-year-old wrong (Cameron, 1985)) obtained the first satisfactory solution to this problem by taking account of elastic distortion and viscosity-pressure effects. In Ertel's analysis it was assumed that the shape of the elastically deformed solids in a highly loaded lubricated contact is the same as the shape produced in a dry Hertzian contact. Ertel's approach produced an excellent account of the physical mechanism of the lubrication process in highly loaded EHL line contacts.

Not until the middle years of the present century has most of the work on elastohydrodynamic lubrication dealt with line contacts. A remarkable extention of the classical hydrodynamic lubrication theory for nonconformal contacts was recorded by Kapitza (1955), who presented an elegant analysis of both line and point contacts lubricated by either isoviscous or piezoviscous fluids. However, applying the half-Sommerfeld boundary condition used in Kapitza's analysis violates flow continuity at the cavitation boundary. Archard and Cowking (1965-1966) developed an elastohydrodynamic theory for point contacts of the form encountered between two spheres and thus extended the classical study of Kapitz as Ertel had extended that of Martin. The Hertzian contact zone was assumed to form a parallel film region, and the generation of high pressure in the approach to the Hertzian zone was considered. The results of the Archard and Cowking analysis led to the concept of a side-leakage factor, which represents the proportional reduction in pressure attributable to side leakage. Only in the 1970's did the complete numerical solution of the isothermal elastohydrodynamical lubrication of point contacts successfully emerge. In the years 1974 to 1978, Hamrock and Dowson (1976a, 1976b, 1977a, 1977b, 1978, 1979a, 1979b) published eight papers on EHL lubrication. These papers gave a complete approach to the solution of the elastohydrodynamic lubrication problem for point contacts. Their numerical solutions representative of materials of both high and

low elastic modulus and this enabled them to write expressions for minimum film thickness in both the isoviscous-elastic and piezoviscous-elastic regimes of lubrication as follows:

Isoviscous-elastic

$$H_{min} = 7.43\ U^{0.65}\ W^{-0.21}(1 - 0.85e^{-0.31k}) \qquad (1.1)$$

Piezoviscous-elastic

$$H_{min} = 3.63\ U^{0.68}\ G^{0.49}\ W^{-0.073}(1 - e^{-0.68k}) \qquad (1.2)$$

Brewe et.al. (1979) have obtained a film thickness equation for the lubrication of fully flooded, rigid, isoviscous point contacts through a numerical analysis that used a more realistic Reynolds condition for the film rupture in the exit region. It was found that the minimum film thickness had the same speed, viscosity, and load dependence as Kapitza's classical solution. However, the incorporation of the Reynolds boundary condition resulted in an additional geometry effects. The results can be written as:

Isoviscous-rigid

$$H_{min} = 128\alpha \left\{ \frac{1}{1 + (2/3)\alpha} \frac{U}{W} [0.131\ TAN^{-1}\left(\frac{\alpha}{2}\right) + 1.683] \right\}^2 \qquad (1.3)$$

1.4 The Objective of Present Work

Equations (1.1), (1.2), and (1.3) thus represent the minimum film thickness formula for three of the four regimes of lubrication of nonconformal contacts. However, full solutions

have not been available for the regime of piezoviscous-rigid lubrication with the same measure of confidence.

It is the first purpose of this work to study the piezoviscous-rigid regime of lubrication and to present results which will carry the same measure of confidence as those already available for the other three regimes of lubrication. This will not only enable the minimum film thickness to be calculated with greater accuracy in the piezoviscous-rigid regime, but will also complete the map of lubrication regimes of nonconformal contacts. The extended set of solutions includes the geometric effect where radius ratio less than one and the influence of lubricant entrainment direction which are not presented in equations (1.1), (1.2), and (1.3) (Jeng, et al., 1985). The results of the present work enable the lubricant film thickness to be predicted with increased confidence for a wide range of machine elements.

Over the last 30 or so years, major strides have been made in the understanding of the mechanism of fluid lubrication in nonconformal machine elements as reviewed above. To obtain a better understanding of the failure mechanism in machine elements, the next generation of elastohydrodynamic lubrication analyses should incorporate such effects as non-Newtontian fluids, surface roughness, and temperature. The second contribution of this work is the development of an improved numerical method of calculating elastic deformation in contact stresses. Incorporating an accurate elastic deformation calculation in the EHL numerical

scheme is necessary to reach the higher upper range of EHL parameters as indicated in Houpert and Hamrock (1985) and provides a means to study surface roughness effects on elastohydrodynamic lubrication and micro-elastohydrodynamic lubrication. A piecewise biquadratic polynomial is used to approximate the pressure distribution on the whole domain analyzed. The deformation of every node is expressed as a linear combination of the nodal pressures whose coefficients can be combined into an influence coefficient matrix. It has been proved that this approach has higher numerical accuracy and smaller computer storage size for the influence coefficient matrix.

This improved elasticity calculation is successfully incorporated into the EHL numerical scheme. Using this revised numerical technique, the surface roughness effects on the elastohydrodynamic lubrication of point contact is studied as an attempt to extend the ideal elastohydrodynamic lubrication model to the real bearing systems. This is the third major feature of this study. Surface roughness effects play a significant role in determining the fatigue life of nonconformal contact lubrication. The introduction of surface roughness effects by a study of Reynolds equation with random variables constitutes a fundamental contribution to stochastic continuum mechanics.

The analysis is based on a Reynolds equation modified through surface topography. Within the approximation of the second order perturbation approach to stochastic flow, only two parameters

govern the pressure developed by the film. In dimensionless form these are Λ, the ratio of nominal film thickness to rms roughness amplitude and γ, the ratio of the correlation lengths parallel and perpendicular to the lay direction of the surface texture. Conditions typical of an EHL contact in the piezoviscous-elastic regime entrained in pure rolling on rough bearing are demonstrated. The results are compared with smooth surface solutions.

Furthermore, the fourth phase of this work consists of experiments designed and conducted to study the transient EHL effects in instrument ball bearings. A parched subregime of elastohydrodynamic lubrication, lying between starved and mixed, is proposed to describe results of these experiments. A system is parched if oil films outside the Hertzian contacts are so thin they do not flow under service accelerations. Parched operation requires the least driving torque and provides the best spin definition possible of any lubrication regime. The results are directly applicable to other nonconformal contacts such as gears, roller bearings, etc.

Chapter 2

RELEVANT EQUATIONS

The study of fluid film lubrication is, from a mathematical standpoint, the application of a reduced form of the Navier-Stokes equation in association with the continuity equation. The resulting differential equation was formulated by Reynolds (1886) in the wake of a classical experiment by Tower (1883) in which the existence of a thin fluid film was detected from measurement of pressures within the lubricant.

The Reynolds equation contains viscosity and density terms. These properties of the lubricants depend on pressure when isothermal conditions are considered; hence it is necessary to deal with the pressure-viscosity and pressure-density formula. The Reynolds equation also contains the film thickness as a parameter. The film thickness is a function of the geometry and the elastic behavior of the contacting solids. The governing equations that describe fluid film lubrication will be developed in this chapter.

2.1 Reynolds equation

The equations of motion for a Newtonian fluid are known as the Navier-Stokes equations. They are derived by applying to a fluid the principles of conservation of momentum. The basic equation of fluid-film lubrication, the Reynolds equation, can be derived from the reduced form of the Navier-Stoke equation (representing the conservation of momentum) and continuity

equations (representing the conservation of mass). A general form of the Reynolds equation can be established in the restriction of the following assumptions:

(1) Inertia and body force terms are negligible compared with the pressure and viscous terms, i.e. $(\rho g h^2/\eta u) \ll 1$ and $((\rho u h/\eta)(h/\ell)) \ll 1$ where u is a characteristic fluid velocity, h is characteristic of the film thickness, η is the characteristic viscosity, ρ is the characteristic density, and l is a characteristic length in the flow direction and g is gravity.

(2) The radius of curvature of the solids bounding the oil film is large compared with the thickness of the lubricant film, $h/R \ll 1$.

The detail derivations can be found in Dowson (1962) or Hamrock and Dowson (1982). The general form of the Reynolds equation can be referred to cartesian coordinates as follows:

$$\frac{\partial}{\partial x}\left(\frac{\rho h^3}{12\eta}\frac{\partial p}{\partial x}\right) + \frac{\partial}{\partial y}\left(\frac{\rho h^3}{12\eta}\frac{\partial p}{\partial y}\right) = \frac{\partial}{\partial x}\left[\frac{\rho(u_{ax} + u_{bx})h}{2}\right] + \frac{\partial}{\partial y}\left[\frac{\rho(u_{ay} + u_{by})h}{2}\right] + \frac{\partial}{\partial t}(\rho h) \qquad (2.1)$$

where

u_{ax} surface velocity of solid a in x direction

u_{bx} surface velocity of solid b in x direction

u_{ay} surface velocity of solid a in y direction

u_{by} surface velocity of solid b in y direction

If the surface velocities are assumed to be a constant, thus the Reynolds equation for steady state conditions can be expressed as:

$$\frac{\partial}{\partial x}\left(\frac{\rho h^3}{\eta}\frac{\partial p}{\partial x}\right) + \frac{\partial}{\partial y}\left(\frac{\rho h^3}{\eta}\frac{\partial p}{\partial y}\right) = 12\left[u_x\frac{\partial(\rho h)}{\partial x} + u_y\frac{\partial(\rho h)}{\partial y}\right] \quad (2.2)$$

where

$u_x = (u_{ax} + u_{bx})/2$

$u_y = (u_{ay} + u_{by})/2$

By introducing u and θ, where $u = \sqrt{u_x^2 + u_y^2}$,

$\theta = \text{TAN}^{-1}(u_x/u_y)$ equation (2.2) becomes

$$\frac{\partial}{\partial x}\left(\frac{\rho h^3}{\eta}\frac{\partial p}{\partial x}\right) + \frac{\partial}{\partial y}\left(\frac{\rho h^3}{\eta}\frac{\partial p}{\partial y}\right) = 12u\left[\cos\theta\frac{\partial(\rho h)}{\partial x} + \sin\theta\frac{\partial(\rho h)}{\partial y}\right] \quad (2.3)$$

2.2 Pressure-Viscosity Formula

It is generally known that the viscosity of a lubricant is a function of temperature and pressure and a generally accepted relation which describes the viscosity-pressure dependency is the Barus (1893) equation:

$$\eta = \eta_o e^{\alpha p} \quad (2.4)$$

where

η viscosity at gage pressure

η_o viscosity at atmosphere pressure

α pressure-viscosity coefficient of lubricant

Unfortunately, pressure-viscosity data seldom follow this simple relation, and it is valid as a resonable approximation only in a moderate-pressure range.

Roelands (1966) in a more extensive experimental study of the effect of pressure on the viscosity of lubricants has developed an empirical formula written as:

$$\log \eta + 1.200 = (\log \eta_0 + 1.200) \left(1 + \frac{p}{2000}\right)^Z \qquad (2.5)$$

where

p gauge pressure kgf/cm^2

Z viscosity index, a dimensionless constant

Rearranging terms gives:

$$\eta = \eta_0 (1 + p/2000)^Z \times 10^{1.2[1 + (p/2000)^Z - 1]} \qquad (2.6)$$

The temperature effect is normally accounted for in η_0.

2.3 Pressure-Density Formula

The variation of density with pressure is roughly linear at low pressures, but the rate of increase falls away at high pressures. From Dowson and Higginson (1966), the dimensionless density for mineral oil can be written as

$$\bar{\rho} = \frac{\rho}{\rho_0} = 1 + \frac{sp}{1 + tp} \qquad (2.7)$$

where s and t are constants that depend on the fluid

2.4 Elasticity Equation

From Timoshenko and Goodier (1951), the elastic deformation at a point (x, y) of a semi-infinite solid subjected to pressure p at the point (x', y') can be written as

$$d(d) = \frac{2p\, dx'\, dy'}{\pi E' r} \qquad (2.8)$$

The elastic deformation at a point (x', y') due to the pressure over the domain is thus

$$d = \frac{2}{\pi} \iint_A \frac{dx'\, dy'}{\left[(y - y')^2 + (x - x')^2\right]^{1/2}} \qquad (2.9)$$

The evaluation of this equation will be discussed more fully in Chapter 4.

2.5 Film Shape

The separation of two rigid solids a and b having radii of curvature (r_{ax}, r_{ay}) and (r_{bx}, r_{by}) in the vicinity of the point of closest approach can be considered as geometrically equivalent to a solid of principal radii (R_x, R_y) adjacent to a plane as shown in figure 2.1. The geometrical requirement is that the separation of the ellipsoidal solids in the initial and equivalent situation should be the same at equal values of x. The effective radii of curvature can be expressed as

$$\frac{1}{R_x} = \frac{1}{r_{ax}} + \frac{1}{r_{bx}}$$

$$\frac{1}{R_y} = \frac{1}{r_{ay}} + \frac{1}{r_{by}} \qquad (2.10)$$

It is assumed that convex surfaces exhibit positive curvature and concave surfaces negative curvature. If the center of curvature lies within the solid, the radius of curvature is positive; if the center of curvature lies outside the solid, the radius is negative.

The separation of two rigid solids (fig. 2.1(a)) in which the principal axes of inertia of the two bodies are parallel can be written as

$$S = S_{ax} + S_{bx} + S_{ay} + S_{by} \tag{2.11}$$

where

$$S_{ax} = r_{ax} - \sqrt{r_{ax}^2 - x^2}$$

$$S_{bx} = r_{bx} - \sqrt{r_{bx}^2 - x^2}$$

$$S_{ay} = r_{ay} - \sqrt{r_{ay}^2 - y^2}$$

$$S_{by} = r_{by} - \sqrt{r_{by}^2 - y^2}$$

The separation in terms of the coordinate and the effective radius of curvature (fig. 2.1(b)) is

$$S(x,y) = R_x - \sqrt{R_x^2 - X^2} + R_y - \sqrt{R_y^2 - y^2} \tag{2.12}$$

Thus, the film thickness between two rigid bodies in point contact can be written as

$$h = h_o + S(x,y) \tag{2.13}$$

If elastic deformation is taken into account, the film thickness can be expressed as

$$h = h_o + S(x,y) + d(x,y) \tag{2.14}$$

Chapter 3

PIEZOVISCOUS-RIGID REGIME

In the piezoviscous-rigid regime of lubrication, Marko et al. (1979) proposed a formulae obtained by means of curve fitting of Dowson and Whitaker's (1965) results for line contacts. In the case of point contact, Hamrock and Dowson (1978) proposed an interim measure that Blok's (1952) solution for line contacts might be adjusted by the application of the same "side-leakage factor" as that derived for piezoviscous-elastic condition. Recently, the numerical solution for a compressible Newtonian lubricant exhibiting pressure-viscosity characteristic and subject to Reynolds cavition boundary condition was obtained by Dowson et al. (1983). The formulae from the last two papers describe the "limiting" film thickness generates infinite pressures, as discussed by Blok (1952). However, they do not include the load parameter W, which has a strong effect on film thickness when piezoviscous effects are considered. Houpert (1984) developed a sophisticated general formula by means of curve fitting of Dalmaz's (1979) results. A shortcoming of Dalmaz (1979) work is that he used the Barus exponential formula for pressure-viscosity characteristics which tends to give high values of viscosity compared to results obtained from Roelands formula (Jones, et al. (1975)). Furthermore, Dalmaz's (1979) results for the isoviscous case produced a lower exponent on W/U then Brewe et al. (1979). This appears to be due to starvation effects entering the fully

flooded results from the designation of the inlet boundary condition.

Figure 3.1 obtained from Meuleman et al. (1985) shows the differences between the Barus formula, Rolands formula and the experimental data of Hirst and Moose (1978). It is apparent that the Rolands formula represents the experimental result for the pressure-viscosity relationship more accurately than the Barus formula at high pressures, and the Rolands formula is used in this study. The researchers in the past used the Barus formula and neglected the lubricant compressibility to obtain a straight forward numerical analysis to the resulting linear partial differential equation. The numerical analysis employed in this study is more complicated because the resulting partial differential equation is now nonlinear. But this nonlinear equation is more realistic.

In the current study, the numerical solution for the piezoviscous-rigid regime of lubrication is presented for the full spectrum of conditions. The influence of lubricant entrainment direction has also been studied. The condition that the lubricant entraining vector is not parallel to the minor axis of the contact might arise, for example, in helical, spiral bevel, and hypoid gears. The radius ratio is varied from 0.2 to 64, to cover any contact ranging from something similar to a disk rolling on a plate ($\alpha<1$) to a contact approaching a nominal line contact ($\alpha\rightarrow70$) such as a barrel-shaped roller against a plate. The

influence of the dimensionless speed, load, and materials parameter on minimum film thickness are also investigated. The dimensionless load parameter is varied over a range of an order of magnitude. The dimensionless speed parameter is varied over a range 5.6 times the lowest speed value. Conditions corresponding to the use of solid materials of steel, bronze, and silicon nitride and lubricants of paraffinic and naphthenic mineral oils are considered in obtaining the exponent in the dimensionless materials parameter. Forty-one cases are used to obtain a simple empirical minimum film thickness formula. Contour plots are shown that indicate in detail the pressure developed between the solid.

3.1 Method of Calculation

By introducing the following dimensionless groups

$$\bar{X} = \frac{X}{R_x}, \qquad \bar{Y} = \frac{Y}{R_x}, \qquad \bar{\rho} = \frac{\rho}{\rho_o}, \qquad \bar{\eta} = \frac{\eta}{\eta_o}, \qquad H = \frac{h}{R_x}, \qquad P = \frac{p}{E'}$$

to the equations described in Chapter 2 the set of dimensionless equations that describe the piezoviscous-rigid regime of lubrication can be expressed as follows.

The Reynolds equation is

$$\frac{\partial}{\partial X}\left(\frac{\bar{\rho}\bar{H}^3}{\bar{\eta}}\frac{\partial P}{\partial X}\right) + \frac{\partial}{\partial y}\left(\frac{\bar{\rho}\bar{H}^3}{\bar{\eta}}\frac{\partial P}{\partial Y}\right) = 12U\left[\cos\theta\,\frac{\partial(\bar{\rho}\bar{H})}{\partial x} + \sin\theta\,\frac{\partial(\bar{\rho}\bar{H})}{\partial Y}\right] \qquad (3.1)$$

where

$$U = \eta_o\, u/E'\, R_x$$

The pressure-viscosity formula is from Roelands (1966)

$$\bar{\eta} = \left(\frac{\eta_\infty}{\eta_o}\right)^{[1-(1+PE'/c)^Z]} \tag{3.2}$$

where

$\eta_\infty = 6.31*10^{-5}$ Ns/m^2

$c = 1.96*10^8$ Ns/m^2

The pressure-density formula is from Dowson and Higginson (1966)

$$\bar{\rho} = 1 + \frac{sPE'}{1 + tPE'} \tag{3.3}$$

where s and t are constants that depend on the fluid.

The film thickness formula is

$$H = H_o + \frac{S(X,Y)}{R_x} \tag{3.4}$$

where H_o is central film thickness also minimum film thickness for rigid contacts.

Note the surfaces are considered rigid. Elastic effects will be considered in Chapter 4.

Boundary Condition

The boundary conditions are:

(a) The Reynolds boundary condition is applied in the divergent film. Namely, $P = dP/dX = dP/dY = 0$ at the cavitation boundary.

(b) The pressure on the boundaries of the computation region are assumed to be zero. The fully flooded conjunction is

considered in the present study, i.e., increasing the computation region of the conjunction does not effect the results.

Numerical Analysis

Having defined the density, viscosity and film thickness we are in a position to solve the Reynolds equation subjected to the Reynolds cavitation boundary condition. The dimensionless pressure of P is notorious for its steep gradient, which is not welcomed when performing numerical analysis via relaxation methods. In order to produce a more gentle curve, a parameter is introduced where

$$\phi = PH^{3/2}$$

This substitution also has the advantage of eliminating all terms containing derivatives of products of H and P or H and ϕ. Substituting equation (3.5) into equation (3.1), one obtains

$$H^{3/2}\left[\frac{\partial}{\partial X}\left(\frac{\bar{\rho}}{\bar{\eta}}\frac{\partial \phi}{\partial X}\right)\right] - \frac{3}{2}\phi\frac{\partial}{\partial X}\left(\frac{\bar{\rho}}{\bar{\eta}}H^{1/2}\frac{\partial H}{\partial X}\right) + H^{3/2}\left[\frac{\partial}{\partial Y}\left(\frac{\bar{\rho}}{\bar{\eta}}\frac{\partial \phi}{\partial Y}\right)\right]$$

$$- \frac{3}{2}\phi\frac{\partial}{\partial Y}\left(\frac{\bar{\rho}}{\bar{\eta}}H^{1/2}\frac{\partial H}{\partial Y}\right) = 12\left[\cos\theta\frac{\partial(\bar{\rho}H)}{\partial X} + \sin\theta\frac{\partial(\bar{\rho}H)}{\partial Y}\right] \qquad (3.6)$$

The method of frozen coefficients (sometimes also referred to as Kacanov's method) (1975) is applied to solve this nonlinear partial differential equation. It means that the solution for the set of equations is obtained by updating the nonlinear terms using an iterative procedure until the differences between the pressure variables for successive iterations are as small as desired. Second order central finite difference approximations are used to

the modified form of the Reynolds equation, thus forming a set of algebraic equations that are solved by the Gauss-Seidel iterative method with overrelaxation. For optimal efficiency, a variable-mesh structure (shown in fig. 3.2) is used to enhance the accuracy in the region of high pressure and large pressure gradient.

Normal Applied Load

The normal applied load can be evaluated by

$$w = \iint p(x,y)\, dx\, dy \tag{3.7}$$

The double Simpson's integration technique are applied to the integration.

A typical example of the pressure distribution in the regime of piezoviscous-rigid lubrication is shown in figure 3.3. Figure 3.3(a) is a 3-dimensional pressure distribution. Figure 3.3(b) shows the pressure profile in the center of the conjunction along the rolling direction. It is observed that the pressure profile in the regime of piezoviscous-rigid lubrication is very picky.

3.2 Results

Dimensionless Grouping

From the variables of the numerical analysis the following dimensionless groupings are written:

(1) Dimensionless Film Thickness

$$H = h/R_x \tag{3.8}$$

(2) Dimensionless Load Parameter

$$W = w/E'R_x^2 \tag{3.9}$$

(3) Dimensionless Speed Parameter

$$U = \eta_o u/E'R_x$$

Where

$$u = \sqrt{u_x^2 + u_y^2} \qquad (3.10)$$

(4) Dimensionless Materials Parameter

$$G = E'/p_{iv,as} \qquad (3.11)$$

Where $p_{iv,as}$ = asymptotic isoviscous pressure gradient obtained from Roelands (1966)

(5) Radius Ratio

$$\alpha = R_y/R_x \qquad (3.12)$$

(6) Lubricant Entraining Angle

$$\theta = TAN^{-1} (u_y/u_x) \quad \theta \text{ in degree} \qquad (3.13)$$

The dimensionless film thickness can thus be written as a function of the other five parameters

$$H_o = f(W, U, \alpha, G, \theta) \qquad (3.14)$$

The most important practical aspects of hydrodynamic lubrication of nonconformal contacts is the determination of the minimum film thickness within the contact. Therefore, in the fully flooded results to be presented, the dimensionless parameters (W, U, α, G and θ) will be varied and the effect on the minimum film thickness will be studied. Note that in equation (3.8) through (3.12) by changing the normal applied load w the dimensionless load W is changed but the other dimensionless parameters remain unchanged. Similar statements can be made about changing u in

the dimensionless speed U, and R in the radius ratio.

Influence of Load

The dimensionless parameters U, G, α and θ are kept constant while varying the dimensionless minimum film thickness H_o to get the dimensionless load capacity W at each different H_o. The values at which the remaining parameters U, G, α and θ are held constant during the calculations are $U = 0.16833*10^{-11}$, $G = 4522$, $\alpha = 16$, and $\theta = 0$.

Table 3.1 shows the computed values of load capacities for 10 values of minimum film thickness. From these 10 pairs of data, it is possible to determine a good empirical relationship between the minimum film thickness H_o and the load capacity W:

$$H_o = C_1 W^{C_2} \tag{3.15}$$

By applying a least-square power fit to the 10 pairs of data $[(W_i, H_{oi}), i = 1,2,\ldots,10]$, the values of C_1, C_2 are found to be $C_1 = 2.60615*10^{-12} \approx 2.606*10^{-12}$ $C_2 = -0.88019 \approx 0.880$. From the value of C_2 and equation (3.15), the effect of load on minimum film thickness is written as

$$H_o \propto W^{-0.880} \tag{3.16}$$

In figure 3.4 the variation of dimensionless film thickness with dimensionless load is plotted for 10 data points. A linear plot is observed when plotted on log-log scale. The percentage difference between the minimum film thickness obtained from

computational results (H_o) and the minimum film thickness from the least square fit equation ($\tilde{H}_o$) is expressed as

$$\tilde{D} = [(\tilde{H}_o - H_o)/H_o]*100 \qquad (3.17)$$

Influence of Speed

If the surface velocity u is changed the dimensionless speed parameter U is modified as shown in equation (3.10), but the other dimensionless parameters (H, G, α and θ) remain constant. The values at which these dimensionless parameters were held constant in the calculations performed to determine the influence of speed on film thickness are

$$\alpha = 16, \qquad H_o = 4.8*10^{-6}, \qquad G = 4522, \qquad \theta = 0$$

Values of the dimensionless speed parameter U and the corresponding dimensionless load capacities as obtained from the numerical computations are presented in table 4.2. Since the relationship between the minimum film thickness H_o and the load capacity W has been obtained. The relationship between minimum film thickness and speed parameter can be written in the form as

$$H_o/W^{-0.88} = C_3\, U^{C4} \qquad (3.18)$$

By applying a least-square fit to the 6 pairs of data [(U_1, H_{o1}), $1 = 1,\ldots,6$], the values of C_3 and C_4 are found to be $C_3 = 1.4899*10^{-13} \approx 1.49*10^{-13}$ and $C_4 = 1.2655 \approx 1.266$. From the value obtained for C_4 and equation (3.18), the effect of dimensionless speed on dimensionless film thickness can be written as

$$H_o \propto U^{1.266} \tag{3.19}$$

The data presented in table 3.2 is presented in figure 3.5. As was true for the load versus film thickness results the speed versus film thickness are linear when plotted on a log-log scale.

Influence of Radius Ratio

In order to study the effect of geometry on minimum film thickness, the dimensionless parameters for minimum film thickness H_o, speed U, materials parameter G, and lubricant entrainment direction are held constant at the following values:

$$H_o = 4.8*10^{-6}, \qquad U = 0.1683*10^{-11}, \qquad G = 4522, \qquad \theta = 0$$

Table 3.3 shows the computed values of dimensionless load capacity W for 22 values of radius ratio. It is possible to determine a good empirical relationship between the H and for the condition considered in the computation. The form of relationship chosen after investigating a number of different expressions can be written as

$$1 - (H_o/H_{o,r}) = \tilde{A}e^{\tilde{B}} \tag{3.20}$$

where $H_{o,r}$ is chosen to be the film thickness at rectangular contact.

A least-square exponential curve was fitted to the 22 pairs of data points to obtain values for $\tilde{A}$ and $\tilde{B}$ in equation (3.20). The values of $\tilde{A}$ and $\tilde{B}$ in equation (3.20) obtained from the least-square fit are $\tilde{A} = 0.989 \approx 1.00$ and $\tilde{B} = 0.03866 \approx$

0.0387. Substituting these values of $\tilde{A}$ and $\tilde{B}$ into equation (3.20) the following relationship between the radius ratio and minimum film thickness results,

$$H_o \alpha (1 - e^{-0.0387\alpha}) \qquad (3.21)$$

The effect of radius ratio on film thickness for the 22 data points is shown in figure 3.6. It is most significant that the computed value of $\tilde{A}$ is approximately unity, since this ensures that the minimum film thickness approaches zero as radius ratio goes to zero. Contour plots for three radius ratios (i.e. α of 16, 9, and 4) are shown in figure 3.7 to demonstrate the influence of geometry. Since the isobars in each case are evenly spaced, the pressure gradients can be easily depicted. As the radius ratio increases, the steeper pressure gradients are predominantly along the rolling direction. This implies that the amount of side leakage decreases as radius ratio increases. Figure 3.8 shows the geometry effects in four different regimes of lubrication, i.e. hard EHL (Hamrock and Dowson (1977a)), soft EHL (Hamrock and Dowson (1978)), piezoviscous-rigid, and isoviscous-rigid (Brewe, et al. (1979)), where H_o is the minimum film thickness for rectangular contacts. It is assumed that when $\alpha = 150$, the rectangular contact limit is realized. The ratio $H_{min}/H_{min,r}$ approaches the limiting value very quickly in hard EHL, and most slowly in isoviscous-rigid case.

Influence of Materials Properties

A study of the influence of the dimensionless materials parameter G on minimum film thickness has to be approached with caution since in practice it is not possible to change the physical properties of the materials, and hence the value of G, without influencing the other dimensionless parameters considered earlier. Equations (3.9), (3.10), and (3.11) show that when either the materials of the solids (as expressed in E') or the lubricants (as expressed in η_o and $p_{iv,as}$) are varied, not only does the materials parameter G change, but so do the dimensionless speed U and load W parameters. Only the radius ratio, minimum film thickness and lubricant entrainment direction can be held fixed; and for all results presented in table 3.4, $H_o = 4.8*10^{-6}$ or $= 1.4*10^{-6}$, $\alpha = 16$, and $\theta = 0$ are adopted.

The results obtained from calculations performed for six values of the dimensionless materials parameter are summerized in table 3.4. The general form of these results, showing how the minimum film thickness is a function of dimensionless materials parameter, is

$$\tilde{C} = C_7 \; G^{C8} \qquad (3.22)$$

where

$$\tilde{C} = H_o/[(1 - e^{-0.0387\alpha}) \; U^{1.266} \; W^{-0.880}] \quad ,$$

By applying a least-square power fit to the six pairs of data, the values of C_7 and C_8 are found to be $C_7 = 175.04$ and

$C_8 = 0.386096 \sim 0.386$. The effect of the dimensionless materials parameter on the minimum film thickness is approximated with adequate accuracy as

$$H_o \alpha G^{0.386} \tag{3.23}$$

The variation of dimensionless materials parameter G with dimensionless film thickness H is shown in figure 3.9. The six data points given in table 3.4 are shown in this figure. It is observed that on log-log scale a linear representation of materials parameter versus film thickness is obtained.

Influence of Lubricant Entrainment Direction

If the velocity of the entrainment lubricant is kept constant, but the component velocity in the x direction u and the component velocity in the y direction u is changed, the lubricant entraining angle is modified as shown in equation (3.13), while the other dimensionless parameters (H_o, G and α) remain constant. The values at which these dimensionless parameters are held constant in the calculations performed to determine the influence of lubricant entrainment direction are

$$\alpha = 20, \qquad H_o = 5.6*10^{-6}, \qquad G = 4522, \qquad U = 0.75749*10^{-11}$$

The results obtained from calculation performed for 10 values of the lubrication entrainment direction are summarized in table 3.5. A cosine function was chosen for curve fitting, namely

$$\tilde{T} = C_9 \theta \tag{3.24}$$

where

$$\tilde{T} = \cos^{-1}\left(W^{-0.880}/W_o^{-0.880}\right)$$

W_o denotes the load capacity at $\theta = 0$.

By applying a least square fit to the 10 pairs of data, the values of C_9 was found to be $C_9 = 0.0200027 \approx 0.0200$. Therefore, the effect of the lubricant entrainment direction on the minimum film thickness can be written as

$$H_o \propto \cos(1.146\ \theta) \qquad (3.25)$$

This is shown in figure 3.10. It is significant that when the entraining angle is zero the cosine function turns out to be 1. In other words, there is no effect of lubricant entrainment direction on minimum film thickness. Although the influence of lubricant entrainment direction is investigated for $\alpha = 20$ only, it is found that it can be applied to the cases from $\alpha = 16$ to $\alpha = 30$.

Minimum Film Thickness Formula

The proportionality equations (3.16), (3.19), (3.21), and (3.23) have established how the minimum film thickness varied with the dimensionless load, speed, radius ratio and materials parameter respectively. This enables a composite dimensionless minimum film thickness formula for fully flooded rigid elliptic contact solid lubricated by piezoviscous fluid to be modeled by

$$H = 178G^{0.386}\ U^{1.266}\ W^{-0.880}\ (1 - e^{-0.0387\alpha}) \qquad (3.26)$$

with 85.6 percent confidence (except the small vaule of α) of ±8.92 percent of the value from the numerical analysis. Equation (3.26) can be written in dimensional form as

$$h = 178(1/p_{iv,as})^{0.386} (un_o)^{1.266} w^{-0.880} R_x^{1.494} \times (1 - e^{-0.0387 R_y/R_x}) \qquad (3.27)$$

Note that the effective elastic modulus E' does not appear in this equation. Case (1) to case (41) in table 3.6 gives the forty-one different cases used in obtaining equation (3.26). To gain more confidence in the application of this empirical equation, some other values of dimensionless U and minimum film thickness H_o not in the range for curve fitting were checked. The results are shown in case (52) and case (53) of table 3.6 . The good agreement between the prediction from the minimum film thickness formula and computed results is encouraging.

4.2 Discussion

A numerical solution for the piezoviscous effect in nonconformal rigid contacts lubricated hydrodynamically has been developed. The following remarks can be made:

(1) It was found that the effective elastic modulus E' does not appear in the dimensional film thickness equation. This corresponds to a rigid contact; there is no effect of elastic properties.

(2) In all cases it was found that if the maximum dimensionless viscosity is less than three, the load capacity is no more than 12 percent larger than the load capacity without

piezoviscous effect. This indicates a very small piezoviscous effects. Here, all the data sets used to generate equation (3.26) have the maximum dimensionless viscosity larger than three.

(3) The exponents of dimensionless load capacity and dimensionless velocity in the minimum film thickness equation for the piezoviscous-rigid regime are between those for piezoviscous-elastic regime and isoviscous-rigid regime.

(4) The film thickness formula according to the side-leakage factor proposed by Hamrock and Dowson (1978) is

$$H = 1.66(GU)^{2/3} [1 - \exp(-0.68*(1.03*\alpha^{0.66}))] \qquad (3.28)$$

The more recent formula from the numerical solution by Dowson et al. (1983) is

$$H_o = 1.66(GU)^{2/3} \left(\frac{\alpha}{1 + \alpha}\right)^{0.6} \qquad (3.29)$$

Figure 3.11 compares the minimum film thickness as obtained from equation (3.28) and (3.29) with the present result for $W = 0.6*10^{-6}$ or $0.9*10^{-6}$ and $\alpha = 8$ or 16. It can be seen that the deviations are large for small values of GU. The deviations result because the load parameter W is not included in equations (3.28) or (3.29) , giving erroneous results when the piezovicous effects are small, i.e. GU small, and because the Barus formula is used for the pressure-viscosity correlation in equations (3.28) and (3.29) cause an overestimate of the minimum film thickness.

(5) The film thickness formula proposed by Houpert (1984) by means of curve fitting of the numerical solution of Dalmaz is

$$H_{pvR} = C\, H_{IVR}$$

$$C = \exp(0.265A)$$

$$H_{IVR} = \left[\frac{\left(1 + \frac{2}{3\alpha}\right) \frac{W}{U}}{\left(0.131 \ \mathrm{TAN}^{-1}\left(\frac{\alpha}{2}\right) + 1.683\right) \sqrt{128\alpha}} + 2.6511 \right]^{-2}$$

$$A = 12GU \frac{0.177\alpha}{\alpha + 0.778} H_{IVR}^{-1.5} \qquad (3.30)$$

A comparison of 20 of the 41 cases used to get the present formula (equation (3.26)) is made with the formula proposed by Houpert. Table 3.7 shows the ratio of H_o (equation (3.26)) to H_o (equation (3.30)). The deviation is between 28% to 54%. A possible cause of this difference may be due to Houpert's results imply an incompressible fluid and a Barus pressure-viscosity formula.

3.4 Summary

A procedure for the numerical solution of the complete piezoviscous-rigid regime of lubrication for nonconformal contacts has been demonstrated. In the numerical analysis of the Reynolds equation the parameter $\phi = PH^{3/2}$ was introduced in order to help the relaxation process. A variable-mesh nodal structure was used to provide close spacing in and around the pressure peak. A more realistic formula is used for the pressure viscosity relationship. Lubricant compressibility was also considered.

By using the procedures outlined in the analysis, the influence of the dimensionless load W, speed U, radius ratio α, materials G and lubricant entraining direction θ on minimum

film thickness were investigated. Forty-one cases were used to generate the minimum film thickness relationship

$$H_o = 178G^{0.386} U^{1.266} W^{-0.880} (1 - e^{-0.0387\alpha})$$

The most dominant exponent occurred in association with the speed parameter; the exponent on the load parameter -0.880 was in between the -2 for isoviscous-rigid regime and -0.073 for piezoviscous-elastic regime. The materials parameter also carries a significant exponent, although the range of the parameter in engineering is limited. The geometry effect shows the same curve as in elastohydrodynamical lubrication, but approaches the limiting value much more slowly. The effect of the direction of lubrication entrainment is a cosine function for the geometries studied. The dimensionless load parameter values used in obtaining the preceding equation are varied over a range of one order of magnitude. The dimensionless speed values are varied over 5.6 times the lowest value. The radius ratio is varied from 0.2 to 64 (a configuration approaching a line contact). Conditions corresponding to the use of solid materials of steel, bronze and silicon nitride and lubricants of paraffinic and naphthenic mineral oils are considered in obtaining the exponent in the dimensionless materials parameter. Contour plots are shown that indicate in detail the pressure developed between the solids.

Chapter 4

ELASTIC DEFORMATION OF ELLIPTICAL CONTACTS

In solving various engineering problems, such as the point contact EHL problems and other frictionless contact problems, the elastic surface deformation is often determined by equation (2.9). However, there are two important problems associated with the integration of equation (2.9) as far as numerical methods are concerned. The first problem arises from the singularity at $x = x'$ and $y = y'$. The second is that the amount of work in the numerical integration is considerably large. This is due to the fact that the whole area must be integrated in order to evaluate the deformation at a certain point and that in the repeated calculation, such as in the numerical solution of the EHL problem by means of iteration, the deformation of every node on the finite difference grid must be evaluated for each iteration. The method of dealing with the singularity is to use a polynomial function to approximate the pressure distribution so that the analytical solution for the intergation on the grid element can be obtained. In order to reduce the amount of the calculation an influence coefficient matrix D is introduced, in which the element D_{ij}^{kl} is defined as the deformation occurring at node (k,l) when a unit of pressure had been applied to node (i,j). Consequently equation (2.9) can be described by the following discrete form:

$$d_{kl} = \frac{2}{\pi} \sum^{i} \sum^{j} D_{ij}^{kl} P_{ij} \qquad (4.1)$$

All the values of D_{ij}^{kl} must be completely computed only once, and the deformation can be calculated by only applying the expression (4.1).

These approaches were first successfully developed by Hamrock and Dowson (1974) and applied to the EHL problems. They assume that the pressure on each element can be replaced by a constant value, that is the whole pressure distribution is replaced by blocks of uniform pressure. In this way, an analytical expression for the integration of the deformation is worked out and the deformation of every node expressed as a linear combination of the nodal pressures. In the solution of Ranger, Ettles, and Cameron (1975), a bilinear interpolating function is used to approximate the practical pressure distribution. Evans and Snidle (1981, 1982) employed a different method which was first presented by Biswas and Snidle (1977). For grid elements without singularity, they adopted directly Simpson's rule for integration, and for those with singularity they used a biquadratic polynomial function to express the pressure distribution approximately. In this way, an analytical solution for the integration is developed without direct expression for the deformation as a linear combination of the nodal pressures. Following in these footsteps, Hou Keping, Zhu Dong, and Wen Shizhu (1984) employed the biquadratic polynomial function for approaching the pressure distribution on all grid elements. An influence coefficient matrix is introduced to reduce the amount of calculating work when repeated

calculations of the elastic deformation is needed. A comparison of computing methods by Ranger et al., Biswas and et al., and the authors was presented. It is found that the method proposed by Hou Keping et al. has higher numerical accuracy and uses less computational time than the others. The reason that Hou Keping's method is more accurate than Biswas's is because of the fact that the integrand of the deformation integral varie· very rapidly around the region of singularity and this can lead to significant errors in evaluating the contribution to the total deformation by the area surrounding the singularity. However, for a (2n+1)*(2m+1) finite difference grid, the influence matrix introduced by Hou Keping et al. is composed of (n*m)*(2n*2m*9) elements, which is not welcomed even in today's powerful computer. It means that only a relatively coarse finite difference grid can be used in the EHL problems.

In the present study, a biquadratic polynomial expressed in Lagrange form is used to approximate the pressure distribution on all grid element. An influence matrix whose coefficient is dependent on the geometric factors and the distance between node (k,l) and node (i,j) only is introduced to express the deformation of every node as a linear combination of the nodal pressures. In this way, only (2n*2m*9) elements is needed in the influence matrix for a (2n+1)*(2m+1) equidistant rectangular grid. The computational time and computer storage size for the influence coefficient matrix is tremendously reduced. For example, for a

(21*21) equidistant rectangular grid (m=n=10) the elements of influence matrix is reduced from 36 0000 to 3600. Incorporating this new elasticity approach with reasonable finite difference grid into the EHL problems is now applicable.

4.1 The Form of Analytical Solution

On a nine-node element (e) of any nonequidistant rectangular grid, a biquadratic polynomial is used to approach the pressure function (fig. 4.1)

$$p(x,y) = \sum_{n=1}^{g} \psi_n^e (x,y)\ p_n^e \tag{4.2}$$

where p_n^e stand for pressure at the nine nidal points, $\psi(x,y)$ are nine biquadratic functions which can be expressed as the following

$$\psi(x,y) = \prod_{\substack{r=i-1 \\ r\neq m}}^{i+1} \left(\frac{x - x_m}{x_r - x_m}\right) \prod_{\substack{S=j-1 \\ S\neq n}}^{j+1} \left(\frac{y - y_n}{y_s - y_n}\right) \tag{4.3}$$

$$= a_1 (x^2 + a_2 x + a_3)(y^2 + a_4 y + a_5)$$

$$m = i-1,\ i,\ i+1$$

$$n = j-1,\ j,\ j+1$$

where $a_1 - a_5$ only depend on the grid geometry. The deformation at node (k,l) caused by the pressure distribution on the element (e) is:

$$d_{kl}^e = \frac{2}{\pi} \sum_{n=1}^{g} p_n^e\ I_n^e$$

$$I_n^e = \iint_e \frac{\psi_n^e(x,y)}{\sqrt{x^2 + y^2}}\, dx\, dy \tag{4.4}$$

After evaluating I for all elements, the total deformation results:

$$a_{kl} = \frac{2}{\pi} \sum_{e} \sum_{g} p_n^e \, I_n^e \tag{4.5}$$

By using the nine values I_n^e of every element, the total deformation matrix on the whole region can be composed. If a function FUN(x,y) is defined as follows,

$$\begin{aligned} FUN(x,y) = \frac{a_1}{120} \Big\{ & y \ln(t + x)[120\, a_3 a_5 + 60\, y\, a_3\, a_4 - 20\, y^2(a_5 - 2a_3) \\ & - 15\, y^3\, b_4 - 12\, y^4] + x \ln(t + y)[120\, a_3 a_5 + 60\, x a_2 a_5 \\ & + 20\, x^2\,(2\, a_5 - a_3) - 15\, x^3 b_2 - 12\, x^4] + t[60\, x\, a_3 a_4 \\ & + 60\, y\, a_2 a_5 + xy\,(20\, a_5 + 20\, a_3 - 15 x a_2 - 15 y a_4) \\ & + t^2\,(40\, a_2 a_4 + 30\, y\, a_2 + 30\, x a_4 + 12\, xy)] \Big\} \end{aligned} \tag{4.6}$$

where

$$t = \sqrt{x^2 + y^2}$$

the deformation integral becomes

$$I = [FUN(x_1,y_1) + FUN(x_3,y_3) - FUN(x_1,y_3) - FUN(x_3,y_1)]$$

Since

$$FUN(x,-y) = -FUN(x,y) \text{ and } FUN(-x,y) = -FUN(x,y)$$

it can be proved that $I_{n\,(x,y)}^e = I_{n\,(x,-y)}^e$ and $I_{n\,(x,y)}^e = I_{n\,(-x,y)}^e$. It means that I is an even function with respect to x and y. Therefore the coefficient of the influence matrix depends on the geometric factors of the grid and the distance between the central of the grid point and the

deformation point only. The size of the influence coefficient matrix is thereby tremendously reduced.

4.2 Discussion

Hou Keping et al. have demonstrated the advantage of employing the biquadratic interpolating polynomial for approaching the pressure distribution on all grid elements by comparing the numerical accuracy with the methods proposed by Ranger et al. and Biswas et al. The comparison between the present approach and Hamrock's approach is shown in table 4.1. The results of table 4.1 show that for a given mesh the best accuracy in the calculation of d_{max} and Δh_{max} is obtained by the present approach. The accuracy of Δh_{max} is also shown since it is a measure of the flatness of the film shape under the Hertzian pressure distribution. This aspect is extremely important at high load, where the elastic deformations are two or three orders of magnitude larger than the film thickness.

4.3 Concluding Remarks

In conclusion, the calculation procedure presented here has the advantages of higher numerical accuracy, less computing time and smaller storage size required for the influence matrix and is easier to apply than other methods proposed to date.

Chapter 5

THE EFFECT OF SURFACE ROUGHNESS ON ELASTOHYDRODYNAMIC LUBRICATION OF POINT CONTACT

Detailed studies of surfaces and the quantification of surface features of importance in tribology are recent, mid-twentith century developments. An understanding of the effect of surface roughness on lubrication is important in specifying engineering surface finishes, analyzing bearing failures, and prediciting the mode of lubrication in a practical situation and the breakdown of full film lubrication. The first attempts to include roughness effect considered deterministic striations such as sinusoidal waves oriented parallel or perpendicular to the direction of motion of the bearing components, i.e. longitudinal and transverse roughness (Elrod, 1977). The real bearing surfaces, however, have a more or less random distribution of roughness. The study of surface roughness effects in lubrication has gained increasing attention with the introduction of stochastic concepts by Tzeng and Saibel (1967). Since then stochastic process theory has been utilized on various bearing performances. Tzeng and Saibel (1967) utilized the stochastic approach for a slider bearing with one-dimensional transverse roughness. Christensen and Tonder (1971, 1972, 1973) developed the stochastic Reynolds equation for transverse and longitudinal roughness and use this equation to analyze the hydrodynamic lubrication of slider and journal bearings. These approaches

involve deriving Reynolds type equations which govern the mean pressure in rough bearings, and these equations have been utilized by many workers to predict rough bearing performance. However, these stochastic Reynolds equations are restricted to two types of roughness structures: one-dimensional ridges oriented either transversely or longitudinally. These are the limiting cases of roughness found on real surfaces. The treatment of general random roughness is a recent development. Two approaches have been developed. The first, due to Bush et al. (1982), introduces roughness as a perturbation to the smooth bearing and averages over an ensemble of roughness configurations. The perturbation method is inherently prevented from being applied to bearings in which contacts occurs since the analysis relies on small-amplitude roughness. However, this assumption allows the effects of roughness to be determined from linear equations whereas the basic Reynolds equation is nonlinear. Roughness effects are therefore relatively easy to calculate. The second method is the flow factor model introduced by Patir and Cheng (1978). In their formulation, the actual flow between rough surfaces is equated to an averaged flow between nominally smooth surfaces, while parameters describing the roughness are included in the Reynolds equation through the flow factors, which are obtained by numerical flow simulation or the height readings of a real surface. Thus any type of roughness structure can be analyzed. Another

advantage of this method is that it can be extended to the mixed lubrication regime in which contact between bearing surfaces occurs.

Using the flow factor formulation, Patir and Cheng (1979) performed a calculation on the inlet half of a elastohydrodynamic line contact with the Ertel-like approximation for the inlet shape as described in Chapter 1. Recently, Tripp and Hamrock (1984) did the complete numerical solution of the isothermal elastohydrodynamic lubrication of line contact on rough surfaces with the same flow factor approach.

In the present study the flow factor model developed by Patir and Cheng (1978) is adopted to study the surface roughness effect on the elastohydrodynamic lubrication of point contact, which essentially takes into account the side leakage effect of nonconformal contacts. Conditions typical of an EHL contact in the piezoviscous-elastic regime with a developed pressure spike near the outlet are investigated. The Roelands formula is used for the pressure-viscosity relationship. The lubricant has been assumed to be compressible and the system to be isothermal. Results are presented demonstrating the effect of surface roughness on the film shape, pressure distribution, and coefficient of rolling friction in a ball bearing.

5.1 Background

The general background for the surface roughness and the stochastic aspect of flow will be described in this section. Tensor notation is used for simplicity.

Surface Roughness

The significance of advanced surface research is becoming apparent where surface systems play an important role affecting the behavior of a physical process. The problems in design, such as lubrication, stiffness of joints, strength of parts, fatigue, accuracy of dimensional chains and kinematic trains, dynamics of machine tools, etc., cannot be satisfactorily approached without information about surface configurations that exhibit a profound random character.

In general terms, the roughness of a solid is defined as any departure of the actual surface height from the ideal datum level, also known as nominal level, occurring as a result of the physical and chemical methods used to prepare the final surface as well as microstructure of the material (fig. 5.1).

To describe the rough surfaces in a statistical sense requires knowledge of the height distribution and the correlation function for these heights. These depend upon the scale selected for measurement of surface features and are not intrinsic properties of the surface. The height distribution is the probability that a single point in the surface selected at random lies at or below a given height, while the correlation functions

describe how the probability of finding one point at a given height depends on the heights of the surrounding points. This is best illustrated by the two point correlation function which is the ensemble-averaged product of heights at two points selected at random with fixed spacing between them. For a general surface, correlation depends on direction as well as magnitude of the displacement of the two points and is determined by the typical dimensions of surface features in that direction.

Reynolds Roughness and Stokes Roughness

When Reynolds equation is used to study the surface roughness effect on lubrication, the roughness should be the Reynolds type which requires long wavelength and small amplitude for the asperities relative to film thickness, and is labled Reynolds roughness (Elrod, 1978). If the wavelength is so small as to necessitate the application of the Navier-Stoke equation, it is referred to as Stokes roughness. Only the Reynolds roughness will be considered in this study.

Statistical Aspects of Flow

The primitive parameters of the problem are given in figure 5.1, which shows the x-direction of a lubricant film moving between two rough solid boundaries at heights z_a and z_b. The translational velocities $\vec{u}_a$ and $\vec{u}_b$ of these boundaries lie in the (x,y) plane and are independent of position and time. Thus, there is no rigid-body rotation and no transient effect. The actual surface height $z_{a,b}$ is considered to be simply the

sum of the specified nominal height and a random roughness height $\delta_{a,b}$. The random variable $\delta_{a,b}$ is a stationary stochastic process distributed with standard deviation (rms value) $\sigma_{a,b}$ about zero mean. We need also the standard deviation of the roughness combination $(\delta_b - \delta_a)$, which in cases where cross-correlation is absent will be just $(a_a^2 + a_b^2)^{1/2}$.

For convenience the boundary variables with the following combinations are introduced:

$$\begin{array}{ll} \text{film thickness} & \text{mean surface height} \\ h = z_b - z_b & z = \frac{1}{2}(z_a + z_b) \\ \text{slip velocity} & \text{mean surface velocity} \\ \vec{v} = \vec{u}_b - \vec{u}_b & \vec{u} = \frac{1}{2}(\vec{u}_a + \vec{u}_b) \end{array} \tag{5.1}$$

The volume flow Q_1 per unit width due to the pressure gradient $\partial_1 p$ and the entraining velocity u_1, under the assumptions of the Reynolds equation described in Chapter 2, is given by

$$Q_1 = -\frac{h^3}{12\eta}\partial_1 p + hu_1 \tag{5.2}$$

The continuity equation for incompressible flow $\partial_1 Q_1 = -\partial h/\partial t$ is applied to derive the Reynolds equation for this problem:

$$\partial_1\left(\frac{h^3}{12\eta}\partial_1 p\right) = -v_1 \partial z_1 \tag{5.3}$$

where the Euler transform has been used to interchange time and space derivative of h.

The central idea for the flow factor method is to recast the flow vector Q_i in terms of the averaged pressure and film thickness, p^* and h^* replacing their true fluctuating values p and h. To achieve this, the effects of roughness must be included explicitly. The form introduced by Patir and Cheng for incompressible laminar flow is:

$$Q_i = - \frac{h^{*3}}{12\eta} \phi^p_{ij} \partial_j p^* + h^* U_i - \frac{\sigma}{2} \phi^s_{ij} V_j \qquad (5.4)$$

where tensors ϕ^p_{ij} and ϕ^s_{ij} are termed, respectively, the pressure (or Poiseuille) and shear flow factors. The shear flow factor ϕ^s_{ij} accounts for flow produced by roughness in the presence of slip even when the pressure gradient vanishes. ϕ^p_{ij} can be thought as a correction factor, comparing the mean pressure flow in rough bearings to that of smooth bearings having the same nominal geometry, namely additional entrainment due to roughness under pure rolling conditions. Fluctuations in flow are now fully incorporated into the flow factors. It is central to the method to assume these fluctuations are negligible compared to those of p and h. The continuity condition $\partial_i Q_i = -\partial h/\partial t$ may now be applied to Q^*_i instead of Q_i yielding

$$\partial_i \left(\phi^p_{ij} \frac{h^{*3}}{12\eta} \partial_j p^* \right) = - V_j \partial_i \left(z\delta_{ij} + \frac{1}{2} \sigma \phi^{s^*}_{ij} \right) \qquad (5.5)$$

This is the modified Reynolds equation for surfaces in translational motion. At this stage, Patir and Cheng adopted the direct approach of numerical simulation of the roughness surfaces

to obtain the flow factors. Tripp (1983) extended the flow factor model proposed by Patir and Cheng (1978) and expressed the flow factors on the roughness parameters in simple closed form by analytical method. In his approach, the pressure term is expanded as a perturbation series by regular perturbation approximation. Then green function technique is applied to solve the terms in the series. It is found that to second order the flow factors are determined by just two parameters: the rms surface height referenced to h, which in the usual notation becomes the film parameter $\Lambda = h/\sigma$, and the anisotropy of typical surface asperities given by γ the ratio of the two-point correlation lengths parallel and perpendicular to the lay direction of the surface texture. Purely transverse, isotropic, and purely logitudinal roughness structures correspond to $\gamma = 0, 1, \infty$, respectively. Surfaces with $\gamma > 1$ are longitudinally oriented (fig. 5.2). In this study, the flow factors express as a function of the film parameter Λ and the anisotropy index γ proposed by Tripp (1983) are used.

5.2 Method of Calculation

For an incompressible lubricant, the modified Reynolds equation for surfaces in translational motion is introduced in last section for generality. For compressible lubricant, the modified Reynolds equation for rotational motion about fixed axes has slight differences from equation (5.5) since now the density is included in the flow vector and the term $\partial(\rho h)/\partial t = 0$ in the

continuity equation is zero. The corresponding form of equation (5.5) becomes

$$\partial_i\left(\phi^{p^*}_{ij}\,\frac{\rho h^{*3}}{12\eta}\,\partial_j p^*\right) = u_1\,\partial_1(\rho h) - \frac{1}{2}\,\sigma v_j\,\partial_1\,\rho\,\phi^{s^*}_{ij} \qquad (5.6)$$

The flow factors are locally deterministic and a second order perturbation calculation using Gaussian forms both for the height distribution and the two-point autocorrelation function (Tripp, 1983) yields the result

$$\left.\begin{aligned} \phi^{p^*}_{xx}(\Lambda,\gamma) &= 1 + 3\,\frac{\gamma-2}{\gamma+1}\,\Lambda^{-2} \\ \phi^{p^*}_{yy}(\Lambda,\gamma) &= \phi^{p^*}_{xx}(\Lambda,\tfrac{1}{\gamma}) \\ \phi^{s^*}_{xx}(\Lambda,\gamma) &= \frac{3}{\gamma+1}\,\Lambda^{-1} \\ \phi^{s^*}_{yy}(\Lambda,\gamma) &= \phi^{s^*}_{xx}(\Lambda,\tfrac{1}{\gamma}) \end{aligned}\right\} \qquad (5.7)$$

with all other components zero. In this representation the x and y directions coincide with the roughness axes determined by the surface lay, from which the general case is readily obtained by coordinate rotation. The forms given by equation (5.7) are compared with the results in Patir and Cheng (1978, 1979) to those computed directly from an ensemble of generated rough surfaces with generally good agreements shown by figures 5.3 and 5.4 in the physically realistic range of Λ.

Choosing the pure rolling condition for illustrative purposes, the flow vector of equation (5.4) in explicit notation is

$$\left.\begin{aligned} Q_x &= -\frac{h^{*3}}{12\eta}\phi^{*p}_{xx}\frac{\partial p^*}{\partial x} + u_x h^* \\ Q_y &= -\frac{h^{*3}}{12\eta}\phi^{*p}_{yy}\frac{\partial p^*}{\partial y} + u_y h^* \end{aligned}\right\} \qquad (5.8)$$

Applying the continuity equation to equation (5.8) leads by an Euler transform to the Reynolds equation appropriate to the case illustrated in this study:

$$\frac{\partial}{\partial x}\left(\phi^{p^*}_{xx}\frac{\rho h^{*3}}{\eta}\frac{\partial p^*}{\partial x}\right) + \frac{\partial}{\partial y}\left(\varphi^{p^*}_{yy}\frac{\rho h^{*3}}{\eta}\frac{\partial p^*}{\partial y}\right) = 12u\left[\cos\theta\frac{\partial(\rho h^*)}{\partial x} + \sin\theta\frac{\partial(\rho h^*)}{\partial y}\right] \qquad (5.9)$$

The following dimensionless groups are introduced for nondimensionalization

$$X = \frac{x}{b}\ ,\ Y = \frac{y}{a}\ ,\ \bar{\rho} = \frac{\rho}{\rho_o}\ ,\ \bar{\eta} = \frac{\eta}{\eta_o}\ ,\ H^* = \frac{h^*}{R_x}\ ,\ p^* = \frac{p^*}{E'} \qquad (5.10)$$

where a and b are semimajor and semiminor axis of contact ellipse.

By substituting these dimensionless groups into the governing equations (5.9), (2.6), (2.7), and (2.14), the dimensionless equations describing the piezoviscous-elastic lubrication on rough bearings is obtained.

The modified Reynolds equation is

$$\frac{\partial}{\partial\bar{X}}\left(\phi^{p^*}_{xx}\frac{\bar{\rho}H^{*3}}{\bar{\eta}}\frac{\partial p^*}{\partial\bar{x}}\right) + \frac{\partial}{\partial\bar{Y}}\left(\phi^{p^*}_{yy}\frac{\bar{\rho}H^{*3}}{\bar{\eta}}\frac{\partial P^*}{\partial\bar{Y}}\right) = 12U\left[\cos\phi\frac{\partial(\bar{\rho}H)}{\partial\bar{x}} + \sin\theta\frac{\partial(\bar{\rho}H)}{\partial\bar{Y}}\right] \qquad (5.11)$$

where $U = \eta_0 u/E'R_x$

The pressure-viscosity formula from Roelands (1966) is

$$\bar{\eta} = \left(\frac{\eta_\infty}{\eta_0}\right)^{[1-(1+p^*E'/c)^Z]} \tag{5.12}$$

where $\eta_\infty = 6.31*10^{-5}$ Ns/m and $c = 1.96*10^8$ Ns/m^2.

The pressure-density formula from Dowson and Higginson (1966) is

$$\bar{\rho} = 1 + \frac{sP^*E'}{1 + tP^*E'} \tag{5.13}$$

where s and t are constants that depend on the fluid.

The film thickness formula is

$$H^* = H_0^* + \frac{s(\bar{X},\bar{Y})}{R_x} + \frac{d(\bar{X},\bar{Y})}{R_x} \tag{5.14}$$

Boundary Conditions

The boundary conditions are similar to what have been described in chapter 2 for piezoviscous-rigid lubrication.

(a) At the cavitation boundary,

$$p^* = \frac{dP^*}{d\bar{X}} = \frac{dP^*}{d\bar{Y}} = 0$$

This condition is commonly known as the Reynolds condition.

(b) At the edges of the computation zone the pressure is zero. The fully flooded conjunction is considered.

Numerical Analysis

The modified Reynolds equation (5.11) for P is transformed into an equation for $\Phi = P^* H^{*3/2}$ and discretized by central

finite difference expansion on a uniform grid scaled to the Hertzian contact ellipse. This scale is chosen instead of the effective radius R_x introduced in Chapter 2 for piezoviscous-rigid lubrication because it's found that it can speed up the convergence process when the elastic deformation is taken into account. Thus a load capacity has to be specified in the beginning to determine the major and minor axes of the Hertzian ellipse instead of giving a specific H_o to get a certain load capacity. It means that an extra outer loop has to be satisfied in addition to the convergence of pressure distribution through the method of frozen coefficients. Hence, the nominal dimensionless separation of the rigid solids H has to be adjusted to compensate for the difference between the actual load obtained by integration of the convergent pressure distribution through the method of frozen coefficients and the initially assumed load. A flow chart is show in figure 5.5. A damping factor is always necessary for each iteration through the method of frozen coefficients to get a convergent pressure distribution. Extensive computing time is required since the elastic deformation is involved in the film thickness formula. The numerical scheme described in Chapter 4 is adopted for the calculation of elastic deformation.

Coefficient of Friction

The shear force per unit length acting on solid a can be written as

$$f_a = \int \left(\eta \frac{du}{dz}\right)_{z=z_a} dx \qquad (5.15)$$

Integrating the reduced Navier-Stokes equation for dp/dx across the film gives

$$\eta \frac{du}{dz} = \frac{[2(z - z_a) - h]}{2} \frac{dp}{dx} - \frac{\eta(u_a - u_b)}{h} \qquad (5.16)$$

Substituting this equation into equation (5.15) gives

$$f_a = -\int \left[\frac{h}{2} \frac{dp}{dx} + \frac{\eta(u_a - u_b)}{h}\right] dx \qquad (5.17)$$

The shearing force per unit length acting on solid b can be written as

$$f_b = \int \left(\eta \frac{du}{dz}\right)_{z=z_b} dx \qquad (5.18)$$

Making use of equation (5.16) gives equation (5.18) as

$$f_b = \int \left[\frac{h}{2} \frac{dp}{dx} - \frac{\eta(u_a - u_b)}{h}\right] dx \qquad (5.19)$$

The normal pressure p acting on the two solids also has a net x-component $w_x = w_{ax} + w_{bx}$ which can be expressed by

$$w_x = \int h \frac{dp}{dx} dx \qquad (5.20)$$

The shear and pressure forces thus balance, satisfying the equilibrium condition

$$f_a - f_b + w_x = 0 \qquad (5.21)$$

For a pure rolling condition, we have

$$f_a = - f_a = - \frac{1}{2} \int h \frac{dp}{dx} dx \qquad (5.22)$$

in which the explicit appearance of n in equations (5.15) and (5.18) is now hidden. The coefficient of rolling friction for either solid a or b is given by

$$\mu = \left| f^* \right| / \mu \qquad (5.23)$$

where the expectation value of the shear force is given in second order perturbation theory by

$$f^* = - \frac{1}{2} \int h^* \frac{dp^*}{dx} \left(1 + \frac{3}{\gamma + 1} \Lambda^{-2} \right) dx \qquad (5.24)$$

5.3 Results and Discussion

The results for a steel bearing in a pure rolling condition is presented. The values of the parameters are shown in table 5.1. Equation (5.7) for the pressure flow factor along the x direction shows a crossover from impeded to enhanced flow along the rolling direction as γ increases through the critical value 2. Representative of asperities on either side of this crossover we have examined the isotropic case, $\gamma = 1$ and the case where asperity are longer in the flow direction by a factor $\gamma = 3$. The range of the film parameter Λ_{mo} studied is from 2 to 10, where $\Lambda_{mo} = h_{mo}/\sigma$, h_{mo} demotes the minimum film thickness for the contact operation with smooth surfaces.

Filmshape Effects

Values of the minimum and central film thickness as a function of Λ_{mo} for $\gamma = 1$ and $\gamma = 3$ are shown in figures 5.6 and 5.7. Values are normalized to the smooth value for comparison. (The same normalization procedure will be followed in studying the variation of pressure distribution and coefficient of friction. The smooth curves joining the computed points have been sketched simply to aid visualization.) For $\gamma = 1$ the minimum and central film thickness grows as Λ_{mo} becomes smaller, while for $\gamma = 3$ minimum and central film thickness decreases as Λ_{mo} becomes smaller. This trend is consistent with the results obtained by Tripp and Hamrock (1984) on line contact of incompressible lubricant but more pronounced. However, this significant filmshape effect agrees with their recent results (Tripp and Hamrock, 1985) on line contact of compressible lubricant by incorporating the improved elasticity calculation into the EHL numerical scheme. It is also noted that isotropic or transverse asperity has stronger effect than longitudinal asperity for the point contact case.

Pressure Effect

The variation of pressure spike under different values γ of Λ and is provided in figure 5.8. For $\gamma = 3$ the pressure spike grows as Λ_{mo} becomes smaller, while for $\gamma = 1$ pressure spike decreases as Λ_{mo} becomes smaller. The work of Tripp and Hamrock (1984) didn't observe any significant change in pressure

spike. A more recent work (Tripp and Hamrock, 1985) indicates that there are small variation in the line contact case of incompressible lubricant and slightly more variation in the line contact case of compressible lubricant.

Rolling Friction Effects

Results of the coefficient of rolling friction calculations based on equation (5.24) are plotted in figure 5.9. For $\gamma = 3$, rolling friction grows as Λ_{mo} becomes smaller, while for $\gamma = 1$, rolling friction grows as Λ_{mo} becomes larger. The logitudinal texture $\gamma = 3$ produces smaller change in μ. The result of Tripp and Hamrock (1984) on the line contact of incompressible lubricant indicate that rolling friction grows as becomes smaller for both $\gamma = 1$ and 3, longitudinal texture showing the larger effect. However, in their recent work on line contact of the compressible lubricant, it was found that rolling friction increases for isotropic or transverse roughness, but decreases for longitudinal roughness $\gamma > 2$, and the friction effect grows as Λ_{mo} becomes smaller. This trend is consistent with the results presented here.

5.4 Concluding Remarks

The flow factor model proposed by Patir and Cheng is adopted to study surface roughness effects on elastohydrodynamic lubrication of a point contact. The flow factors are obtained from Tripp's analytical approach.

The numerical method presented in Chapter 3 incorporating the improved elasticity calculation described in Chapter 4 is used to solved the modified Reynolds equation successfully. The system we have investigated is a compressible, isothermal, Newtonian fluid with Roelands viscosity entrained in pure rolling.

Results are obtained for a range of film parameter Λ_{mo} from 2 to 10. Anisotropy effects are included by studying both isotropic asperities $\gamma = 1$ and asperities three times longer on average in the flow direction than that transverse to it, $\gamma = 3$. The surface roughness effect on film shape, pressure distribution, and rolling friction are presented.

Chapter 6

PARCHED ELASTOHYDRODYNAMIC LUBRICATION

A starved subdivision of EHL was originally developed because the fully flooded numerical solution as applied to instrument ball bearings calculated films which were much too thick. A starvation correction for a reduced oil supply was constructed by assigning an arbitrary upstream location for the beginning of pressure build up (Orcutt and Cheng, 1966; Castle and Dowson, 1972). Calculated films indeed became thinner as the inlet miniscus was brought toward the Hertz area, and the correspondence was confirmed for film thickness measured by interferometry in a ball-on-plane geometry (Wedeven et al., 1971). As a result, most starved elastohydrodynamic calculations presently use some form of inlet miniscus position criterion.

However, the inlet miniscus position starvation, which is a steady state theory, cannot apply to instrument ball bearings. These have no inlet miniscus because they operate without any free bulk oil, and show long term transients in film thickness (Kingsbury, 1984). Since inlet miniscus position starvation has become entrenched in the literature (Hamrock and Dowson, 1981). It seems useful to define a parched elastohydrodynamic lubrication framework which would be able to accommodate at least instrument ball bearings.

Parched lubrication is used in instrument bearings for two reasons: the minimum torque demand and because the spin axis

defined in space by a pair of parched bearings is the most stable of any lubrication regime.

The work presented below was performed with Dr. E. Kingsbury of C.S. Draper Laboratory during his stay at NASA Lewis Reaearch Center as an NRC fellow.

6.1 Parched Transient

A ball bearing is parched if oil films are so thin outside the Hertz contacts that there is no flow under service accelerations. This is the situation in instrument bearings.

As described by Singleterry (1966), it is reasonable to say that oil films are immobile outside the Hertz areas in a parched bearing. This means that there is no inflow back into the Hertz track between ball passes in a parched bearing.

The oil under pressure inside a Hertz contact on the other hand is not immobile. It may be very viscous but as rolling continues it is gradually forced sideways out of the track. Since it is not replaced (absent a special oil replacement system), there is a long term transient in film thickness. Such transients in instrument ball bearings have been recognized for many years (Archibald and Blasingame, 1963; Horch, 1963). Neither fully flooded nor starved EHL theory allows for transients. Both calculate film thickness from material properties, geometry, and kinematics, using a steady state formulation; thickness is a time-constant dependent variable. In contrast, a parched EHL film

thickness is given or set as an independent variable at the start of a calculation or experiment.

6.2 Basic Speed Ratio

Basic speed ratio (BSR) is a characteristic number describing the kinematic configuration of an angular contact ball bearing. It is defined as

$$B = \dot{\delta}/S \tag{6.1}$$

where $\dot{\delta}$ is the ball spin angular velocity and S is the total speed of the bearing, i.e., the algebraic difference in race angular velocities. For perfect ball-race coupling and zero ball centrifugal force B is independent of bearing mode, i.e., inner, outer, counter, or joint rotation. For zero slip and no dynamic effects

$$B = \frac{d_m^2 - d_\ell^2 \cos^2 \beta}{2\, d_\ell\, d_m} \tag{6.2}$$

where the bearing geometry is defined by the pitch diameter d_m, the ball diameter d_ℓ and the zero load zero speed contact angel β. The first-order basic speed ratio is a function of geometry only.

The basic speed ratio can be measured extremely accurately in a bearing run in the counter race rotation mode at zero ball orbit rate. For stationary ball centers individual spin rates can easily be obtained to 1 part in 10^5, and the BSR computed from its definition. Since the first order BSR is a geometric constant, any measured change reflects some deviation from the

first order assumptions. This is useful for example in determining running conditions where specific assumptions break down, and in evaluating numerical modes of bearing performance (Kingsbury, 1984).

In a successful running bearing balls and races are separated by an EHL film. Since ball spin is driven by traction forces through this film, BSR gives a sensitive measurement of ball-lubricant-race coupling (Kingsbury, 1980). For perfect coupling (no lubricant, zero drag slip), BSR has a maximum value set by bearing geometry that decreases with increasing spin drag slip. Coupling, in turn, depends on film rheology and thickness.

6.3 Experimental Consideration

In the experiment to be described here a parched, retainerless 108 size bearing was run under pure axial load in the counter race rotation mode for zero ball orbit rate. No lubricant make up system was used so the oil lost from or modified within the Hertz areas was not replaced. The resulting transient in ball-lubricant-race coupling was followed by measuring the basic speed ratio of the bearing (Kingsbury, 1980).

An initial uniform parched EHL film can be established on bearing balls by taking them from a dilute solution of oil in a volatile solvent. Its thickness can be adjusted by changing concentration and estimated by weighing. The lubricant deposited in this way for these tests is SRG mineral oil.

Figure 6.1 shows the counter rotation fixture which was built for 108 size bearings. Table 6.1 gives measured geometry for the single 108 bearing which was used in all test. All tests were run at a total speed of 62 Hz (3720 rpm) and axial load of 1344 N. The resulting bearing operating parameters are given in table 6.2.

6.4 Observation

Figures 6.2 and 6.3 show transients found in the 108 bearing: basic speed ratio is plotted against time. The independent variable in the tests is the initial film thickness, $2*10^{-7}$ m for figure 6.2, and $8*10^{-8}$ m for figure 6.3.

General behavior in the two tests is the same: an initial decrease (not shown in fig. 6.2 because it was over too quickly to get a reading of speed ratio), a constant period, then a linear increase. The differences are an extreme time compression and generally higher levels of speed ratio for the thinner film.

The thin film test was stopped after 436 s because each ball, originally spinning about a fixed, stable axis, had begun to tumble. This is taken to show a significant change in the net surface traction moment applied to the ball through its EHL films (Dormgold and Klaus, 1968), a precursor of penetration and surface damage. No sign of tumbling was seen in the thick-film test, which was suspended after 20 000 s.

6.5 Discussion

The decreasing part of figure 6.2 is not understood. It has been seen in many other tests and is tentatively ascribed to some

average rearranging of the original film coverage, which is not really "uniform" after deposition.

The constant parts of figures 6.2 and 6.3 can be explained assuming they really show a small increasing trend which present measuring techniques for speed ratio are too coarse to resolve. They result as fluid oil pumped sideways out of the Hertz track under repeated high pressure transients. Oil is not replaced since there is no flow in a parched EHL film outside Hertzian contacts. Fluid mechanics (Kingsbury, 1973) or plasticity equations would describe transient thinning of a parched EHL film. In addition to the variable rheologic circumferential slip measured by basic speed ratio, an angular contact bearing always produces constant kinematic pivoting slips (Kingsbury, 1984). As the EHL film thins, shear rates due to this slip increase, concentrating mechanical shear energy into smaller and smaller Hertz volumes. When the concentration is high enough polymerization or oxidation reactions are activated, chemically (irreversibly) solidifying the lubricant. The linear increase in speed ratio (coupling) shown in figures 6.2 and 6.3 are attributed to this process (Kingsbury, 1978). The rate at which degradation reactions occur is proportional to $\exp(-Eh/Ttu)$, where E is an activation energy, T is a limiting shear stress, h is film thickness, u is (pivoting) slip velocity, and t is contact transient time. Reaction rate increases exponentially as thickness decreases, without any film penetration.

In the experiment degradation is detected by washing balls taken from a parched test with the solvent used to deposit virgin oil. The parched oil film is gone, inside and outside the Hertz track, but a light brown insoluble polymeric film remains. Diffuse light photographs then show the amount and placement of degradation product. The polymer is gone after wiping with a soft cloth, and there is no evidence of surface damage. The polymer was unpenetrated during running. This is one justification for separation of the parched and mixed EHL regimes.

6.6 Summary and Conclusions

Elastohydrodynamic lubrication does not go directly from starved to mixed, at least in instrument ball bearings. The intervening parched regime is characterized by zero lubricant flow outside the Hertz area, slow crossflow inside the Hertz area, and long term transients in film thickness. Parched EHL treats initial film thickness as an independent variable, in contrast to classical EHL which calculates thickness from other variables. Failure of a parched film is by oxidation or polymerization rather than by asperity penetration. The degradation reactions are activated by mechanical shear. Infinite steady state parched operation of a bearing therefore requires an oil makeup system with inflow adjusted to crossflow. Parched operation requires the least driving torque and gives the best spin axis definition possible in a given bearing.

CHAPTER 7

SUMMARY

The lubrication of nonconformal contacts is characterized by poor conformity, low contact area, and high unit loading. The form of lubrication normally found in nonconformal contacts is elastohydrodynamic lubrication. Depending on the effects of the elastic deformation and the variation of the viscosity with pressure, four regimes of lubrication can be defined, isoviscous-rigid, isoviscous-elastic, piezoviscous-rigid, and piezoviscous-elastic. In this literature, several aspects of lubrication of nonconformal contacts are presented.

The first objective of this work is the development of representations of minimum film thickness results for piezoviscous-rigid regime of lubrication which carries the same measure of confidence as those already available for the other three regimes of lubrication. This does not only enable the minimum film thickness to be calculated with greater accuracy in the piezoviscous-rigid regime. It also completes the map of lubrication regimes of nonconformal contacts. The compressible Newtonian fluid with Roelands viscosity is considered. The extended set of solutions includes geometry effects where radius ratio less than 1 and the influence of lubricant entrainment direction. The results provide a basis for the analysis and design of a wide range of machine elements operating in the piezoviscous-rigid regime of lubrication.

The second major feature of this study is to propose a new numerical method of calculating elastic deformation in contact stresses. The improved elastic deformation calculation uses a biquadratic polynomial to approximate the pressure distribution on the whole domain analyzed, and the deformation of every node is expressed as a linear combination of the nodal pressures whose coefficients can be combined into an influence coefficient matrix. This approach has the advantages of higher numerical accuracy, less computing time and smaller storage size requirement for the influence matrix.

The third purpose of this study is to extend the ideal elastrohydrodynamic lubrication to the real bearing systems in order to get a better understanding of the failure mechanism in machine elements. The improved elastic deformation calculation is successfully incorporated into the EHL numerical scheme. Using this revised numerical technique, surface roughness effects on the elastohydrodynamic lubrication of point contact is studied as an attempt to extend the ideal elastohydrodynamic lubrication to the real bearing systems. The flow factor model is adopted to study surface roughness effect on the elastohydrodynamic lubrication of point contact. In this formulation, the actual flow between rough surfaces is equated to an averaged flow between nominally smooth surfaces, while parameters describing the roughness are included in the Reynolds equation through flow factors. The system selected is a compressible isothermal Newtonian fluid with

Roelands viscosity. Conditions typical of an EHL contact in the piezoviscous-elastic regime entrained in pure rolling on rough bearing are investigated. Results are presented demonstrating the effect of surface roughness on the film shape, pressure distribution, and rolling friction in a ball bearing.

Furthermore, the fourth phase of this work consists of experiments designed and conducted to study the transient EHL effects in instrument ball bearings. A parched subregime of elastohydrodynamic lubrication, lying between starved and mixed, is thereby proposed to describe instrument ball bearing behavior. The parched regime is characterized by zero lubricant flow outside the Hertz area, slow crossflow inside the Hertz area and long term transients in film thickness. A parched bearing has the least driving torque demand and best spin axis definition possible from any lubrication regime.

REFERENCES

Archard, J.F., and Cowking, E.W. (1965-1966) "Elastohydrodynamic Lubrication at Point Contacts," Proc. Inst. Mech. Eng., London, 180 (3B), 165-167.

Archibald, F.R., and Blasingame B.P. (1963) "The Jog Mechanism in Gyroscopes," Air, Space and Instruments, S. Lees, ed., McGraw-Hill, pp. 498-502.

Barus, C. (1893) "Isotherms, Isopiestics, and Isometrics Relative to Viscosity," Am. J. Sci., Vol 45, pp. 87-96.

Biswas, S., and Snidle, R.W., (1977) "Calculation of Surface Deformation in Point Contact EHD," ASME J. Lubr Tech., Vol. 99, No. 3, pp. 313-317.

Blok, H. (1952) "Discussion of Paper by E. McEwen" J. Inst. Petrol., Vol. 38, p. 683.

Brewe, D.E., Hamrock, B.J., and Taylor, C.M. (1979) "Effect of Geometry on Hydrodynamic Film Thickness" ASME, J. Lubr. Tech., Vol. 101, No. 2, pp. 231-239.

Bush, A.W., Skinner, P.H., and Gibson, R.D. (1982) "Surface Roughness Effect in Point Contact Elastohydrodynamic Lubrication," Wear 83, pp. 285-301.

Cameron, A. (1985) "Righting a 40-year-old wrong": A.M. Ertel - the true author of 'Grubin's ehl' solution" Tribology International, Vol. 18, No. 2, pp. 92.

Christensen, H., and Tonder, K. (1971) "The Hydrodynamic Lubrication of Rough Bearing Surfaces of Finite Width," Journal of Lubrication Technology, Trans. ASME Series F, Vol. 93, p. 324.

Christensen, H., and Tonder, K. (1972) "Waviness and Roughness in Hydrodynamic Lubrication," Proc. Instn. Mech. Engrs., Tribology Grp., vol. 186, pp. 807.

Christensen, H., and Tonder, K. (1973) "The Hydrodynamic Lubrication of Rough Journal Bearings," Journal of Lubrication Technology, Trans. ASME Series F, p. 166.

Dalmaz, G. (1979) "Le film mince visqueux dans les contacts hertziens en regimes hydrodynamique et elastohydrodynamique" Docteur d'Etat Es sciences Thesis, I.N.S.A. Lyon.

Dowson, D., and Higginson, G.R. (1959) "A Numerical Solution to the Elastohydrodynamic Problem," J. Mech. Eng. Sci., Vol. 1, No. 1, pp. 6-15.

Dowson, D. (1962) "A Generalized Reynolds Equation for Fluid-Film Lubrication," Int. J. Mech. Sci. Pergamon Press Ltd., Vol. 4, pp. 159-170.

Dowson, D., and Whitaker, A.V. (1965) "The Isothermal Lubrication of Cylinder" ASLE Trans., Vol 8, No. 3, pp. 224-234.

Dowson, D., and Higginson, G.R. (1966) "Elastohydrodynamic Lubrication" Pergamon Press.

Dowson, D., and Hamrock, B.J., (1976) "Numerical Evaluation of the Surface Deformation of Elastic Solids Subjected to a Hertzian Contact Stress," ASLE Transactions, Vol. 19, No. 4, pp. 279-286.

Dowson, D., Dunn, J.F., and Taylor, C.M. (1983) "The Piezoviscous Fluid Rigid Solid Regime of Lubrication" Proc. Instn. Mech. Engrs., Vol 197c, pp. 43-52.

Dormgold, L.D., and Klaus, E.E. (1968) "The Physical And Chemical Characteristics of an Homologous Series of Instrument Oils," Bearings Conference Proceedings, Dartmouth College, Paper No. 9.

Elrod, H.G. (1977) "A Review of Theories for the Fluid Dynamic Effects of Roughness on Laminar Lubricating Films," Proc 4th Leeds-Lyon Symp on Tribology, Lyon, (D. Dowson, C.M. Taylor, M. Godet and D. Berthe, eds., Mechanical Engineering Publications, London, 1978), pp. 11-26.

Ertel, A.M. (1984) "Die Berechnung der hydrodynamischen Schmierung gekrummter oberflaschenron unter hoher Belastung und Relativbewegung," Fortschr.Ber. VDIZ., Reihe 1, No. 115.

Evans, H.P., and Snidle, R.W., (1981) "The Isothermal Elastohydrodynamic Lubrication of Spheres," ASME Journal of Lubrication Technology, Vol. 103, No. 4, pp. 547-557.

Evans, H.P., and Snidle, R.W., (1982) "The Elastohydrodynamic Lubrication of Point Contacts at Heavy Loads," Proc. Roy. Soc., (London), Series A, Vol. 382, pp. 183-199.

Fucik, S., Kratochvil, A., and Necas, J. (1975) "Kacanov's method and its application," Rev. Roum. Math. Pures et Appl., Vol. 20, pp. 907-916.

Grubin, A.N. (1949) "Fundamentals of the Hydrodynamic Theory of Lubrication of Heavily Loaded Cylindrical Surfaces," in Investigation of the Contact Machine Components, Kh. F. Ketova, ed. Translation of Russian Book No. 30, Central Scientific Institute for Technology and Mechanical Engineering, Moscow, Chap. 2. (Available from Dept. of Scientific and Industrial Research, Great Britain, Transl. CTS-235, and from Special Libraries Association, Chicago, Trans. r-3554.)

Hamrock, B.J., and Dowson, D. (1974) "Numerical Evaluation of Surface Deformation of Elastic Solids Subjected to Hertzian Contact Stress," NASA TN D-7774.

Hamrock, B.J., and Dowson, D., (1976a) "Isothermal Elastohydrodynamic Lubrication of Point Contacts, Part I-Theoretical Formulation," ASME J. Lubr. Tech., Vol. 98, No. 2, pp. 223-229.

Hamrock, B.J., and Dowson, D. (1976b) "Isothermal Elastohydrodynamic Lubrication of Point Contacts, Part II-Ellipticity Parameter Results," ASME J. Lubr. Tech., 98 (3), 375-378.

Hamrock, B.J., and Dowson, D. (1977a) "Isothermal Elastohydrodynamic Lubrication of Point Contacts, Part III-Fully Flooded Results," ASME J. Lubr. Tech., 99 (2), 264-276.

Hamrock, B.J., and Dowson, D. (1977b) "Isothermal Elastohydrodynamic Lubrication of Point Contacts, Part IV-Starvation Results," ASME J. Lubr. Tech., 99 (1), 15-23.

Hamrock, B.J., and Dowson, D. (1978) "Elastohydrodynamic Lubrication of Elliptical Contacts for Materials of Low Elastic Modulus, Part I-Fully Flooded Conjunction," ASME J. Lubr. Tech., 100 (2), 236-245.

Hamrock, B.J., and Dowson, D. (1979a) "Elastohydrodynamic Lubrication of Elliptical Contacts for Materials of Low Elastic Modulus, Part II-Starved conjunction," ASME J. Lubr. Tech., 101 (1), 92-98.

Hamrock, B.J., and Dowson, D. (1979b) "Minimum Film Thickness in Elliptical Contacts for Different Regimes of Fluid-Film Lubrication," in Proceedings of Fifth Leeds-Lyon Symposium on Tribology on 'Elastohydrodynamics and Related Topics,' D. Dowson, C.M. Taylor, M. Godet, and D. Berthe, eds., Mechanical Engineering Publications, Bury ST. Edmunds, Suffolk, 22-27.

Hamrock, B.J., and Dowson D. (1981) "Ball Bearing Lubrication - The Elastohydrodynamics of Elliptical Contacts", John Wiley and Sons, New York.

Hirst, W., and Moore, A.J. (1979) "Elastohydrodynamic Lubrication at High pressure, Part 2 Non-Newtonian Behavior", Proc. R. Soc., London, A. No. 365, pp. 537-565.

Horsch, J.D. (1963) "Correlation of Gyro Spin Axis Ball Bearing Performance with the Dynamic Lubricating Film," ASLE Trans., Vol. 6, No. 2, pp. 112-124.

Houpert, L.H. (1984) "The Film Thickness in Piezoviscous Regime; Film thickness Lubrication Regimes Transition Criteria" ASME, J. Lubr. Tech., Vol. 106, No.3, pp. 375-385.

Houpert, L.G., and Hamrock, B.J. (1985) "Fast Approach for Calculating Film Thickness and Pressure in Elastohydrodynamically Lubricated Contacts at High Loads," Submit to ASME and ASLE joint conference, Atlanta, Georgia.

Jeng, Y.R., Hamrock, B.J., and Brewe, D. (1985) "Piezoviscous Effects in Nonconformal Contacts Lubricated Hydrodynamically", presented at the ASLE annual meeting, Las Vegas, Nevada, May 6-9. To appear.

Jones, W. R., and Winer, W.O., et al. (1975) "Pressure-Viscosity Measurements for Several Lubricants to $5.5*10^8$ Newtons per Square Meter ($8*10^4$ psi) and 149 C (300 F)" ASLE Trans., Vol. 18, No. 4, pp. 249-262.

Kapitza, P.L. (1955) "Hydrodynamic Theory of Lubrication during Rolling" Zh. Tekh. Fiz., Vol. 25, No. 4, pp. 747-762.

Kingsbury, E. (1973) "Cross Flow in a Starved EHD Contact," ASLE Trans., Vol. 16, No. 4, pp. 276-280.

Kingsbury, E. (1978) "Lubricant Breakdown in Instrument Ball Bearings," ASME J. Lubr. Tech. Tech., Vol. 100, No. 3, pp. 386-394.

Kingsbury, E. (1980) "Dynamic and Coupling Influences on Basic Speed Ratio of an Angular Contact Ball Bearing," Wear, Vol. 63, pp. 189-196.

Kingsbury, E. (1982) "Ball Motion Perturbation in an Angular Contact Ball Bearing," ASLE Trans., Vol. 25, No. 3, pp.279-282.

Kingsbury, E. (1984a), "Transient Effects in Starved Ball Bearings," NASA Conference Publication 2300, Vol. II, pp. 641-663.

Kingsbury, E. (1984b) "Pivoting and Slip in an Angular Contact Ball Bearing," ASLE Trans., Vol. 27, No. 3, pp. 259-262.

Markho, P.A., and Clegg, D.B. (1979) "Reflection on Some Aspects of Lubrication of Concentrated Line Contacts" ASME, J. Lubr. Tech., Vol. 101, pp. 528-531.

Martin, H.M. (1916) "The Lubrication of Gear Tooth" Engineering (London), Vol. 102, pp. 119-121.

Meuleman, P.K., Lubrecht, A.A., and Napel, W.E. (1985) "Traction in Elastohydrodynamic Lubrication- High Contact Pressure Experiments and a Thrmal Roelands-Eyring-Maxwell Model" Research Report nr. WB, Twente University of Technology, The Netherlands.

Orcutt, F.K., and Cheng, H.S. (1966) "Lubrication of Rolling Contact Instrument Bearings," Gyro Spin Axis Hydrodynamic Bearing Symposium, Vol. 2, MIT Instrumentation Laboratory, Paper No. 5.

Patir, N., and Cheng, H.S. (1978) "An Average Flow Model for Determining Effects of Three-Dimensional Roughness on Partial Hydrodynamic Lubrication," ASME J. Lubr. Tech., 100; pp. 12-17.

Patir, N., and Cheng, H.S. (1979) "Effect of Surface Roughness Orientation on the Central Film Thickness in E.H.D. Contacts," Proc 5th Leeds-Lyon Symp on Tribology, Leeds, (D. Dowson, C.M. Taylor, M. Godet and D. Berthe, eds., Mechanical Engineering Publications, London) pp. 15-21.

Ranger, A.P., Ettles, C.M.M., and Cameron, A., (1975) "The Solution of the Point Contact Elastohydrodynamic Problem," Proc. Roy. Soc., (London), Series A, Vol. 346, pp. 227-244.

Reynolds, O. (1886) "On the Theory of Lubrication and Its Application to Mr. Beauchamp Tower's Experiments, Including an Experimental Determination of the Viscosity of Olive Oil," Philos. Trans. R. Soc. London, 177, 157-234.

Roelands, C.J.A. (1966) "Correlational Aspect of the Viscosity-Temperature-Pressure Relationship of Lubricating Oils" Druk V.R.B., Groningeon, Netherlands.

Singleterry, C.R. (1966) "Some Factors Affecting the Movement of Oil Over Metal Surfaces," Gyro Spin Axis Hydrodynamic Bearing Symposium, Vol. 2, MIT Instrumentation Laboratory, Paper no. 12.

Timoshenko, S., and Goodier, J.N. (1951) Theory of Elasticity, McGraw-Hill.

Tower, B. (1883) "First Report on Friction Experiments (Friction of Lubricated Bearings)," Proc. Inst. Mech. Eng., London, 632-659.

Tripp, J.H. (1983) "Surface Roughness Effects in Hydrodynamic Lubrication: The Flow Method," ASME J. Lub. Tech., Vol 105, pp. 458-465.

Tripp, J.H., and Hamrock, B.J. (1984) "Surface Roughness Effects in Elastohydrodynamic Contacts," Proc 11th Leeds-Lyon Sym. on Tribology, Lyon, (to appear).

Tripp, J.H., and Hamrock, B.J. (1985), To Appear.

Tzeng, S.T., and Saibel, E. (1967) "Surface Roughness Effect on Slider Bearing Lubrication," ASLE Trans, Vol. 10, pp. 334.

Wedeven, L.D., Evans, D., and Cameron, A. (1971) "Optical Analysis of Ball Bearing Starvation," ASME Journal of Lubrication Technology, Vol. 93, No. 3, pp. 349-363.

TABLE 3.1 - EFFECT OF DIMENSIONLESS LOAD PARAMETER ON MINIMUM FILM THICKNESS

Dimensionless load parameter	Minimum film thickness		Percentage Difference
	Obtained from computational result	Obtained from least square fit	
$W*10^7$	H_o*10^6	$\tilde{H}_o*10^6$	D
0.90971	4.1	4.13	0.77
0.89091	4.2	4.21	0.20
0.85159	4.4	4.38	-0.48
0.80860	4.6	4.78	-0.37
0.77376	4.8	4.76	-0.75
0.74467	5.0	4.93	-1.45
0.68766	5.2	5.29	1.64
0.65859	5.5	5.49	-0.18
0.64956	5.6	5.56	-0.77
0.63293	5.8	5.69	-1.98

TABLE 3.2 - EFFECT OF DIMENSIONLESS SPEED PARAMETER ON MINIMUM FILM THICKNESS

Dimensionless speed parameter	Dimensionless load parameter	Minimum Film Thickness		Percentage difference
		Obtained from computational result	Obtained from least square fit	
$U*10^{11}$	$W*10^{6}$	H_o*10^{6}	$\tilde{H}_o*10^{6}$	D
0.21883	0.11750	4.8	4.68	-2.56
0.20120	0.11009	4.8	4.83	0.72
0.18516	0.88950	4.8	4.84	0.76
0.16833	0.77377	4.8	4.85	0.96
0.15150	0.67629	4.8	4.77	-0.53
0.13466	0.58454	4.8	4.68	-2.58

TABLE 3.4 - EFFECT OF DIMENSIONLESS MATERIALS PARAMETER ON MINIMUM FILM THICKNESS

Solid material	Lubricant	Dimensionless parameter			Minimum film thickness		Percentage difference
		Materials	Speed	Load	Obtained from computational result	Obtained from least square fit	
		G	$U*10^{11}$	$W*10^{7}$	H_o*10^{6}	$\bar{H}_o*10^{6}$	D
Steel	Paraffinic	4522	0.16832	0.77376	4.8	4.681	-2.48
Bronze	Paraffinic	2310	0.32957	1.51499	4.8	4.682	-2.45
Silicon nitride	Paraffinic	6785	0.11218	0.51571	4.8	4.682	-2.45
Steel	Naphthenic	7031	0.48123	1.18602	1.4	1.441	2.92
Bronze	Naphthenic	3591	0.94227	2.32216	1.4	1.441	2.92
Silicon nitride	Naphthenic	10549	0.32073	0.79047	1.4	1.441	2.92

TABLE 3.3 - EFFECT OF ELLIPTICITY PARAMETER ON MINIMUM FILM THICKNESS

Radius ratio	Dimensionless load parameter	Minimum film thickness		Percentage difference
		Obtained from computational result	Obtained from least square fit	
α	$W*10^6$	H_o*10^6	$\tilde{H}_o*10^6$	D
64	1.61064	4.8	4.805	0.10
61	1.59341	4.8	4.804	0.09
59	1.56632	4.8	4.828	0.58
58	1.55278	4.8	4.842	0.89
54	1.49756	4.8	4.900	2.09
49	1.42381	4.8	4.969	3.52
42	1.13262	4.8	5.044	5.09
34	1.17520	4.8	5.065	5.52
30	1.09985	4.8	5.039	4.99
27	1.04072	4.8	4.994	4.04
20	0.88157	4.8	4.669	-2.83
18	0.83509	4.8	4.691	-2.27
16	0.77377	4.8	4.615	-3.84
12	0.60153	4.8	4.636	-3.42
10	0.53541	4.8	4.764	-7.57
8	0.45598	4.8	4.236	-11.66
4	0.28576	4.8	3.445	-28.22
1	0.12031	3.0	1.953	-34.91
0.8	0.09028	3.0	2.019	-32.70
0.6	0.09548	2.0	1.447	-27.65
0.4	0.05424	2.0	1.593	-20.36
0.2	0.02073	1.5	1.874	24.23

TABLE 3.5 - EFFECT OF LUBRICANT ENTRAINMENT DIRECTION ON MINIMUM FILM THICKNESS

Lubricant entrainment direction	Dimensionless load parameter	Minimum film thickness		Percentage diffenence
		Obtained from computational result	Obtained from least square fit	
θ	$W*10^6$	H_o*10^6	$\bar{H}_o*10^6$	D
0	0.14965	5.6	5.60	-0.00
5	0.14841	5.6	5.56	-0.69
10	0.14532	5.6	5.54	-1.03
15	0.14043	5.6	5.52	-1.49
20	0.13427	5.6	5.50	-1.80
25	0.12708	5.6	5.50	-1.80
30	0.11941	5.6	5.54	-1.14
35	0.11902	5.6	5.60	-0.00
40	0.10200	5.6	5.49	-1.94
45	0.09278	5.6	5.33	-4.88

TABLE 3.6 - DATA SHOWING EFFECT OF LOAD, SPEED, RADIUS RATIO MATERIAL PARAMETER AND LUBRICANT ENTRAINMENT DIRECTION ON MINIMUM FILM THICKNESS

Case	Dimensionless load parameter	Dimensionless speed parameter	Radius ratio	Dimensionless materials parameter	Lubricant entrainment direction	Minimum film thickness		Percentage difference	Results
						Obtained from computational results	Obtained from least square fit		
	$W*10^7$	$U*10^{11}$	a	G	ø	H_0*10^6	H_0*10^6	D	
1	0.00971	0.16033	16	4522	0	4.1	4.13	0.72	Load
2	0.00971					4.2	4.21	0.24	
3	0.05159					4.4	4.38	-0.47	
4	0.00860					4.6	4.58	-0.38	
5	0.77376					4.8	4.76	-0.74	
6	0.74467					5.0	4.93	-1.44	
7	0.68746					5.2	5.11	-1.65	
8	0.65055					5.5	5.49	-0.17	
9	0.64956					5.6	5.56	-0.76	
10	0.63293					5.8	5.69	-1.97	
11	1.17505	0.21862				4.0	4.60	-4.20	Speed plus case 5
12	1.00859	0.20120					4.35	-0.94	
13	0.88950	0.18516					4.39	-0.94	
14	0.67625	0.15150					4.69	-2.20	
15	0.58454	0.13466					4.60	-4.22	
16	1.51499	0.32951		2310			4.64	-0.33	Material plus case 5
17	0.5357	0.11218		6765			4.64	-2.33	
18	0.11866	0.48123		703		1.4	1.38	-2.14	
19	2.32216	0.9422		359			1.38	-2.14	
20	0.78047	0.32078		10544			1.38	-2.14	
21	1.61064	0.16033	64	4522		4.8	4.96	3.32	Radius ratio plus case 5
22	1.59341		6				4.95	3.13	
23	1.56637		59				4.98	3.02	
24	1.55276		58				4.99	4.14	
25	1.49756		54				5.06	5.37	
26	1.42381		49				5.13	6.85	
27	1.33262		42				5.21	8.47	
28	1.17520		34				5.22	8.92	
29	1.09885		30				5.20	8.37	
30	1.04[illegible]		28				5.15	7.36	
31	0.88157		20				4.94	2.92	
32	0.83509		18				4.84	0.88	
33	0.62153		12				4.77	-0.72	
34	0.5354		10				4.44	-3.64	
35	0.45598		8				4.38	-4.82	
36	0.29571		4				3.56	-25.9	
37	0.12037					3.0	2.02	-32.82	
38	0.09078	0.0				3.0	2.08	-30.53	
39	0.05548	0.0				2.0	1.50	-25.23	
40	0.05424	0.0				2.0	1.66	-17.20	
41	0.02013	0.0				1.5	1.94	29.65	
42	1.49645	0.75745	20		0	5.6	5.51	1.60	Lubricant entrainment direction
43	1.48427				5		5.55	0.85	
44	1.45318				10		5.53	1.25	
45	1.4043				15		5.50	1.78	
46	1.34264				20		5.49	1.98	
47	1.27083				25		5.48	2.14	
48	1.19408				30		5.52	1.42	
49	1.10916				35		5.58	0.30	
50	1.02002				40		5.5[illegible]	-1.65	
51	0.92715				45		5.34	-4.64	
52	0.10874	0.25745	16		C	5.8	5.89	1.55	
53	0.1400	0.53[illegible]	20			15.5	14.5	-6.45	

TABLE 3.7 - COMPARISON BETWEEN THE PRESENT RESULT AND THE EQUATION PROPOSED BY HOUPERT

Case	$\frac{H_o \text{ (Houpert)}}{H_o \text{ (Jeng)}}$
1	1.52
2	1.50
3	1.42
4	1.38
10	1.20
11	1.54
12	1.46
13	1.40
16	1.34
17	1.34
18	1.28
19	1.28
20	1.28
21	1.37
24	1.36
30	1.35
34	1.36
37	0.969
38	0.968
39	0.927

TABLE 4.1 - COMPARISON OF THE ELASTIC DEFORMATIONS OBTAINED WITH TWO METHODS (UNIT CM)

[$E = 21.97$ MN/cm; $R_x = R_y = 0.5558$ cm; $F = 8.964$ N]

NX	NY	$\frac{d_{max}}{d_{Hertz}} - 1$		Δh_{max}	
		H D	New Approach	H D	New Approach
15	15	1.183×10^{-2}	1.225×10^{-3}	1.652×10^{-6}	8.173×10^{-7}
19	19	6.329×10^{-3}	2.161×10^{-4}	1.264×10^{-6}	6.042×10^{-7}
31	31	2.448×10^{-3}	1.320×10^{-5}	6.888×10^{-7}	3.042×10^{-7}

H D: Hamrock and Dowson (1974)

TABLE 5.1 - MATERIAL AND LUBRICANT PROPERTIES FOR THE ILUSTRATIVE EXAMPLES

ELASTIC MODULUS OF STEEL BALLS, E		2.00×10^{11}	N/m^2
POISSON'S RATIO FOR STEEL, ν		0.3	
INLET VISCOSITY OF PARAFFINIC LUBRICANT, η_0		4.11×10^{-2}	Ns/m^2
CONSTANTS IN ROELANDS MODEL, η_∞		6.31×10^{-5}	Ns/m^2
	Y_c	1.96×10^{8}	N/m^2
ROELANDS VISCOSITY-PRESSURE INDEX, Z		0.67	
EFFECTIVE BALL RADIUS, R_x		1.11125×10^{-2}	m
SPECIFIC LOADING OF BALLS, F		8.5	N
ROLLING SPEED, u_x		1.0×10^{-1}	m/s
DIMENSIONLESS EHL PARAMETERS,	U	1.683×10^{-12}	
	W	3.134×10^{-7}	
	G	4522.2	
	H_{mo}	6.4237×10^{-6}	
	k	6	
	θ	0	

TABLE 6.1 - 108 BEARING GEOMETRY

Bore	0.04 m (1.57 in.)
Ball diameter	9.53×10^{-3} m (0.375 in.)
Pitch diameter	5.273×10^{-2} m (2.076 in.)
Contact angle	15.67 degrees
Inner cross race curvature	0.54
Outer cross race curvature	0.58
Ball complement	17

TABLE 6.2 - BEARING OPERATING PARAMETERS

Mean Hertz stress	1×10^{9} N/m (150000 psi)
Inner major Hertz width	1.38×10^{-3} m (0.054 in.)
Inner ellipticity ratio	6.16
Outer major Hertz width	1.01×10^{-3} m (0.04 in.)
Outer ellipticity ratio	3.26
Nominal ball spin rate	167 Hz (10000 rpm)
Nominal inner race rate	36 Hz (2160 rpm)
Nominal outer race rate	26 Hz (1560 rpm)
Total ball-race pivoting rate	6.13 Hz (363 rpm)
Entrainment velocity	5 m/s (197 in/s)

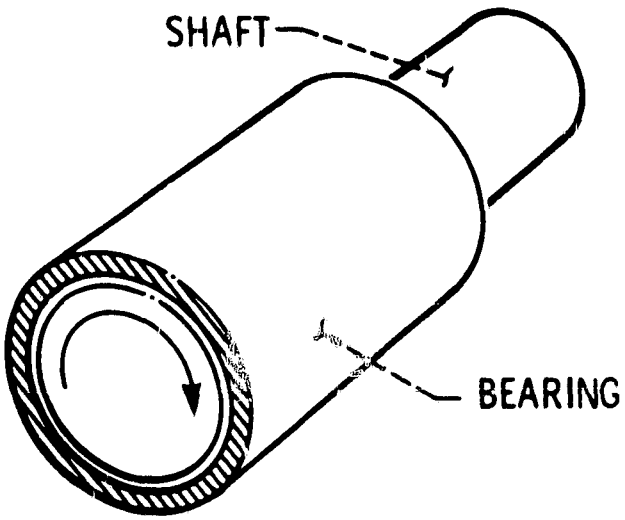

SLIDING SURFACE BEARING. HIGH CONFORMITY, LARGE EFFECTIVE CONTACT AREA AND LOW UNIT LOADING

Figure 1.1. - Conformal surfaces.

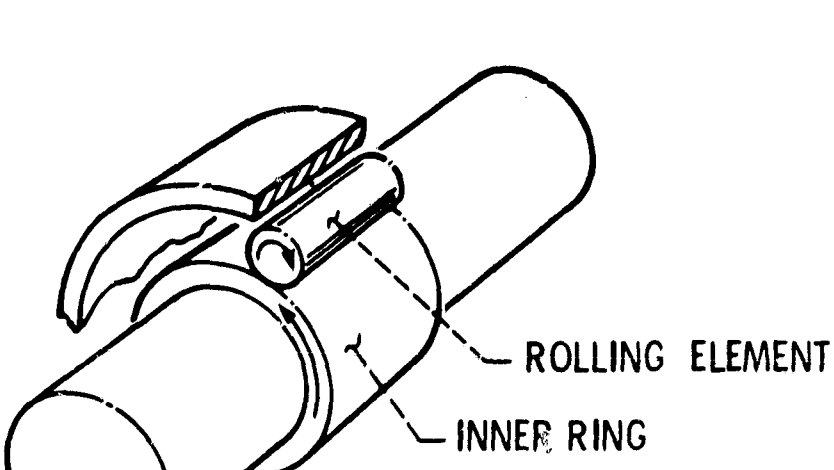

ROLLING ELEMENT BEARING. POOR CONFORMITY, SMALL CONTACT AREA, HIGH UNIT LOADING

Figure 1. 2. - Nonconformal surfaces.

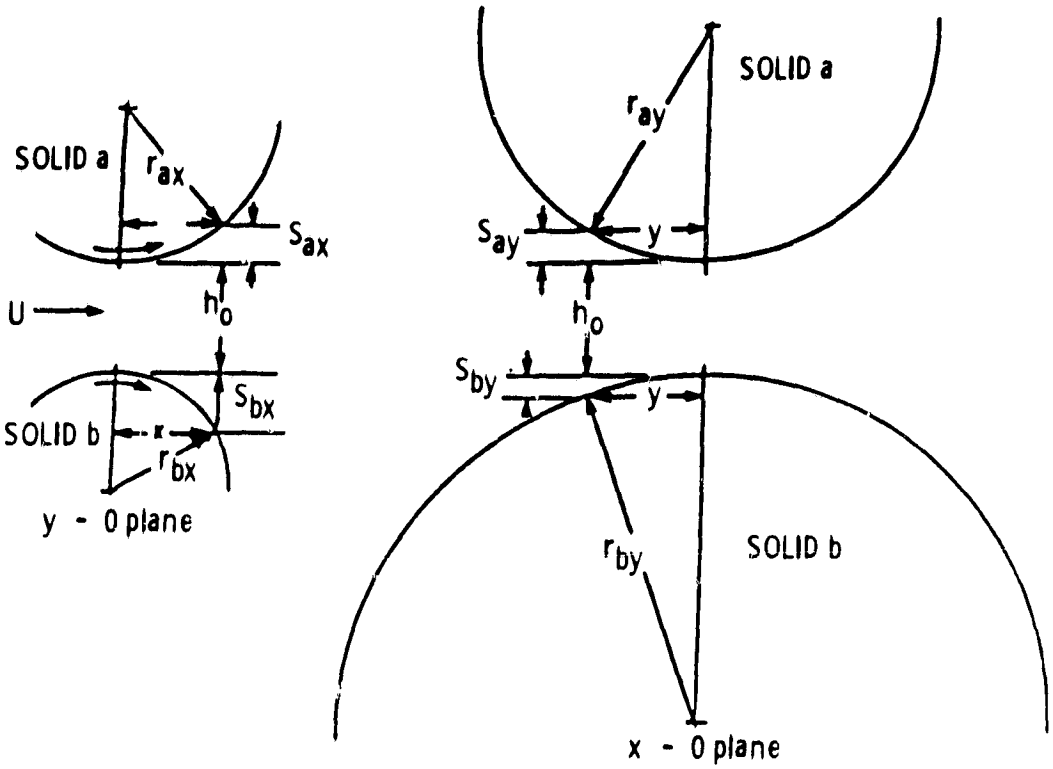

(a) Two rigid solids separated by a lubricant film.

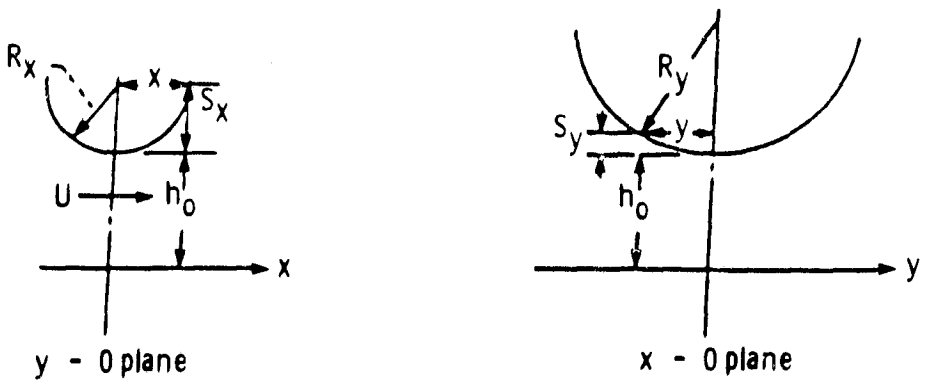

(b) Equivalent system of a rigid solid near a plane separated by a lubricant film.

Figure 2.1 Contact geometry.

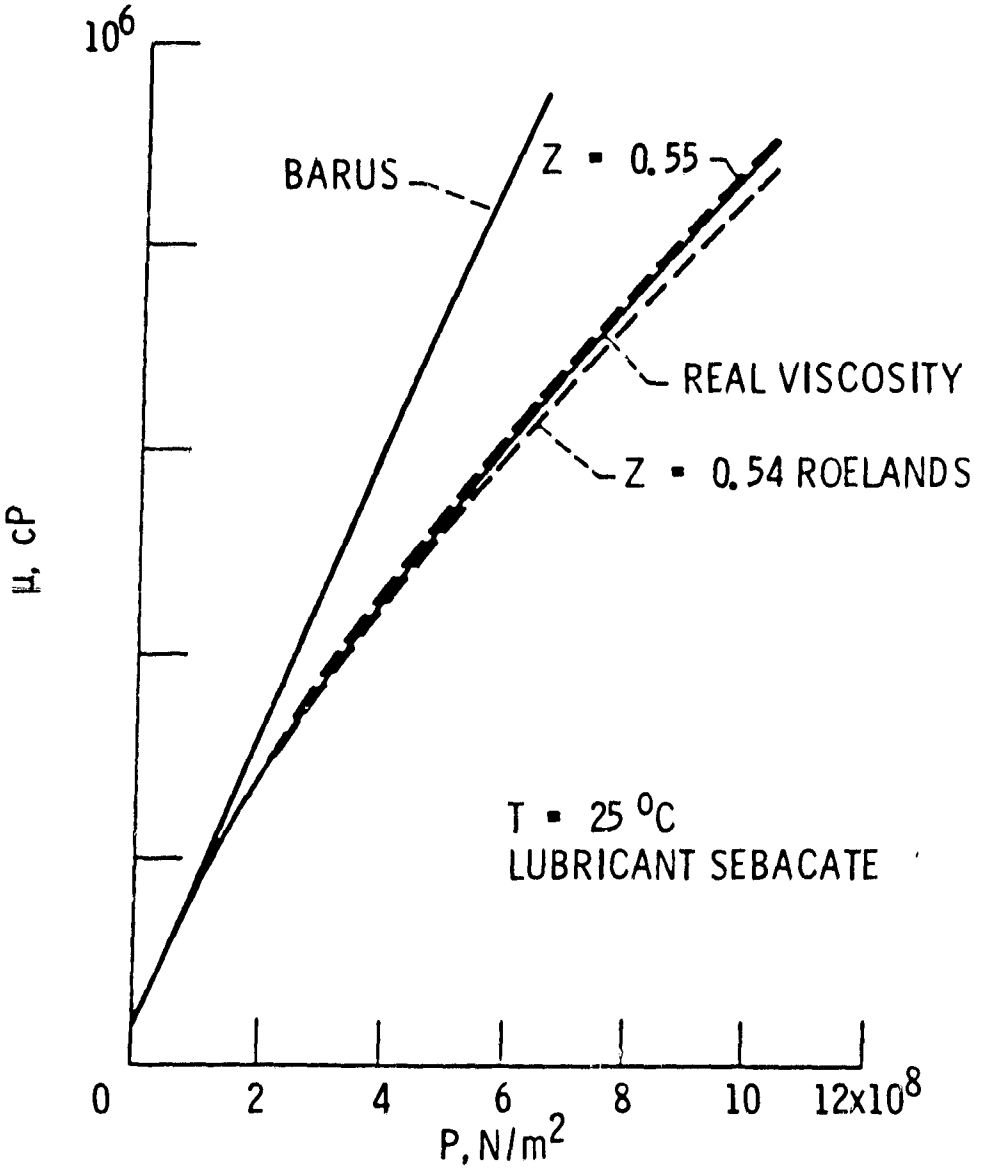

Figure 3.1 Viscosity as a function of pressure.

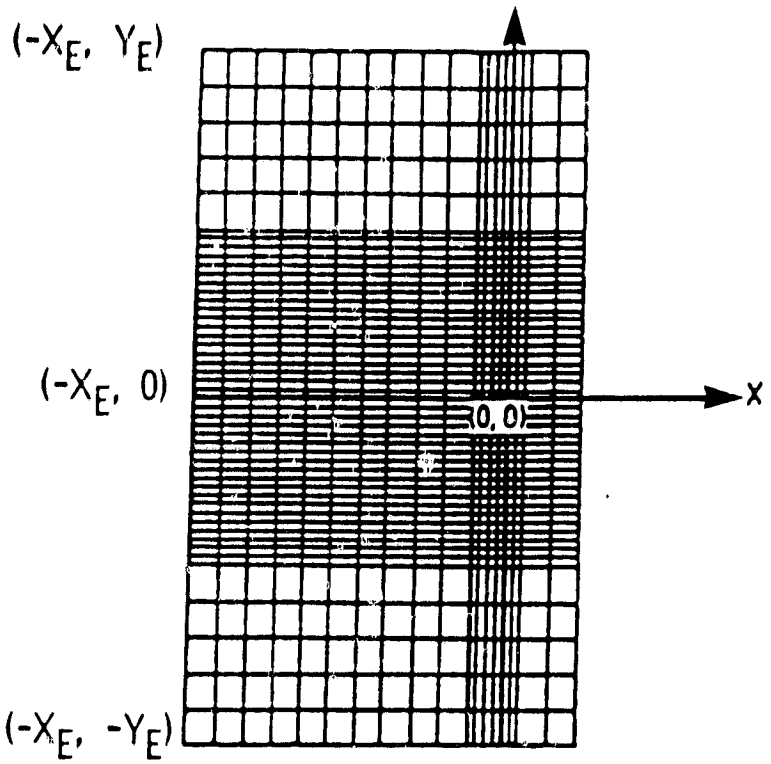

Figure 3.2 Variable nodal structure used for numerical calculations.

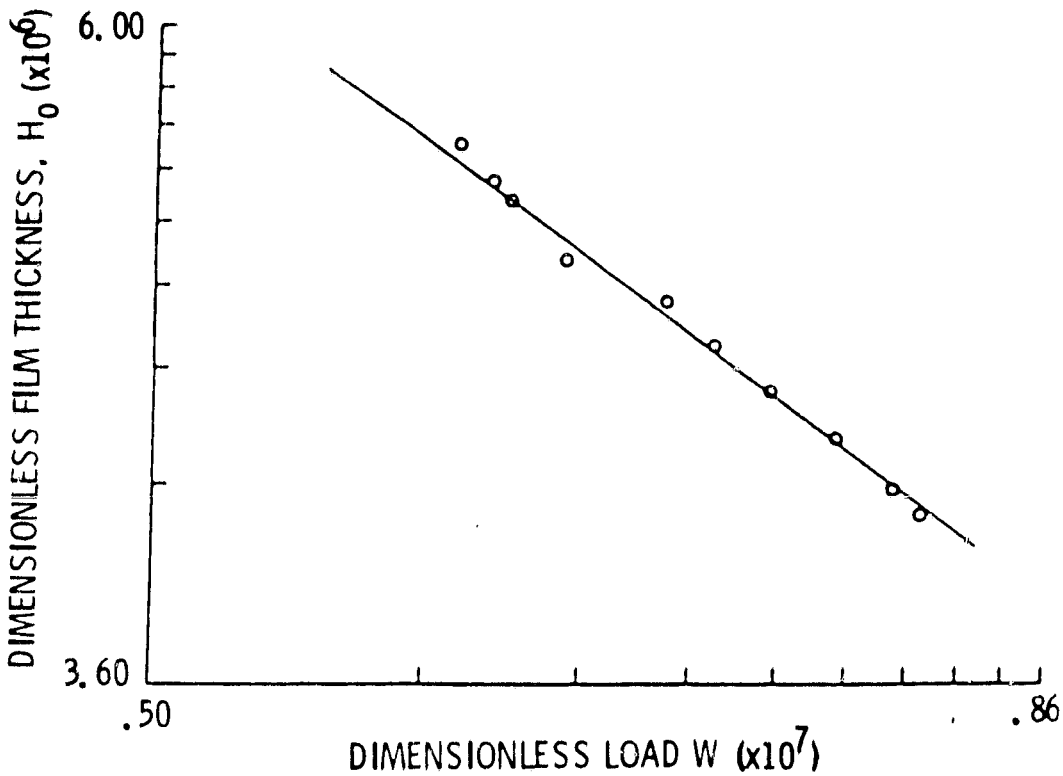

Figure 3.3 The variation of dimensionless minimum film thickness with dimensionless load.

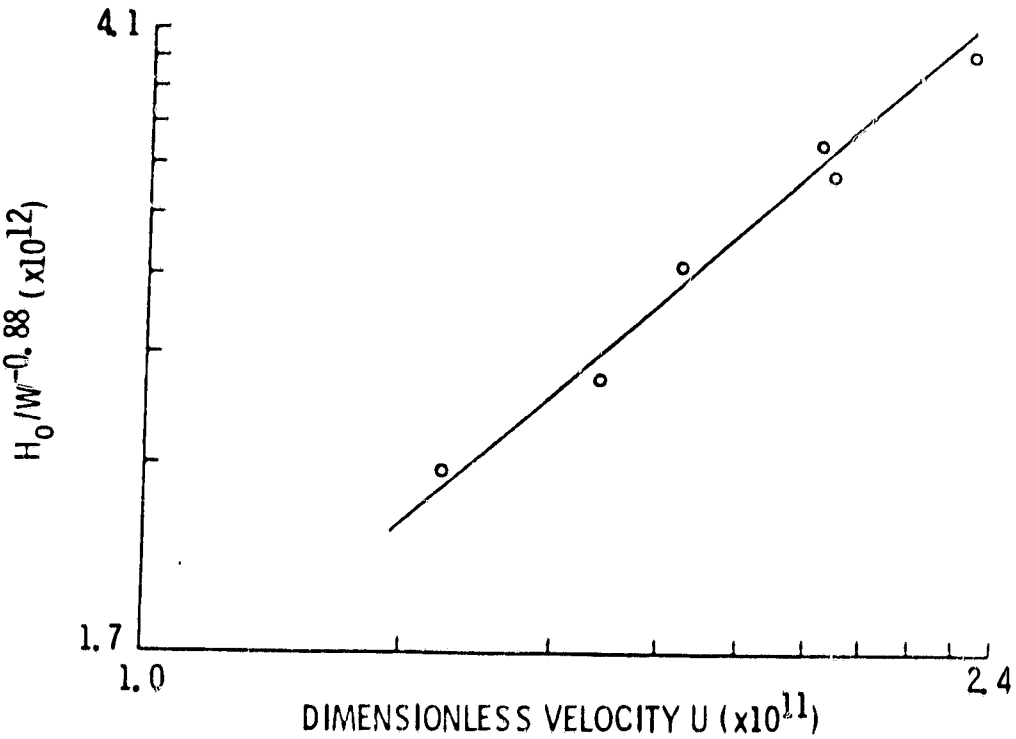

Figure 3.4 The variation of dimensionless minimum film thickness with dimensionless velocity.

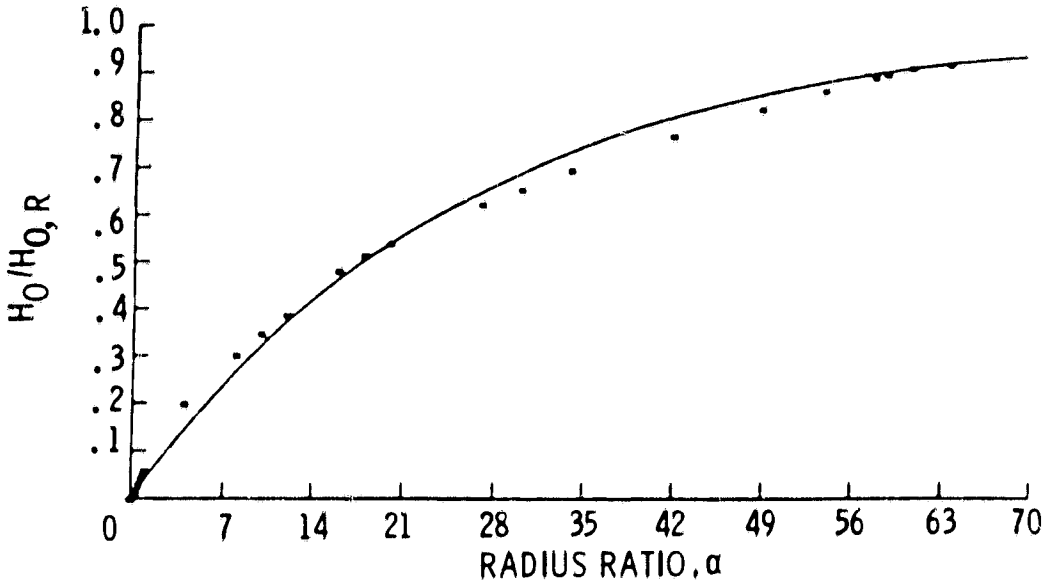

Figure 3.5 The influence of radius ratio on dimensionless minimum film thickness.

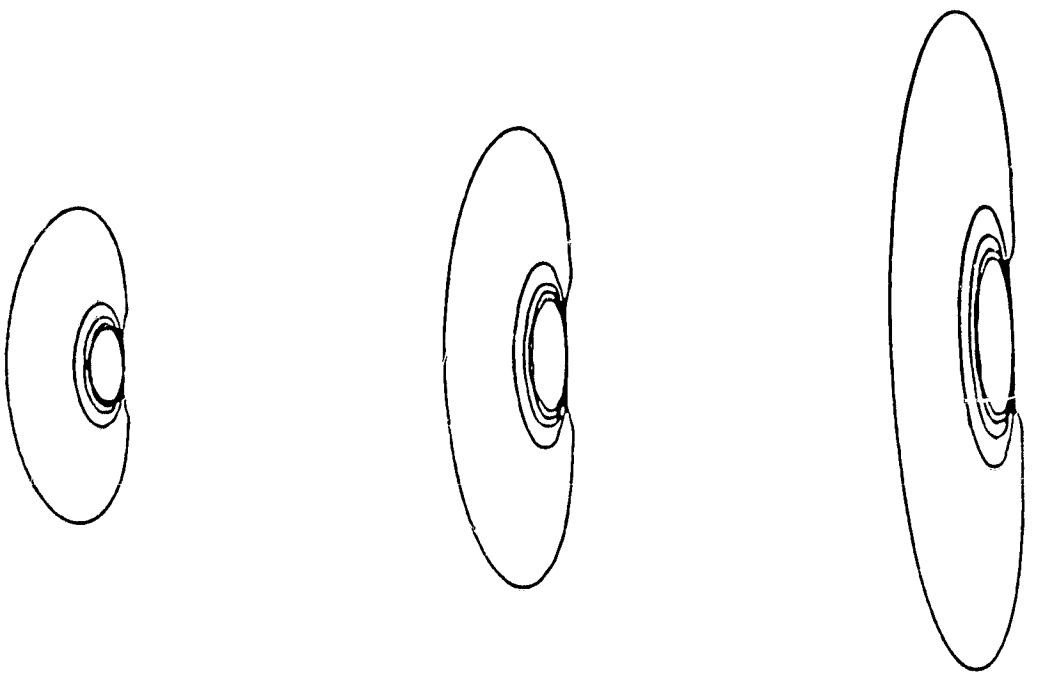

α = 4 α = 8 α = 16

Figure 3.6 Pressure contour for three radius ratios.

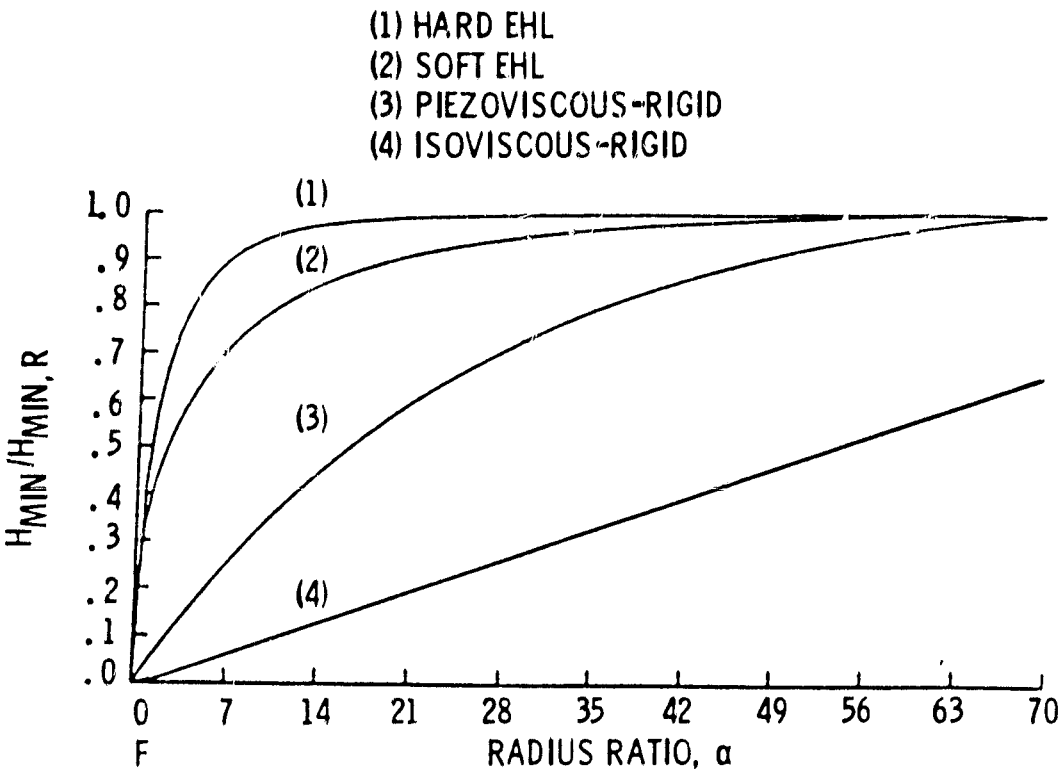

Figure 3.7 Comparison of the geometry effects in four different regimes of lubrication.

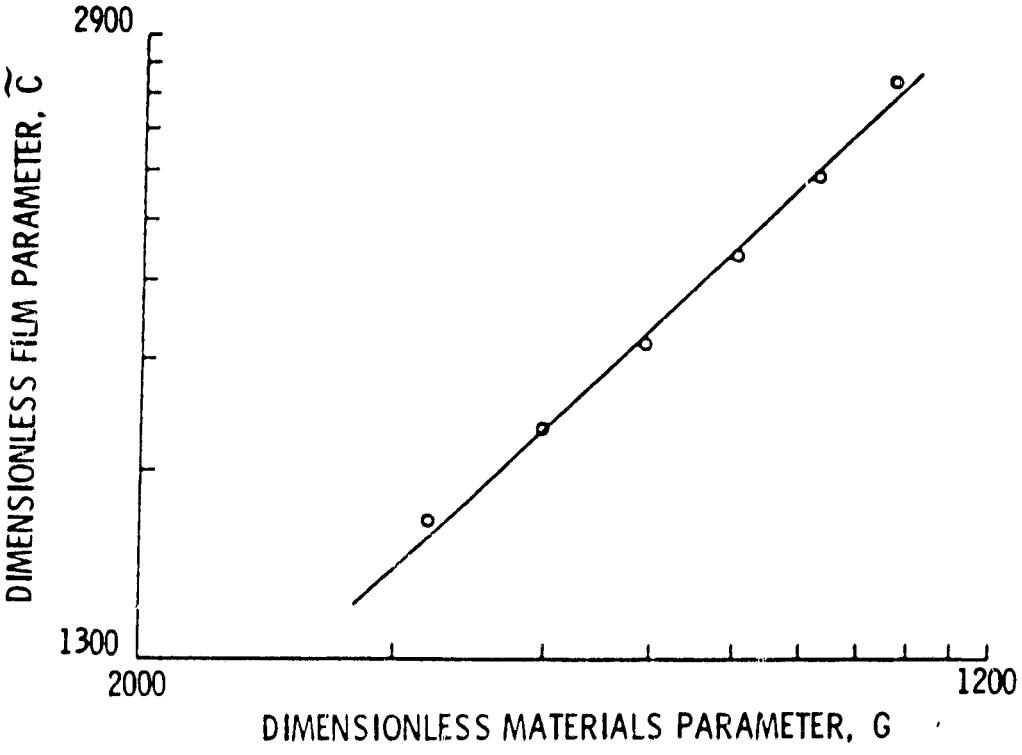

Figure 3.8 The variation of dimensionless minimum film thickness with dimensionless materials parameter.

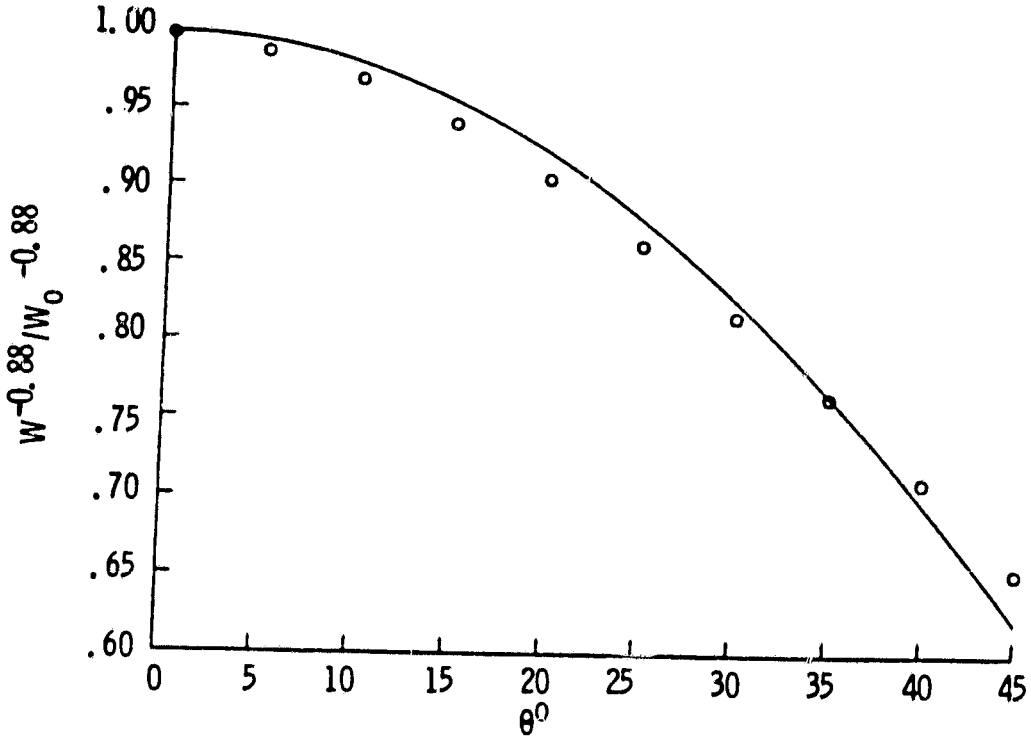

Figure 3.9 The variation of minimum film thickness with the lubricant entrainment direction.

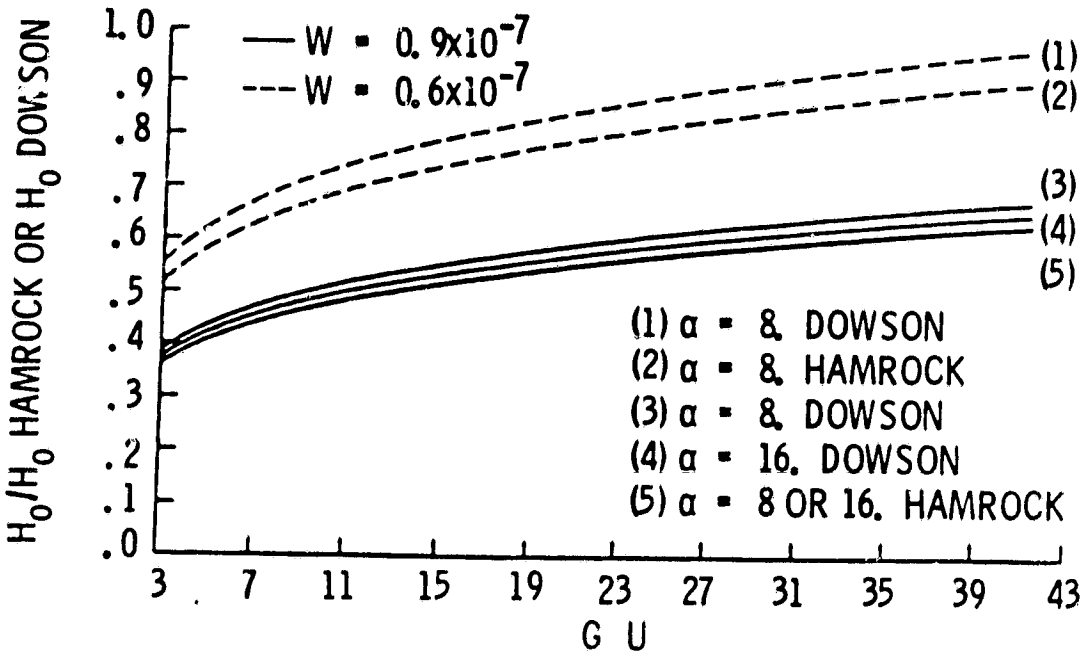

Figure 3.10 Comparison between different minimum film thickness formulae.

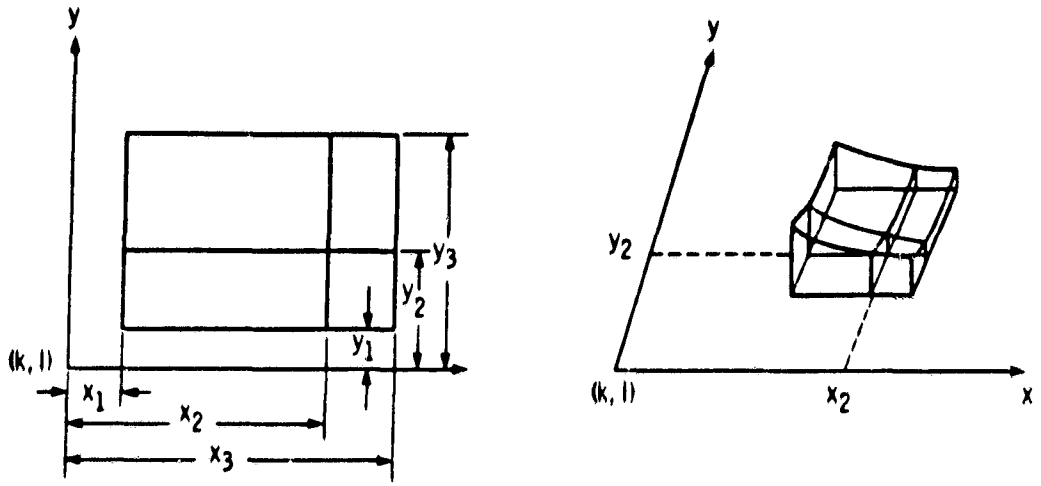

(a) Rectangular elements with nine nodes.

(b) Representation of pressure distribution by paraboloidal surfaces.

Figure 4.1 Coordinate system for the computing element.

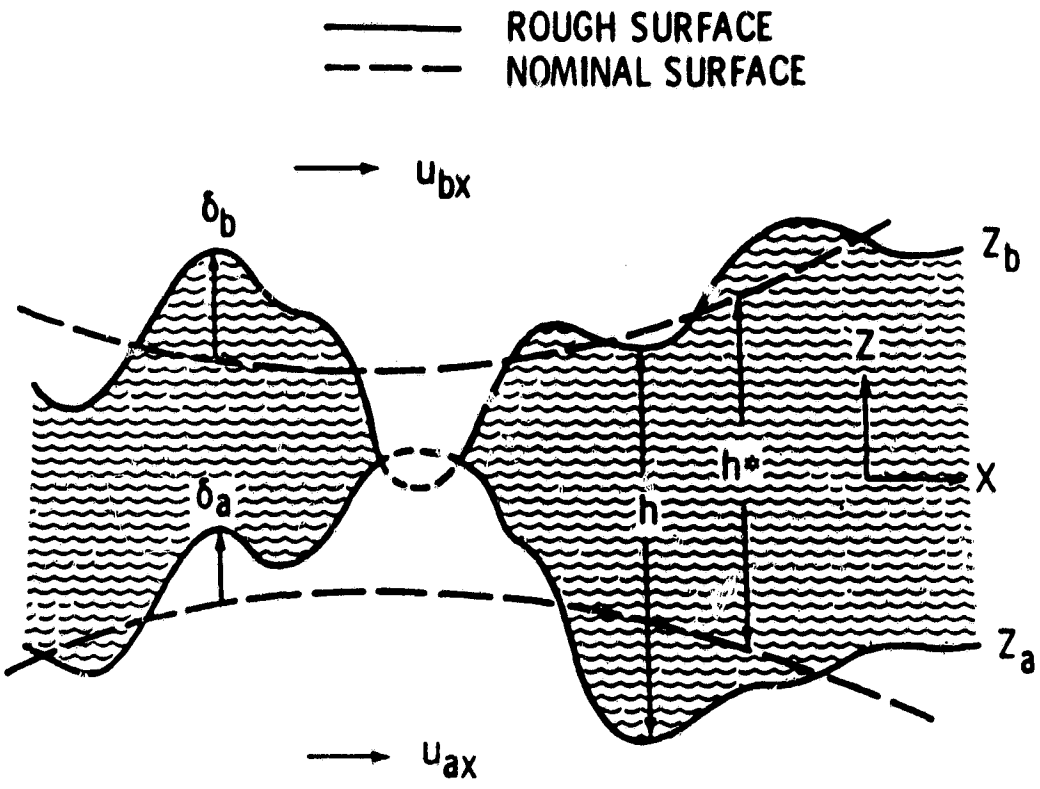

Figure 5.1 Lubrication of moving rough surfaces.

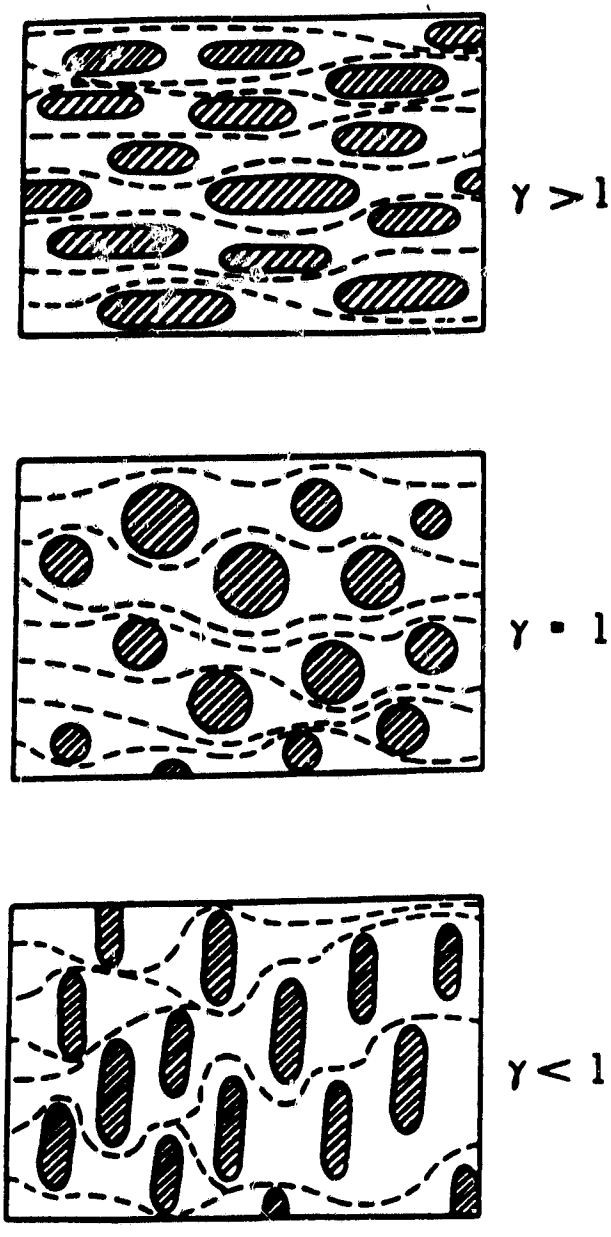

Figure 5.2 Typical contact areas for longitudionally oriented ($\gamma > 1$), isotropic ($\gamma = 1$) and transversely oriented ($\gamma < 1$) surfaces.

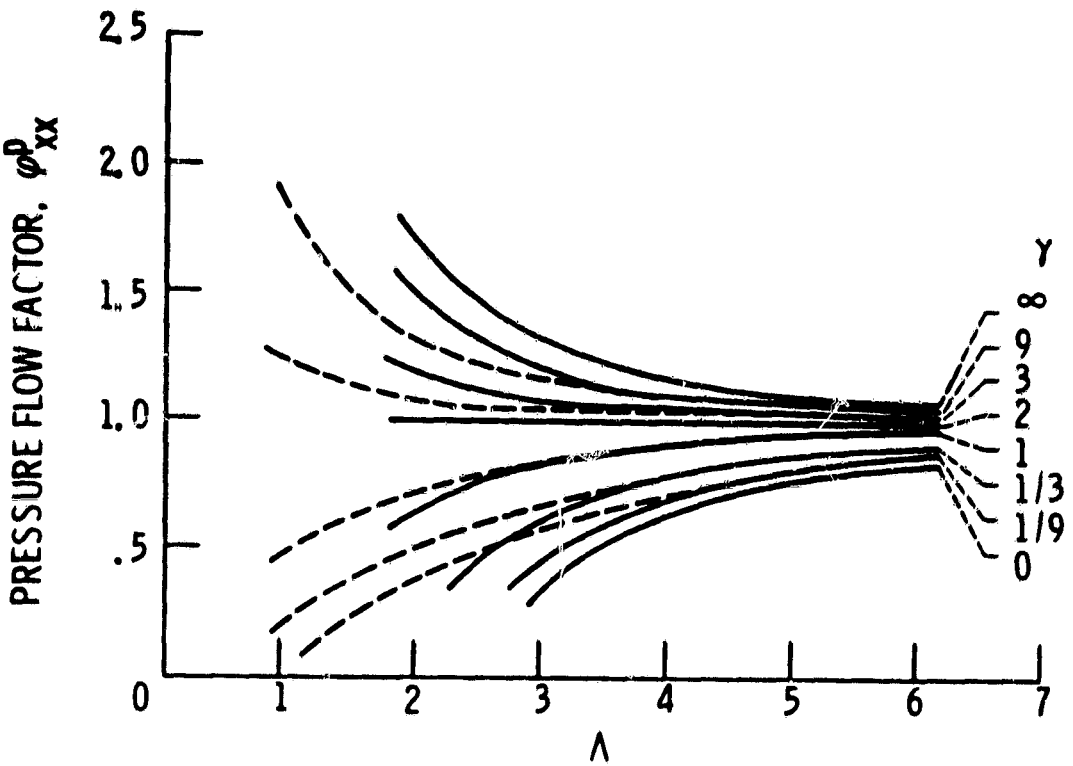

Figure 5.3 Comparison of pressure flow factor calculated from equation (5.7) (solid line) with those of Patir and Cheng (1978) (dashed line).

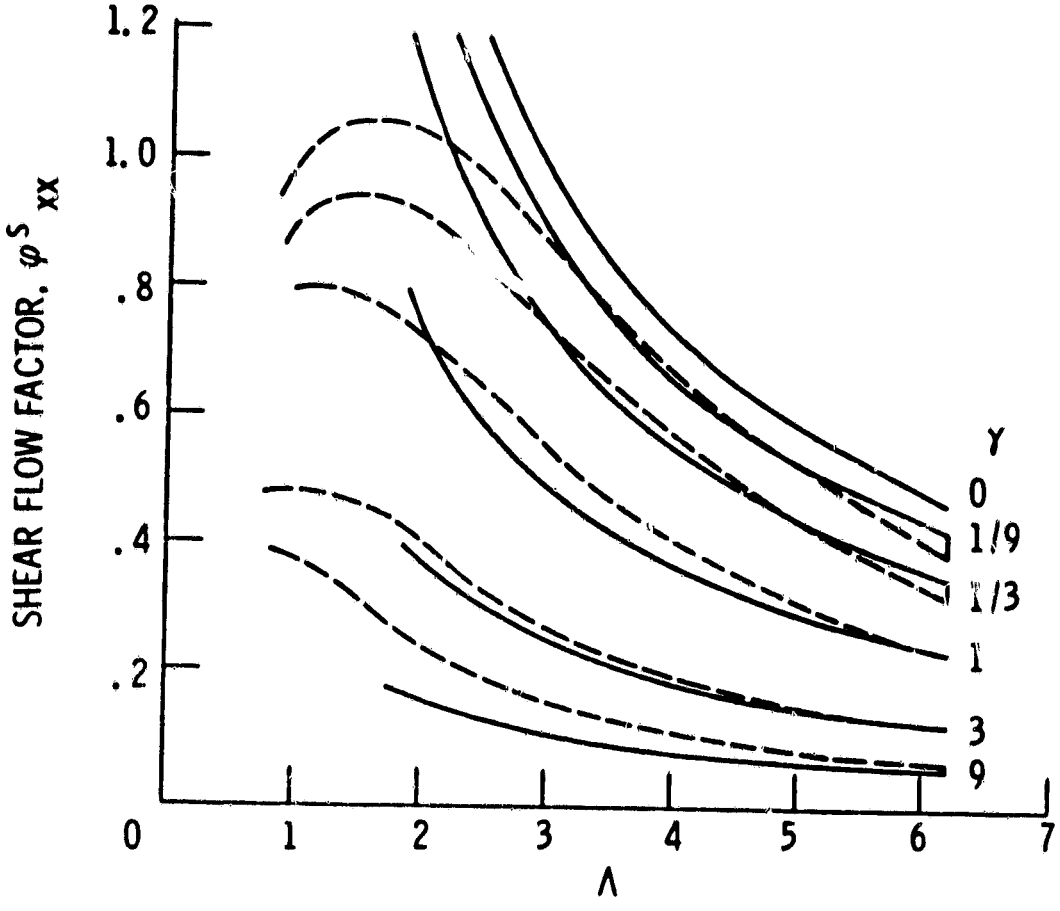

Figure 5.4 Comparison of shear flow factor calculated from equation 5.7) (solid line) with those of Patir and Cheng (1979) (dashed line).

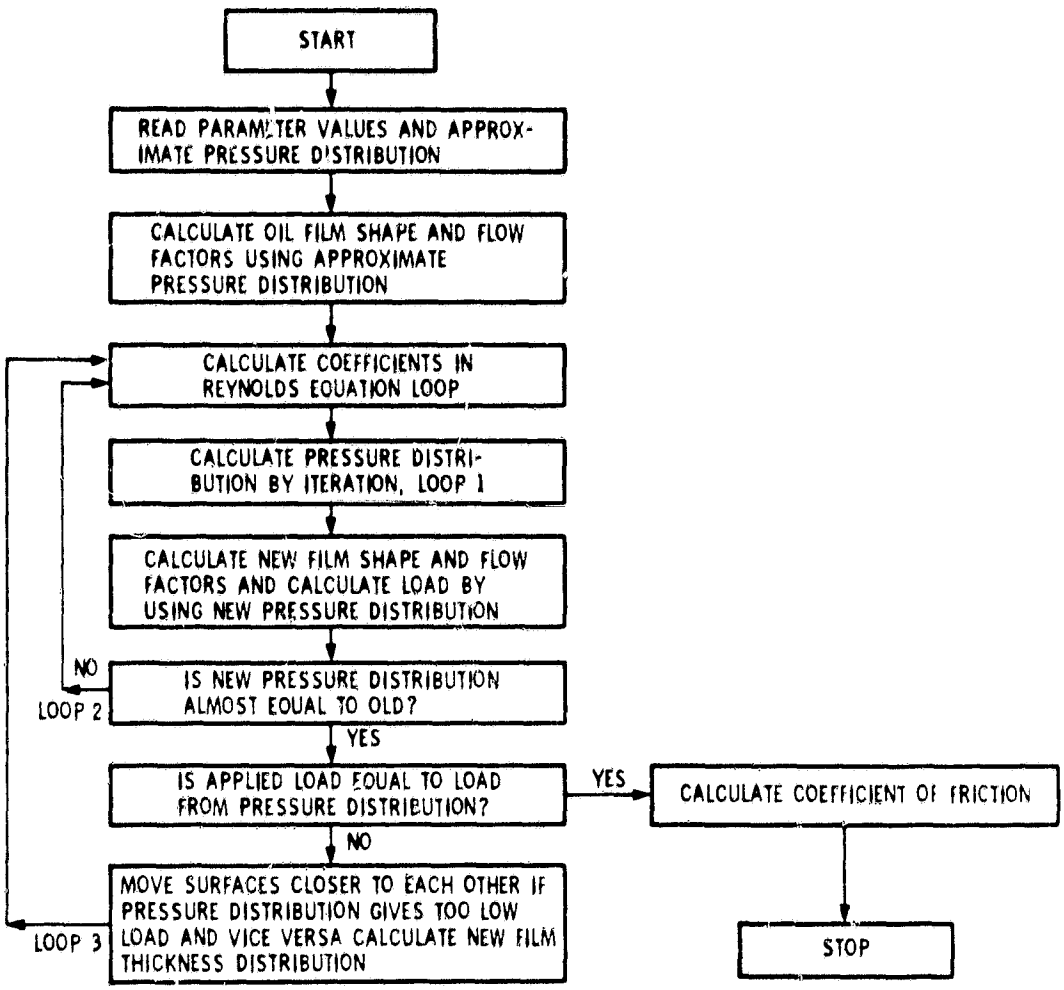

Figure 5, 5 - Flow chart of computer code.

CS-65-234

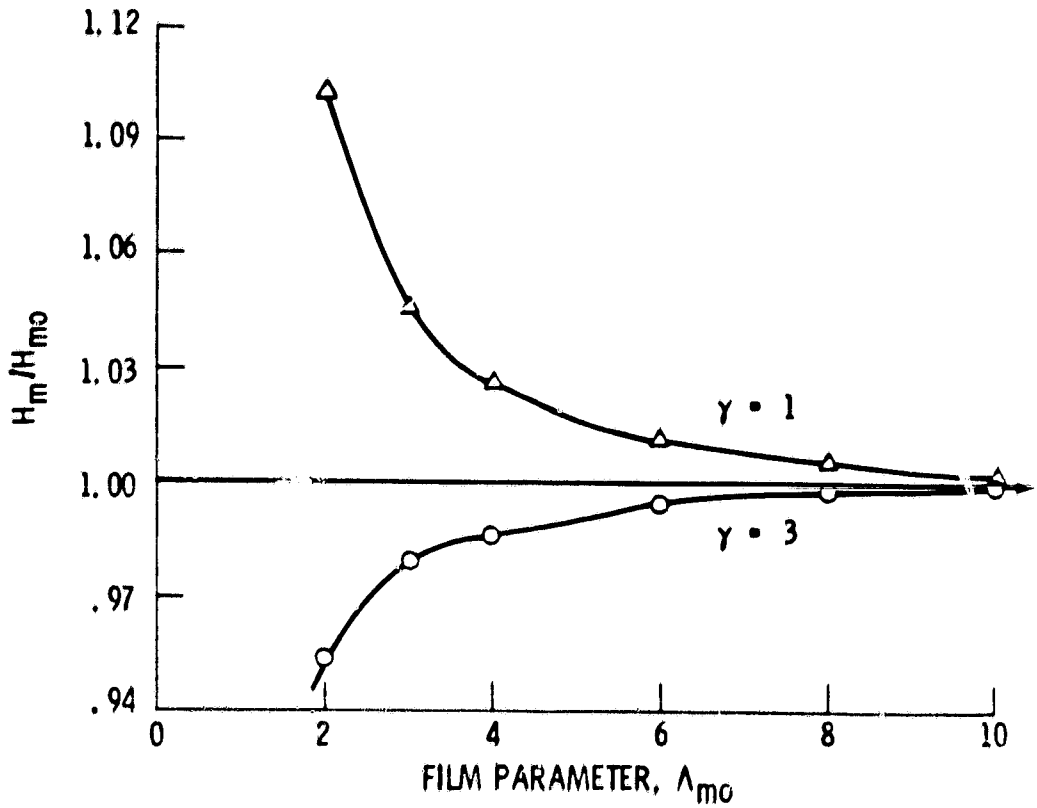

Figure 5.6 Variation of minimum film thickness at constant load with film parameter for different asperity anistropy.

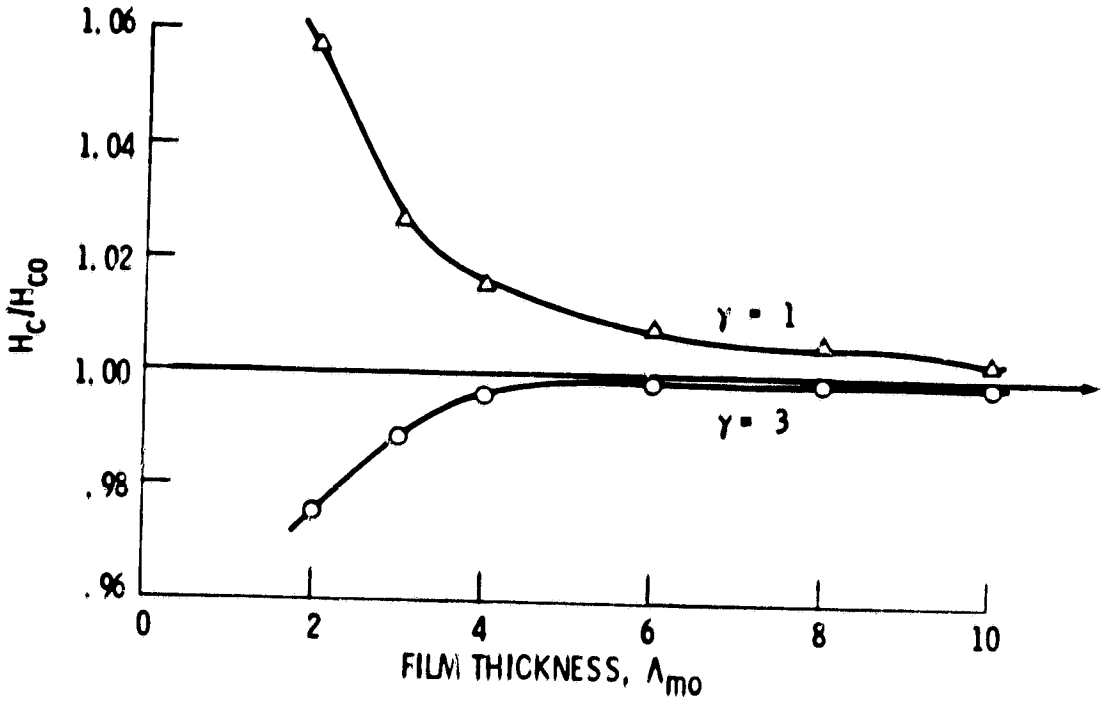

Figure 5.7 Variation of central film thickness at constant load with film parameter for different asperity anisotropy.

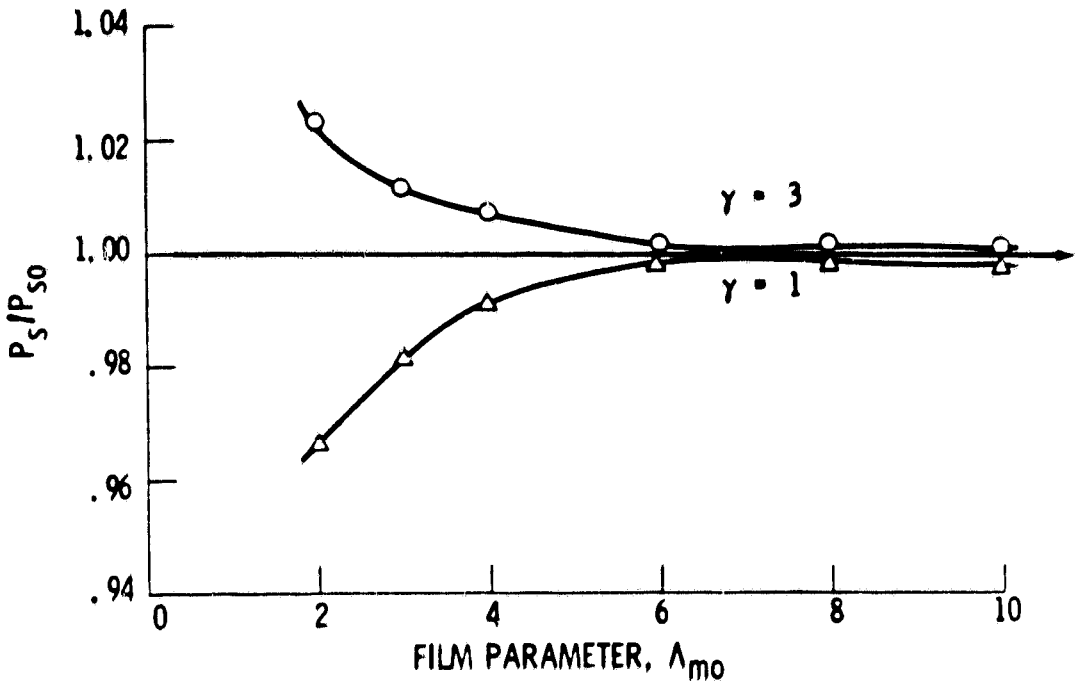

Figure 5.8 Variation of pressure spike at constant load with film parameter for different asperity anisotropy.

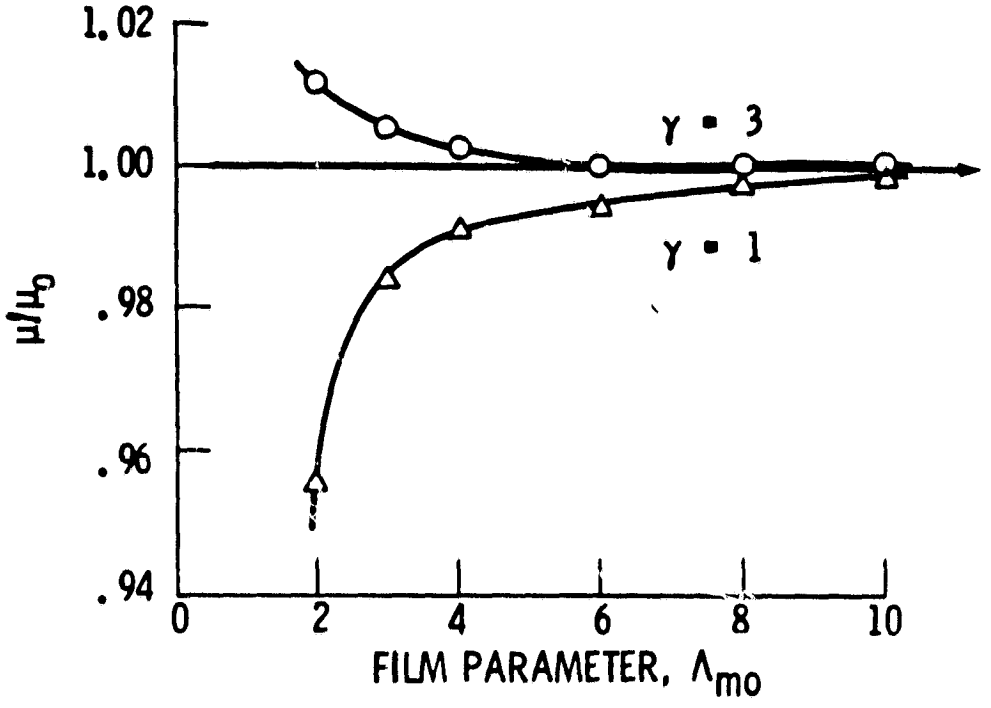

Figure 5.9 Variation of rolling friction coefficient at constant load with film parameter for different asperity anisotropy.

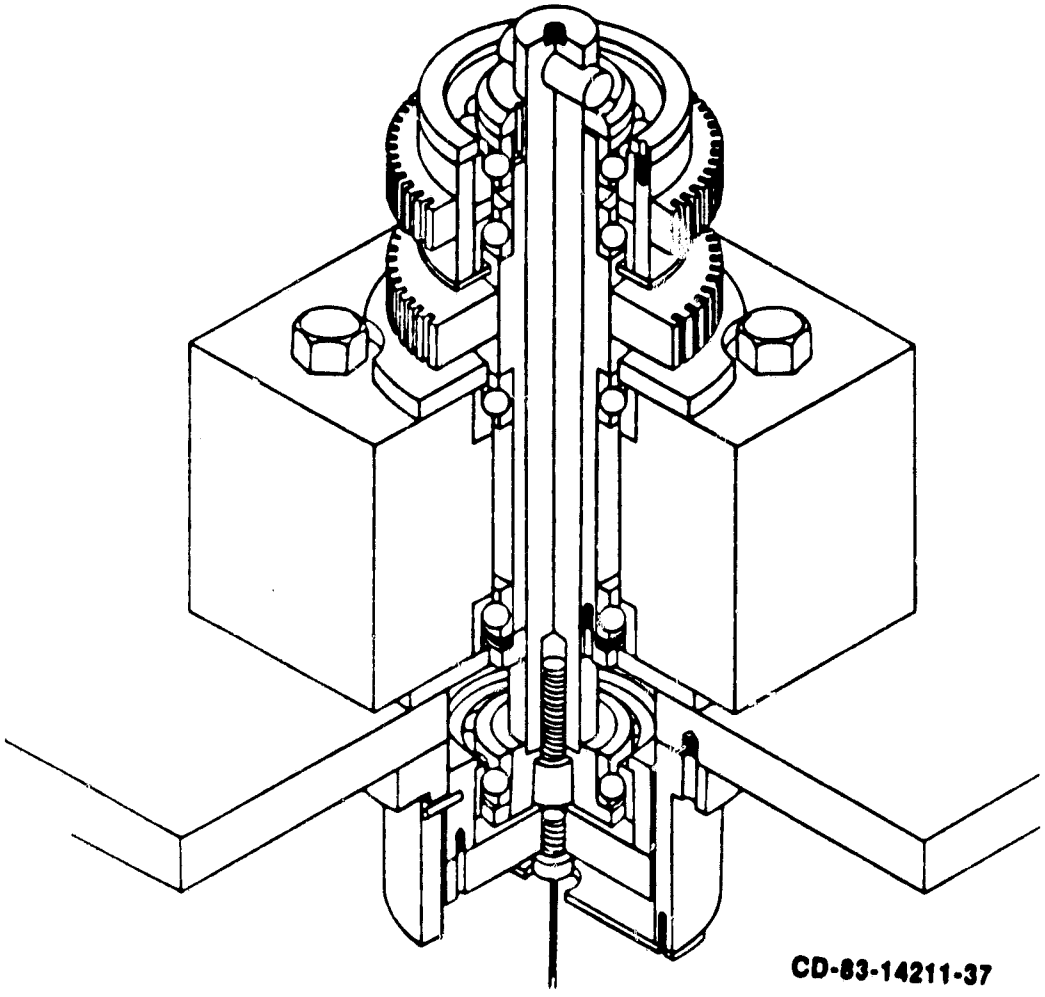

Figure 6.1 Apparatus.

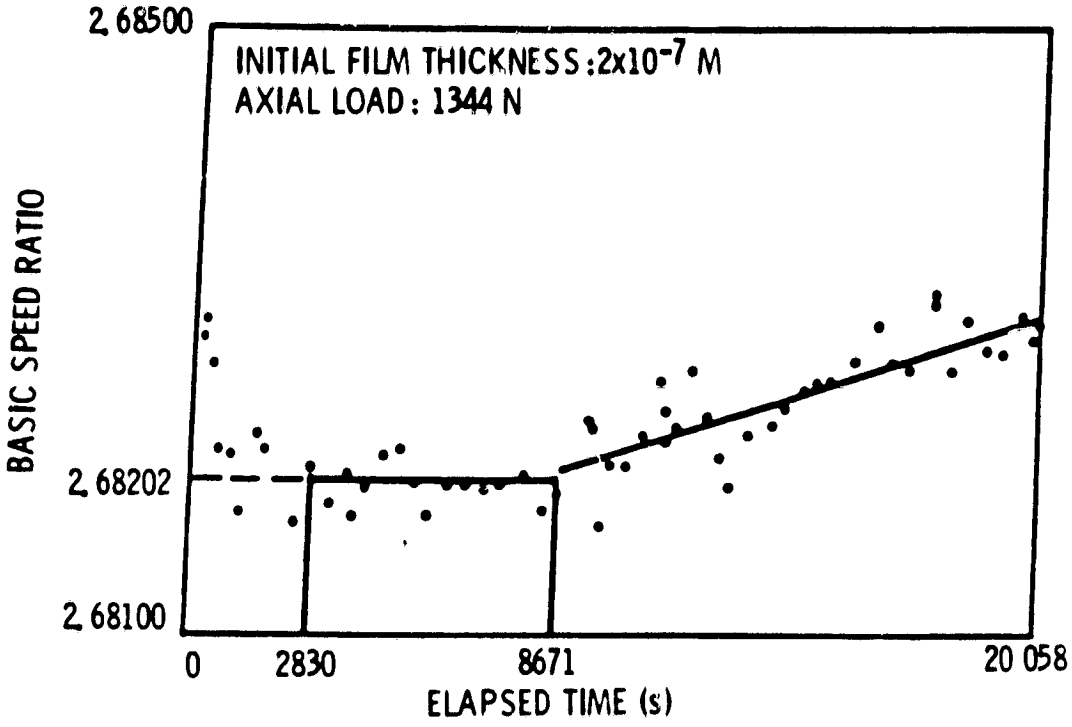

Figure 6.2 Basic speed ratio versus time (thick film).

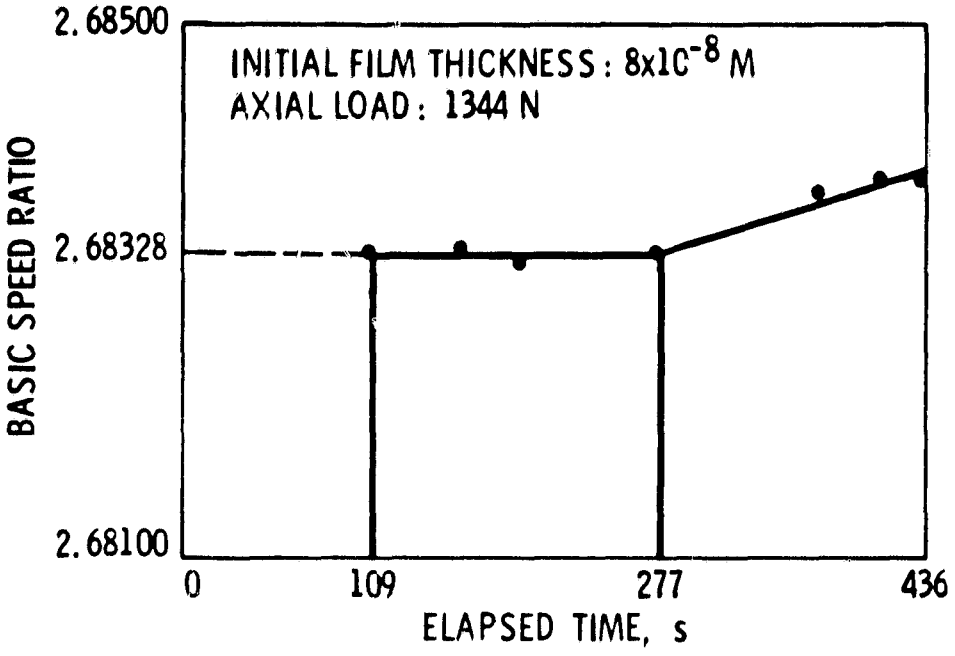

Figure 6.3 - Basic speed ratio versus time (thin film).

CS-85-2727

APPENDIX 1

THE VARIABLE-MESH NODAL STRUCTURE

A variable-mesh nodal structure was used to provide close spacing in and around the pressure spike. This help to minimize the errors that can occur because of large gradients in the high-pressure region. The locations of the pressure spikes from Kapitza (1955) are determined by setting $(\partial P/\partial X) = (\partial P/\partial Y) = 0$ and solving for X and Y as follows:

$$X_{pk} = -\sqrt{\frac{2H_o}{3}}$$

$$Y_{pk} = 0$$

The fine spacing are determined so that there are 2 or 3 nodes between H_o and X_{pk}. An interative program is developed to set up the variable-mesh nodal structure. The nodal structure used was varied depending on anticipated pressure distribution. A nodal structure is used when a good convergence is observed by changing the nodal structure then it is used for similar pressure distribution.

Appendix 2

COMPUTER PROGRAM LIST 1

PROGRAM NAME	UTILITY
NODAL	Set up the variable-mesh structure
MAIN	Mainprogram used to input the variable-mesh strucutre.
PVRH	subprogram used to analyze the lubrication of piezoviscous-rigid regime.

```
000020 C     NODAL
000100          IMPLICIT REAL*8(A-H,O-Z)
000200          NAMELIST /OUT/NX,NY,NCGF,NZON2,JZON,HIN,HO,ZC1,ZC2,ZD1,ZE1,XNODF,XI,YI,NXY,NXPK,XPK
000300          DATA HIN/0.12D0/
000400          DATA HO,ALPHA/2.0D-5,20.0D0/
000500          DATA NODE,NCGF/1,12/
000600          DATA ZC1,ZD1/100.0D0,100.0D0/
000700          SPACE=DSQRT(2./3.*HO)*0.5
000800          XP=1.-SPACE*2.0
000820          XPK=1.11125*XP
001000          ZE1=NODE/SPACE
001100 5        WRITE(6,100)FZONE1,FZONE,FCZONE,XF
001200 100      FORMAT(1X,'INPUT NZON1,NZON2,IFNODE',1X,4D16.8,1X,'(FZONE1,FZONE,FCZONE,XF,INDE)')
001300          READ(5,150)NZON1,NZON2,IFNODE
001400 150      FORMAT(3I3)
001500          FCZONE=IFNODE/ZD1
001600          FZONE1=NZON1/ZE1
001700          FZONE=NZON2/ZE1
001800          XF=1.+FZONE-FZONE1+FCZONE
001900          IF(FZONE1.LE.0.15)GO TO 5
002000          IF(FZONE.LE.0.196)GO TO 5
002100 E        IF(XF.LE.1.1225)GO TO 5
002200          WRITE(6,110)FZONE1,FZONE,FCZONE,XF,INDE
002300 110      FORMAT(1X,'INPUT INDE',4D16.8,1X,I1)
002400          READ(5,120)INDE
002500 120      FORMAT(I1)
002600          IF(INDE.EQ.1) GO TO 5
002700          CZONE=(NCGF-1)/100.0D0
002800          XI=1.-FZONE1-CZONE
002900          X=1.-XI
003000          XNODF=XI+CZONE
003100          NX=NCGF+NZON2+IFNODE
003200          NXPK=NCGF+NZON1-NODE
003300          Y=ALPHA*DSQRT(1.-(1.-1./ALPHA*(HIN-HO-1.+DSQRT(1.-X*X)))**2)
003400          YI=8.4895358D0-Y
003500 6        WRITE(6,200) ZC2,YZONE
003600 200      FORMAT(1X,'INPUT NY,JZON,IND',2D16.8,'(ZC2,YZONE)')
003700          READ(5,250)NY,JZON,IND
003800 250      FORMAT(3I3)
003900          NYF=NY-JZON
004000          YZONE=Y-(JZON-1)/ZC1
004100          ZC2=NYF/YZONE
004200          IF(IND.EQ.1)GO TO 6
004300          NXY=NX*NY
004400          WRITE(6,OUT)
004420          WRITE (4,OUT)
004500          STOP
004600          END
```

```
000020 C MAIN
000100       IMPLICIT REAL*8(A-H,O-Z)
000200       DIMENSION H(59400),PR(59400)
000300       REAL*4 XE(450),XG(132),YG(132),YGC(899),HS(59400),PRS(59400)
000400          REAL*4 XMI(450)
000500       COMMON/STARTV/HIN,HO,XNODF,ZC1,ZC2,ZD1,ZE1,XI,YI
000600       COMMON/STARTI/JZON,NCGF,NZON2,IDE,NXPK
000700 C     INPUT
000800       NX=132
000900       NY=270
001000       NCGF=13
001100       NZON2=110
001200       JZON=60
001300       IDE=1
001400       HIN=0.15D0
001500          HO=4.8D-6
001600       ZC1=100.0D0
001620          ZC2=164.00806139334D0
001800       ZD1=100.0D0
001801          ZE1=559.01701103495D0
001802          XNODF=0.83900311041810
001805          XI=0.71900311041810D0
001820          YI=6.6191109841981D0
002300          NXPK=102
002400       M=1
002500 C
002600 C    M=-1: READS IN FORMATTED INPUT AND BYPASSES THE INITIAL
002700 C    CALCULATION OF THE PRESSURE DISTRIBUTION
002800 C
002900 C    M=0: READS IN HEXADECIMAL INPUT AND BYPASSES THE INITIAL
003000 C    CALCULATION OF THE PRESSURE DISTRIBUTION
003100 C
003200 C    M=+1: CALCULATES AN INITIAL GUESS
003300 C
003400     1 CONTINUE
003500       NXY=NX*NY
003600       NYM1=2*NY-1
003700       CALL RIGID3(NX,NY,NXY,NYM1,H,PR,PRS,HS,XG,YG,YGC,XE,XMI,M)
003800       STOP
003900       END
```

```
000020 C     PVRH
 00100       SUBROUTINE RIGID3(NX,NY,NXY,NYM1,H,PR,PRS,HS,XG,YG,YGC,XE,XMI,M)
 00200       IMPLICIT REAL*8(A-H,O-Z)
 00300       REAL*4 XMIN,XLEN,YMIN,XE(NY),XMI(NY)
 00400       REAL*4 XG(NX),YG(NX),YGC(NYM1),HS(NXY),PRS(NXY)
 00500       REAL*4 FN,US,WS,ALPHA,HI,XMAX,XCENTS,YCENTS,YMAX,PRMXS,XPK
 00600       REAL*4 XNODFS,XDEL,YDEL,HMINS,PMIN,HMAX
 00700       NAMELIST/INPUT/RAX,RAY,RBX,RBY,RX,RY,SMU,SMV,EP,PL
 00800       NAMELIST/RADIUS/RAX,RAY,RBX,RBY,RX,RY,SMU,SMV,PHEE,ALPHA,NXPK,XI,YI
 00900       NAMELIST/OUTPUT/PBAR,PCHECK,FBAR,FCHECK,SUM3,HO,HIN,WOU
 01000       DIMENSION DENS(64680),VIS(64680),XMU(64680),ZPR(64680),PHI(64680)
 01100       DIMENSION A(64680),B(64680),C(64680),DLZ(64680),XL(64680)
 01200       DIMENSION XM(64680)
 01300       DIMENSION S(64680),H(NXY),PR(NXY)
 01400       COMMON/STARTV/HIN,HO,XNODF,ZC1,ZC2,ZD1,ZE1,XI,YI
 01500       COMMON/STARTI/JZON,NCGF1,NZON2,IDE,NXPK
 01600       COMMON/CTRINF/FN,US,WS,ALPHA,HI,XMAX,XCENTS,YCENTS,YMAX,PRMXS,XPK
 01700       COMMON/CTR/XNODFS,XDEL,YDEL,HMINS,PMIN,HMAX
 01800       COMMON/CTRINT/NCGF
 01900          REAL*4 FMTX,PRD(305,999)
 02000 C
 02100 C     INPUT
 02200 C
 02300       MPARA=0
 02400       NVISC=0
 02500       MWT=0
 02600 C
 02700 C     MPARA=1:  THE PARABOLIC APPROXIMATION WILL BE USED
 02800 C     NVISC=0:  THE ISO-VISCOUS SOLUTION IS DETERMINED
 02900 C     MWT=1:  PARTIALLY CONVERGED SOLUTION IS STORED ON TAPE IN CASE OF
 03000 C     CRASH
 03100 C
 03200          M=1
 03300       ROSM=1.0D0
 03400       MAUR=0
 03500       JENN=0
 03600       ZZZ=1.0D0
 03700       PI=3.14159265359D0
 03800       PIVAS=4858.7D0
 03900       VISO=4.11D-6
 04000       VA=0.0D0
 04100       VB=0.0D0
 04200       Z=.67D0
 04300       ELPHA=5.82744D-6
 04400       BETA=1.68348D-5
```

```
004500        VISE=.0000000631D0
004600        ORF=1.9D0
004700        ZE2=ZD1
004800        NCGF=NCGF1
004900        XCENT=1.00D0
005000        YCENT=8.48953585D0
005100 C
005200 C     M=-1: READS IN FORMATTED INPUT AND BYPASSES THE INITIAL
005300 C     CALCULATION OF THE PRESSURE DISTRIBUTION
005400 C
005500 C     M=0: READS IN HEXADECIMAL INPUT AND BYPASSES THE INITIAL
005600 C     CALCULATION OF THE PRESSURE DISTRIBUTION
005700 C
005800 C     M=+1: CALCULATES AN INITIAL GUESS
005900 C
006000 975    CONTINUE
006100        DEL1=.1D0
006200        MAXS2=1
006300        DEL3=.1D0
006400        HMIN=10.0D0
006500        HMAX=10.0
006600        PRSVMX=.1D-18
006700        PRMX=.1D-18
006800 976    CONTINUE
006900        HIN=HIN
007000        NX1=NX-1
007100        NY1=2*NY
007200        HI=HIN
007300           READ(7,INPUT)
007400 C
007500 C       CURVATURE SUM AND DIFFERENCE
007600 C
007700        RX=(1./RAX)+(1./RBX)
007800        RY=(1./RAY)+(1./RBY)
007900        RHO=RX+RY
008000        GAMMA=(RX-RY)/RHO
008100        ALPHA=RX/RY
008200 C
008300        XCENTS=XCENT/RX
008400        YCENTS=YCENT/RX
008500        XNODFS=XNODF/RX
008600        YM=YCENT
008700        XN=XCENT
008800 C
008900 C     DIMENSIONLESS PARAMETER GROUPING
```

```
009000 C
009100       V=SQRT(SMU**2+SMV**2)
009200       THETA=ATAN(SMV/SMU)
009300       U=VISO*RX*V/EP
009400       US=U
009500       HO=HO
009600       PHEE=1./(1.+(2.*RY)/(3.*RX))
009700       Q1=VISE/VISO
009800       Q2=EP/19608.5268
009900       Q5=ELPHA*EP
010000       Q6=BETA*EP
010100  4    CONTINUE
010200       ZC=ZC1
010300       SA=1./ZC
010400       SB=1.0/ZD1
010500 C
010600 C      INITIAL GUESS
010700 C
010800       IF (M) 5,6,7
010900   5   CONTINUE
011000       READ(5,700) (PR(N),N=1,NXY)
011100       READ(5,700) (H(N),N=1,NXY)
011200  700  FORMAT(8D10.5)
011300       GO TO 7
011400   6   CONTINUE
011500       READ (5) (PR(N),N=1,NXY)
011600   7   CONTINUE
011700       Y=YI
011800       DO 13 J=1,NY
011900       X=XI
012000       DO 12 I=1,NX
012100       ZD=ZD1
012200       N=I+(J-1)*NX
012300       JTWIN=NY1-J
012400       IF(J.GE.JZON) ZC=ZC2
012500       YGC(J)=Y/RX
012600       YGC(JTWIN)=2.*YCENTS-YGC(J)
012700       XG(I)=X/RX
012800       NVMF=NCGF+(J-1)*NX
012900       NVMB=NVMF+NZON2
013000       IF(N.GE.NVMF .AND. N.LT.NVMB) ZD=ZE1
013100       IF(N.GE.NVMB) ZD=ZE2
013200       SQX=((X-XN)/RX)**2
013300       SQY=((Y-YM)/RX)**2
013400       IF (MPARA .EQ. 1) GO TO 23
013500       S(K)=(1./RX)+(1./RY)-DSQRT((1./RX)**2-SQX)-DSQRT((1./RY)**2-SQY)
```

```
      GO TO 8
75    S(N)=(RX*SQX+RY*SQY)/2.
8     CONTINUE
      IF(M.EQ.1) GO TO 9
      GO TO 10
9     CONTINUE
      PR(N)=.1D-8
10    CONTINUE
      IF (J.EQ.1 .OR. I.EQ.1 .OR. I.EQ.NX) PR(N)=0.0D0
      IF(PR(N).GT.0.) GO TO 11
      PR(N)=0.D0
11    CONTINUE
      IF(J.EQ.NY) YG(I)=PR(N)
      IF (PR(N).LT.PRSVMX) GO TO 12
      PRSVMX=PR(N)
      NHOLD=N
12    X=X+1./ZD
13    Y=Y+1./ZC
C
C     FILM THICKNESS
C
14    CONTINUE
      DO 19 J=1,NY
      DO 18 I=1,NX
      N3=I+(J-1)*NX
      H(N3)=HO+RX*S(N3)
      IF (H(N3) .GE. HIN) PR(N3)=0.0D0
      IF (H(N3) .GE. HIN) H(N3)=HIN
      IF (H(N3).GT.HMIN) GO TO  17
      HMIN=H(N3)
      HMINS=HMIN
      NSAVE=N3
17    CONTINUE
      PHI(N3)=PR(N3)*(H(N3)**1.5)
18    CONTINUE
19    CONTINUE
      IF (M .EQ. 1) GO TO 20
      WRITE(6,900) (PR(N),N=1,NXY)
900   FORMAT(1H ,2HPR/70(1H ,10D13.5/))
      WRITE(6,1100) NSAVE,HMIN
1100  FORMAT(1H ,6HNSAVE=,I10,10X,5HHMIN=,D16.5)
      WRITE(6,1200) PRSVMX,NHOLD
1200  FORMAT(1H ,7HPRSVMX=,D16.5,10X,6HNHOLD=,I10)
20    CONTINUE
      WRITE(6,RADIUS)
```

```
018100          WRITE(6,1106) NX,NY,NZON2,JZON
018200 1106     FORMAT(1X,'NX=',I6,' NY=',I6,' NZON2=',I6,' JZON=',I6)
018300 C
018400 C      INITIAL VISCOSITY AND DENSITY CALCULATION
018500 C
018600        DO 21 N=1,NXY
018700        DENS(N)=1.+(Q5*PR(N))/(1.+Q6*PR(N))
018800        VIS(N)=Q1**(1.-(1.+Q2*PR(N))**Z)
018900        XMU(N)=DENS(N)/VIS(N)
019000 21     CONTINUE
019100 C
019200 C      RELAXATION COEFFICIENTS A,B,C,D,L,AND M
019300 C
019400 22     CONTINUE
019500        SUM=0.0D0
019600        ZC=ZC1
019700        ZF=ZC1
019800        DO 24 J=2,NY
019900        DO 23 I=2,NX1
020000        ZD=ZD1
020100        ZE=ZD
020200        N=I+(J-1)*NX
020300        NVMF=NCGF+(J-1)*NX
020400        NVMB=NVMF+NZON2
020500        IF(J.GE.JZON) ZF=ZC2
020600        IF(J.GT.JZON) ZC=ZC2
020700        IF(N.GE.NVMF .AND. N.LT.NVMB) ZE=ZE1
020800        IF(N.GT.NVMF .AND. N.LE.NVMB) ZD=ZE1
020900        IF(N.GE.NVMB) ZE=ZE2
021000        IF(N.GT.NVMB) ZD=ZE2
021100        V1=((ZE*ZD)/(ZE+ZD))**2.
021200        V2=((ZE)**2.)*(ZD-ZE)/(ZD+ZE)
021300        V3=(ZE**3.)*(ZE+2.*ZD)/((ZE+ZD))**2.
021400        V4=(ZD**3.)*(2.*ZE+ZD)/((ZE+ZD))**2.
```

```
      V5=(ZD/ZE)**2.*V2
      C2D=ZC**2-ZF**2
      C3P1=ZC+2.*ZF
      C3P2=2.*ZC+ZF
      CF=(ZF/(ZC+ZF))**2
      CF1=(1./(ZC+ZF))**2
      CP=(ZC+ZF)**2
      Z1=.5*ZD
      Z2=ZC/(ZC+ZF)
      Z3=Z1**2
      Z4=Z2**2
      N1=N+1
      N2=N-1
      N3=N+NX
      N4=N-NX
      IF (J.EQ.NY) N3=N4
      Y0=XMU(N)
      Y1=XMU(N1)
      Y2=XMU(N2)
      Y3=XMU(N3)
      Y4=XMU(N4)
      Y5=H(N1)
      Y6=H(N2)
      Y7=H(N)
      Y8=H(N3)
      Y9=H(N4)
      Y10=Y1*DSQRT(Y5)
      Y11=Y2*DSQRT(Y6)
      Y12=Y3*DSQRT(Y8)
      Y13=Y4*DSQRT(Y9)
      Y14=Y0*DSQRT(Y7)

      A(N)=V1*Y2+V2*Y0+V3*Y1
      B(N)=Z4*(Y3*ZF**2-C2D*Y0+ZC*C3P1*Y4)
      C(N)=V4*Y2-V5*Y0+V1*Y1
      DLZ(N)=CF*(ZF*C3P2*Y3+C2D*Y0+ZC**2*Y4)
      XL1=Y2*4.*Z3-(ZD-ZE)**2*Y0+Y1*ZE**2+CF1*(Y3*ZF**2*CP-C2D**2*Y0+ZC**2*CP*Y4)
      XL2=1.5/(Y7**1.5)
      XL3=Y11*(V4*Y6-Y7*4.*Z3+Y5*V1)+Y14*(-V5*Y6+(ZD-ZE)**2*Y7+Y5*Y2)+
     Y10*(V1*Y6-ZE**2*Y7+V3*Y5)
      XL4=CF1*(Y12*ZF**2*(ZF*C3P2*Y8-CP*Y7+Y9*ZC**2)+Y13*ZC**2 -
     1*(Y8*ZF**2-CP*Y7+ZC*C3P1*Y9)+Y14*C2D*(ZF**2*Y8+C2D*Y7-ZC**2*Y9))
      XL(N)=XL1+XL2*(XL3+XL4)
      XM1=12.*U/(Y7**1.5)
      XM2=((ZE**2.*DEMS(N1)*Y5/(ZD+ZE)+(ZD-ZE)*DEMS(N)*Y7-ZD**2.*      -
     1Y6/(ZD+ZE))*DCOS(THETA)
      XM3=(Y8*ZF**2*DEMS(N3)+C2D*DEMS(N)*Y7-Y9*ZC**2*DEMS(N4))*DSIN(THETA)
      XM(N)=XM1*(XM2+Z2/ZC*XM3)
   23 CONTINUE
   24 CONTINUE
   25 SUM=0.0D0
C
C     RELAXATION FORMULA
C
      DO  30 J=2,NY
```

```
026900            MENDA=0
027000          MEND=0
027100          DO  29 I=2,NX1
027200          MN=I+(J-1)*NX
027300          MNA=MN+1
027400          MNB=MN-1
027500          MNC=MN+NX
027600          MND=MN-NX
027700          IF(J.EQ.NY) MNC=MND
027800          ZPR(MN)=PHI(MN)-ORF*(PHI(MN)+(XM(MN)-A(MN)*PHI(MNA)-B(MN)*PHI(MND)-
                C(MN)*PHI(MNB)-DLZ(MN)*PHI(MNC))/XL(MN))
027900 26       CONTINUE
028000          IF (H(MN) .GE. HIN) GO TO 127
028100          IF (ZPR(MN).LE.0.) GO TO  27
028200             STDN=STDN+DABS(ZPR(MN))
028300             SERR=SERR+DABS(ZPR(MN)-PHI(MN))
028400          GO TO  28
028500 127        ZPR(MN)=0.0D0
028600             MENDA=MENDA+1
028700             IF(MENDA.EQ.1)XMI(J)=XG(I)
028800             GO TO 28
028900 27       ZPR(MN)=0.0D0
029000          MEND=MEND+1
029100          IF (MEND .EQ. 1) XE(J)=XG(I)
029200 28       PHI(MN)=ZPR(MN)
029300 29       CONTINUE
029400 30       CONTINUE
029500 31       CONTINUE
029600          MAUR=MAUR+1
029700 41       CONTINUE
029800 C        IF (MWT.EQ.0) GO TO 66
029900 65       CONTINUE
030000 C        WRITE (8) (PR(I),I=1,NXY)
030100 C        WRITE (8) (H(I),I=1,NXY)
030200 C        REWIND 8
030300 66       CONTINUE
030400          IF (SERR.LT.DEL3) GO TO  311
030500          GO TO 25
030600 C
030700 C        VISCOSITY AND DENSITY ITERATION
030800 C
030900 311      SUM2=0.0D0
031000          WRITE (6,480) MAUR,SERR
031100 480      FORMAT(1H ,5HMAUR=,I8,5X,4HSERR=,D16.5)
031200          MAUR=0
031300          PRMX=.1D-13
031400             ROSM=ROSM1
031500             TDN=0.0
031600             ERR1=0.0
031700             SUM2=0.0
031800             DO 54 J=2,NHY
031900             JP=(J-1)*NX
032000             DO 54 I=2,NXM1
032100             N=I+JP
032200             A(N)=PHI(N)/(H(N)**1.5)
```

```
032300          DLZ(N)=A(N)-PR(N)
032400          TDN=TDN+DABS(A(N))
032500          ERR1=ERR1+DABS(DLZ(N))
032600   54     CONTINUE
032700          ERR=ERR1/TDN
032800        DO 315 J=2,NY
032900        DO 316 I=2,NX1
033000        N=I+(J-1)*NX
033100        PR(N)=(PHI(N)/(H(N)**1.5)+(ROSM-1.)*PR(N))/ROSM
033200        IF (H(N) .GE. HIN) PR(N)=0.0D0
033300        IF(PR(N).LT.PRMX) GO TO 33
033400        PRMX=PR(N)
033500        PRMXS=PRMX
033600        NHOLD=N
033700 33     CONTINUE
033800 C      IF(NVISC.EQ.0) GO TO 316
033900        DENSN=1.+(Q5*PR(N))/(1.+Q6*PR(N))
034000        VISN=Q1**(1.-(1.+Q2*PR(N))**Z)
034100        XMUN=DENSN/VISN
034200        Y99=(XMUN-XMU(N))/XMUN
034300        SUM2=SUM2+DABS(Y99)
034400        DENS(N)=DENSN
034500        VIS(N)=VISN
034600 316    XMU(N)=XMUN
034700 315    CONTINUE
034800        MN1=1
034900 459    CONTINUE
035000        JENN=JENN+1
035100        WRITE(6,810) SUM2
035200 810    FORMAT(1H ,5HSUM2=,D16.5)
035300        IF (ERR.LT.DEL1) GO TO 32
035400        MAXS2=MAXS2+1
035500        GO TO 22
035600 C
035700 C      APPLIED NORMAL LOAD
035800 C
035900 32     CONTINUE
036000        MAXS2=1
036100        WRITE(6,481) JENN
036200 481    FORMAT(1H ,9HJENNIFER=,I8)
036300        JENN=0
036400        MAUR=0
036500        QU4=0.0D0
036600        PSUM=0.0D0
036700        IZON=1
036800        ZD=ZD1
036900        PBAR=0.0D0
037000        PCHECK=0.0D0
037100        MS=2
037200        MF=NCGF
037300        GO TO 483
037400 482    ZD=ZE1
037500        IZON=2
037600        MS=MF
```

```
037700        MF=MS+NZON2
037800        QU4=0.0D0
037900        PSUM=0.0D0
038000        GO TO 483
038100 485    ZD=ZE2
038200        IZON=3
038300        MS=MF
038400        MF=NX
038500        QU4=0.0D0
038600        PSUM=0.0D0
038700 483    CONTINUE
038800        DO 38 I=MS,MF
038900        IM=MOD(I,2)
039000        IMS=MOD(MS,2)
039100        IF(IMS.EQ.1) GO TO 486
039200        QU1=1.0D0
039300        IF(IM.EQ.1) QU1=2.0D0
039400        GO TO 487
039500 486    QU1=2.0D0
039600        IF(IM.EQ.1) QU1=1.0D0
039700 487    CONTINUE
039800        QU5=1.0D0
039900        QU3=0.0D0
040000        IF(I.EQ.MS .OR. I.EQ.MF) QU1=.5D0
040100        IF(I.EQ.MS .OR. I.EQ.MF) QU5=.5D0
040200        JINTG=1
040300        ZC=ZC1
040400        NS=2
040500        NF=JZON
040600        GO TO 35
040700 34     JINTG=2
040800        ZC=ZC2
040900        NS=NF
041000        NF=NY
041100 35     DO 37 J=NS,NF
041200        N=I+(J-1)*NX
041300        JN=MOD(J,2)
041400        JNS=MOD(NS,2)
041500        IF(JNS.EQ.1) GO TO 40
041600           QV1=2.0D0
041700        IF(JN.EQ.1) QV1=4.0D0
041800        IF(J.EQ.NS .OR. J.EQ.NF) QV1=1.0D0
041900        GO TO 37
042000 40        QV1=4.0D0
042100        IF(JN.EQ.1) QV1=2.0D0
042200        IF(J.EQ.NS .OR. J.EQ.NF) QV1=1.0D0
042300 37     QU3=QU3+PR(N)*QV1/ZC
042400        IF(JINTG.EQ.1) GO TO 34
042500        PSUM=PSUM+QU3*QU5/3.0
042600 38     QU4=QU4+QU3*QU1/3.0
042700           PBAR=4.*QU4/(3.*ZD)+PBAR
042800           PCHECK=2.*PSUM/ZD+PCHECK
042900        FBAR=4.*EP/(RX**2)*QU4/(3.*ZD)+FBAR
043000        FCHECK=2.*EP/(RX**2)*PSUM/ZD+FCHECK
```

```
043100        IF(IZON.EQ.2) GO TO 485
043200        IF (IZON.EQ.3) GO TO 36
043300        GO TO 482
043400  36    CONTINUE
043500           WOU=PBAR/(0.411D-5*V*RX)
043600        WRITE (6,OUTPUT)
043700        WS=PBAR
043800  39    CONTINUE
043900        IF (MPARA.EQ.0) GO TO 43
044000        PRMX=.1D-13
044100        PRSVMX=PRMX
044200        HMAX=10.0D0
044300        HMIN=10.0D0
044400        MPARA=0
044500        GO TO 976
044600  43    CONTINUE
044700        IF (NVISC .EQ. 0) GO TO 53
044800        WRITE(6,1600) NSAVE,HMIN
044900  1600  FORMAT(1H ,6HNSAVE=,I10,10X,5HHMIN=,D16.5)
045000        WRITE(6,1700) (PR(N),N=1,NXY)
045100  1700  FORMAT(1H ,2HPR/70(1H,10D13.5/))
045200        WRITE(6,1900) (H(N),N=1,NXY)
045300  1900  FORMAT (1H ,1HH/70(1H ,10D13.5/))
045400        WRITE(6,1800) (PHI(N),N=1,NXY)
045500  1800  FORMAT(1H ,3HPHI/70(1H ,10D13.5/))
045600        WRITE(6,2000) (S(N),N=1,NXY)
045700  2000  FORMAT (1H ,1HS/70(1H ,10D13.5/))
045800        WRITE(6,2100) (DENS(N),N=1,NXY)
045900  2100  FORMAT(1H ,7HDENSITY/70(1H ,10D13.5/))
046000        WRITE(6,2200) (VIS(N),N=1,NXY)
046100  2200  FORMAT(1H ,9HVISCOSITY/70(1H ,10D13.5/))
046200  C
046300  53    CONTINUE
046400        PMIN=.1E-20
046500        PRMX=.1D-20
046600        DO  55 J=1,NY
046700        DO  54 I=1,NX
046800
046900        N=I+NX*(J-1)
047000        JTWIN=NY1-J
047100        PRS(N)=PR(N)
047200           PRD(I,J)=PRS(N)
047300  C        FMTX(1,I,J)=XG(I)
047400  C        FMTX(2,I,J)=YGC(J)
047500  C        FMTX(3,I,J)=PRD(I,J)
047600        HS(N)=H(N)
047700        IF(PR(N).LT.PRMX) GO TO 54
047800        PRMX=PR(N)
047900        PRMXS=PR(N)
048000        NHOLD=N
048100        XPK=XG(I)
048200  54    CONTINUE
048300  55    CONTINUE
048400
```

```
048500           NYMM1=NY-1
048600           DO 56 I=1,NX
048700           N=I+NX*NYMM1
048800           YG(I)=PR(N)
048900 56        CONTINUE
049000           WRITE(6,3100)(XMI(N),N=1,NY)
049100 3100      FORMAT(1X,5HXMI= /70(1X,10D13.5/))
049200        HMAX=H(NVMF+1)
049300        PMIN=PR(NVMF+1)
049400        WRITE(6,3000) PRMX,NHOLD
049500 3000   FORMAT(1H ,5HPRMX=,D16.5,10X,6HNHOLD=,I10)
049600           WRITE(6,3200) VIS(NHOLD)
049700 3200      FORMAT(1X,'VIS(NHOLD)=',D16.5)
049800           WRITE(8) NX,NY,((PRD(I,J),I=1,NX),J=1,NY),(XG(N),N=1,NX),(YGC(N),N=1,NY),PRMXS
049900           NVMB=NCGF+NZON2
050000           WRITE(8)NXY,NCGF,NVMB,JZON
050100 61     CONTINUE
050200        CALL DSPLAY(XE,NY,XPK,PCHECK,PBAR,PRMXS,NHOLD)
050300  63    CONTINUE
050400 64    CONTINUE
050500        STOP
050600        END
```

APPENDIX 3

COMPUTER PROGRAM LIST 2

PROGRAM NAME	UTILITY
CHHR	Calculate the deformation under contact stresses by the method proposed by Hamrock and Dowson.
CNHR	Calculate the deformation under contact stresses by the present approach.

```
000020 C     CHHR
000100           IMPLICIT REAL*8(A-H,O-Z)
000200           REAL*4 XE(70)
000300           DIMENSION XD(150),YD(70),PR(3600)
000400           DIMENSION D(2000)
000500           DIMENSION W(2000),H(2000),S(2000)
000600           DIMENSION DENS(2000),VIS(2000),XMU(2000),PHI(2000)
000700           COMMON/AA/HO,PRX,HMIN,NHSAVE
000800           NAMELIST /INPUT/HO,SMU,SMV,EP,FP
000900           NAMELIST/OUTPUT/G,ALPHA,RBY,XK,PBAR,PCHECK,FBAR,FCHECK,STRS,HAMRK
001000 C         DATA PI/3.1415926535D0/
001100 C         DATA RAX,RAY,RBX/1.11125D0,1.11125D0,1.0D12/
001200 C         ***   ***   ***
001300 C
001400 C         DATA RX/1.11125D0/
001500 C         DATA RAY,RBY/1.11125D0,-1.1861150D0/
001600           DATA XI,YI,MN/0.0,0.0,19/
001700           DATA PI,EP/3.1415926535D0,21.97D06/
001800           DATA FP,RX,RY/8.964D0, 0.5558D0,0.5558D0/
001900 C   ***
002000 C         DATA ZD,ZC/13.0D0,5.0D0/
002100           DATA NX,NHY/39,20/
002200           DATA XM,YM/1.0D0,1.0D0/
002300 C         DATA HO/0.0/
002400 C
002500           HO=0.0
002600 C         RY=1.0/((1.0/RAY)+(1.0/RBY))
002700           NXHY=NX*NHY
002800           NY=2*NHY-1
002900           NXY=NX*NY
003000           NXM1=NX-1
003100 C
003200 C         CURVATURE SUM AND DIFFERENCE
003300 C
003400           PRX=1.0/RX
003500           PRY=1.0/RY
003600           RHO=PRX+PRY
003700           GAMMA=(PRX-PRY)/RHO
003800           ALPHA=PRX/PRY
003900           PAL=1.0/ALPHA
004000           PDAL=PAL*PAL
004100 C
004200 C         INITIAL GUESS FROM SIMPLIFY EQ
004300 C
004400           Q=PI/2.0-1.0
004500           FSS=PI/2.0+Q*DLOG(ALPHA)
004600           ESS=1.0+Q/ALPHA
004700           XKK=ALPHA**(2.0D0/PI)
004800 C
004900 C         ELLIPTIC INTEGRALS ES AND FS
005000 C
005100 C         XK=SQRT(2.0D0)
005200           XK=XKK
```

```
0005300           ES=ESS
0005400           FS=FSS
0005500 C
0005600 C         XK IS THE ELLIPTICITY PARAMATER
0005700 C
0005800           KITER=0
0005900  1        KITER=KITER+1
0006000           AK=SQRT(1.0D0-(1.0D0/(XK**2)))
0006100           CALL CEL(FS,ES,AK,IER)
0006200           XJK=SQRT((2.0*FS-ES*(1.0+GAMMA))/(ES*(1.0-GAMMA)))
0006300           A9=XK-XJK
0006400           XK=XJK
0006500           IF(DABS(A9).GT.1.0D-8) GO TO 1
0006600 C
0006700 C         INITIAL SEMIMAJOR AND SEMIMINOR AXES OF CONTACT ELLIPSE
0006800 C
0006900 C         FP=WD*EP/(PRX*PRX)
0007000           WD=FP*PRX*PRX/EP
0007100           AX1=(6.0*XK*XK*ES*FP/(PI*EP*RHO))**(1.0/3.0)
0007200           BX1=AX1/XK
0007300 C
0007400           PHZMX=1.5*FP/(EP*PI*AX1*BX1)
0007500 C         DDC=PRX*FS*(((4.5*RHO)/ES)*(FP/(PI*EP*XK))**2)**(1.0/3.0)
0007600           DDC=FS*(((4.5*RHO)/ES)*(FP/(PI*EP*XK))**2)**(1.0/3.0)
0007700           WRITE(6,1010) DDC,AX1,BX1
0007800           WRITE(4,1010) DDC,AX1,BX1
0007900  1010     FORMAT(1X,'DDC= ',D12.5,' AX1=',D12.5,' BX1=',D12.5)
0008000 C         PDXK=1.0/(XK*XK)
0008100 C         PXK=1.0/XK
0008200           T3=0.5*PRX*BX1*BX1
0008300           T2=0.5*PRY*AX1*AX1
0008400           Z1=0.5*ZD
0008500           Z2=0.5*ZC/XK
0008600           Z3=Z1*Z1
0008700           Z4=Z2*Z2
0008800           NXM1=NX-1
0008900 C
0009000 C         NODAL STRUCTURE
0009100 C
0009200           DZD= XN/MN
0009300           DZC= YM/MN
0009400           ZD=1.0/DZD
0009500           ZC=1.0/DZC
0009600           HDZD=0.5*DZD
0009700           HDZC=0.5*DZC
0009800           XD(1)=0.0
0009900           YD(1)=0.0
0010000           DO 5 I=2,NX
0010100           XD(I)=XD(I-1)+DZD
0010200 5         CONTINUE
0010300           DO 6 I=2,NY
0010400           YD(I)=YD(I-1)+DZC
0010500 6         CONTINUE
0010600           NCTR=NXHY-NX+MN+1
```

```
C
C         CURVATURE AND HERTZIAN PRESSURE
C
          DO 8 J=1,NHY
          JP=(J-1)*NX
          DO 9 I=1,NX
          N=I+JP
          S20=(YD(J)-YM)**2
          S21=(XD(I)-XN)**2
          SS1=S20+S21
          S(N)=T2*S20+T3*S21
          ECIR=1.0-SS1
          IF (ECIR.LE.0.0) GO TO 7
          PR(N)=PHZMX*ECIR**0.5
C         PRSV(N)=PR(N)
C         H(N)=HO+DDC
          GO TO 9
 7        PR(N)=0.0D0
C         PRSV(N)=PR(N)
C         H(N)=HO+S(N)*PRX
 9        CONTINUE
 8        CONTINUE
C
C         INFLUENCE COEFFICIENT
C
          DXK=XK*XK
          DO 65 JJ=1,NY
          JP=(JJ-1)*NX
          Y2=(JJ-1)*DZC
          CP=(Y2+HDZC)*XK
          CM=(Y2-HDZC)*XK
          DO 85 II=1,NX
          N=II+JP
          X2=(II-1)*DZD
          S1=DSQRT(DXK*(Y2+HDZC)**2+(X2+HDZD)**2)
          S2=DSQRT(DXK*(Y2-HDZC)**2+(X2+HDZD)**2)
          S3=DSQRT(DXK*(Y2+HDZC)**2+(X2-HDZD)**2)
          S4=DSQRT(DXK*(Y2-HDZC)**2+(X2-HDZD)**2)
          DP=X2+HDZD
          DM=X2-HDZD
          D(N)=(DP*DLOG((CP+S1)/(CM+S2))+CP*DLOG((DP+S1)/(DM+S3))+
     *         DM*DLOG((CM+S4)/(CP+S3))+CM*DLOG((DM+S4)/(DP+S2)))*BX1
C
 85       CONTINUE
 65       CONTINUE
C
C      INITIAL FILM THICKNESS VISCOSITY AND DENSITY CALCULATION
C
 10       CONTINUE
          CALL SM2(NX,NY,NHY,NXY,NXHY,XD,YD,D,H,W,S,PR,PHI)
          HNTH=DDC+HO
C      WRITE(6,3401) HMIN,NHSAVE,W(NCTR),H(NCTR)
C      WRITE(6,3401) HMIN,NHSAVE,W(NCTR),H(NCTR)
 3401     FORMAT(3X,' HMIN=',D14.5,' NHSAVE=',I6,' W(NCTR)=',D14.5,' H(NCTR)=',D14.5)
```

```
3016100  312  CONTINUE
3016200       DLW=W(NCTR)/DDC-1.0
3016220       DLW1=(W(NCTR)+W(NCTR-1))/(2.0*DDC)-1.0
3016300       DLH=H(NCTR)-HMIN
3016320       DLH1=(H(NCTR)+H(NCTR-1))/2.0-HMIN
3016400       WRITE (6,300) NX,NY,NHY,MN,FP
3016500       WRITE (4,300) NX,NY,NHY,MN,FP
3016600  300  FORMAT(1X,'NX=',I5,' NY=',I5,' NHY=',I5,' MN=',I5,' FP=',D10.5)
3016700       WRITE (6,250)  ZD,ZC,XI,YI
3016800       WRITE (4,250)  ZD,ZC,XI,YI
3016900  250  FORMAT(1X,'ZD=',D10.4,' ZC=',D10.4,' XI=',D10.4,' YI=',D10.4,1X)
3017000       WRITE(6,500) PHZMX,DLW,DLH,RX,RY,R
3017100       WRITE(4,500) PHZMX,DLW,DLH,RX,RY,R
3017200  500  FORMAT(1X,'PHZMX=',D11.5,' DLW=',D11.5,' DLH=',D11.5,' RX=',
              D11.5,' RY=',D11.5,' R=',D11.5,)
3017220       WRITE(6,600) DLW1,DLH1
3017225       WRITE(4,600) DLW1,DLH1
3017240  600  FORMAT(1X,'DLW1= ',D14.5,' DLH1= ',D14.5)
3017300       DO 50 JW=1,NHY
3017400       IWP=(JW-1)*NX
3017500       IE=IWP+1
3017600       IS=IWP+NX
3017700       PRINT 150,JW
3017800       PRINT 200,(W(M),M=IE,IS)
3017900       PRINT 200,(H(M),M=IE,IS)
3018000       WRITE(6,150) JW
3018100       WRITE(6,200)(W(M),M=IE,IS)
3018200       WRITE(6,200)(H(M),M=IE,IS)
3018300   50  CONTINUE
3018400  150  FORMAT(/5X,'JW=',I5)
3018500  200  FORMAT(/,10(1X,D12.5))
3018600       STOP
3018700       END
```

```
000020 C     CHHR
000100           IMPLICIT REAL*8(A-H,O-Z)
000300           DIMENSION XD(150),YD(70),PR(3600)
000400           DIMENSION D(39,39,9)
000500           DIMENSION W(2000),H(2000),S(2000)
000600           DIMENSION DENS(2000),VIS(2000),XMU(2000),PHI(2000)
000620           COMMON B222,B322,B422,B522,B212,B312,B232,B332,B423,B523,B421,B521
000640           COMMON/AA/HO,PRX,HMIN,NHSAVE
000800           NAMELIST /INPUT/HO,SMU,SMV,EP,FP
000900           NAMELIST/OUTPUT/G,ALPHA,RBY,XK,PBAR,PCHECK,FBAR,FCHECK,STRS,HAMRK
001000 C         DATA PI/3.14159265359D0/
001100 C         DATA RAX,RAY,RBX/1.11125D0,1.11125D0,1.0D12/
001200 C         ***   ***   ***
001300 C
001400 C         DATA RX/1.11125D0/
001500 C         DATA RAY,RBY/1.11125D0,-1.1861150D0/
001600           DATA XI,YI,MN/0.0,0.0,19/
001700           DATA PI,EP/3.14159265359D0,21.97D06/
001800           DATA FP,RX,RY/8.964D0, 0.5558D0,0.5558D0/
001900 C    ***
002000 C         DATA ZD,ZC/13.0D0,5.0D0/
002100           DATA NX,NHY/39,20/
002200           DATA XH,YM/1.0D0,1.0D0/
002300 C         DATA HO/0.0/
002400 C
002500           HO=0.0
002600 C         RY=1.0/((1.0/RAY)+(1.0/RBY))
002700           NXHY=NX*NHY
002800           NY=2*NHY-1
002900           NXY=NX*NY
003000           NXM1=NX-1
003100 C
003200 C         CURVATURE SUM AND DIFFERENCE
003300 C
003400           PRX=1.0/RX
003500           PRY=1.0/RY
003600           RHO=PRX+PRY
003700           GAMMA=(PRX-PRY)/RHO
003800           ALPHA=PRX/PRY
003900           PAL=1.0/ALPHA
004000           PDAL=PAL*PAL
004100 C
004200 C         INITIAL GUESS FROM SIMPLIFY EQ
004300 C
004400           Q=PI/2.0-1.0
004500           FSS=PI/2.0+Q*DLOG(ALPHA)
004600           ESS=1.0+Q/ALPHA
004700           XKK=ALPHA**(2.0D0/PI)
004800 C
004900 C         ELLIPTIC INTEGRALS ES AND FS
005000 C
005100 C         XK=SQRT(2.0D0)
005200           XK=XKK
```

```
005300           ES=ESS
005400           FS=FSS
005500 C
005600 C         XK IS THE ELLIPTICITY PARAMATER
005700 C
005800           KITER=0
005900  1        KITER=KITER+1
006000           AK=SQRT(1.0D0-(1.0D0/(XK**2)))
006100           CALL CEL(FS,ES,AK,IER)
006200           XJK=SQRT((2.0*FS-ES*(1.0+GAMMA))/(ES*(1.0-GAMMA)))
006300           A9=XK-XJK
006400           XK=XJK
006500           IF(DABS(A9).GT.1.0D-8) GO TO 1
006600 C
006700 C         INITIAL SEMIMAJOR AND SEMIMINOR AXES OF CONTACT ELLIPSE
006800 C
006900 C         FP=WD*EP/(PRX*PRX)
007000           WD=FP*PRX*PRX/EP
007100           AX1=(6.0*XK*XK*ES*FP/(PI*EP*RHO))**(1.0/3.0)
007200           BX1=AX1/XK
007300 C
007400           PHZMX=1.5*FP/(EP*PI*AX1*BX1)
007500 C         DDC=PRX*FS*(((4.5*RHO)/ES)*(FP/(PI*EP*XK))**2)**(1.0/3.0)
007600           DDC=FS*(((4.5*RHO)/ES)*(FP/(PI*EP*XK))**2)**(1.0/3.0)
007700           WRITE(6,1010) DDC,AX1,BX1
007800           WRITE(4,1010) DDC,AX1,BX1
007900  1010     FORMAT(1X,'DDC= ',D12.5,' AX1=',D12.5,' BX1=',D12.5)
008000 C         PDXK=1.0/(XK*XK)
008100 C         PXK=1.0/XK
008200           T3=0.5*PRX*BX1*BX1
008300           T2=0.5*PRY*AX1*AX1
008400           Z1=0.5*ZD
008500           Z2=0.5*ZC/XK
008600           Z3=Z1*Z1
008700           Z4=Z2*Z2
008800           NXM1=NX-1
008900 C
009000 C         MODAL STRUCTURE
009100 C
009200           DZD= XM/MM
009300           DZC= YM/MM
009400           ZD=1.0/DZD
009500           ZC=1.0/DZC
009510           RDZD=BX1*DZD
009520           RDZC=AX1*DZC
009530           RZD=1.0/RDZD
009540           RZC=1.0/RDZC
009600           HDZD=0.5*DZD
009700           HDZC=0.5*DZC
009800           XD(1)=0.0
009900           YD(1)=0.0
010000           DO 5 I=2,NX
010100           XD(I)=XD(I-1)+DZD
010200  5        CONTINUE
```

```
010300           DO 6 I=2,NY
010400           YD(I)=YD(I-1)+DZC
010500 6         CONTINUE
010600           NCTR=NXNY-NX+MN+1
010700 C
010800 C         CURVATURE AND HERTZIAN PRESSURE
010900 C
011000           DO 8 J=1,NNY
011100           JP=(J-1)*NX
011200           DO 9 I=1,NX
011300           N=I+JP
011400           S20=(YD(J)-YM)**2
011500           S21=(XD(I)-XM)**2
011600           SS1=S20+S21
011700           S(N)=T2*S20+T3*S21
011800           ECIR=1.0-SS1
011900           IF (ECIR.LE.0.0) GO TO 7
012000           PR(N)=PHZMX*ECIR**0.5
012100 C         PRSV(N)=PR(N)
012200 C         H(N)=HO+DDC
012300           GO TO 9
012400  7        PR(N)=0.0D0
012500 C         PRSV(N)=PR(N)
012600 C         H(N)=HO+S(N)*PRX
012700  9        CONTINUE
012800  8        CONTINUE
012900 C
012920 C         INFLUENCE COEFFICIENT
012940 C
012960           RZE=RZD
012980           RZDE=RZD/2.0
013000           B122=RZD*RZE*RZC*RZC
013020           B112=-RZD*RZDE*RZC*RZC
013040           B132=-RZDE*RZE*RZC*RZC
013060           B123=-B122/2.0
013080           B113=-B112/2.0
013100           B133=-B132/2.0
013120           B121=B123
013140           B111=B113
013160           B131=B133
013180           DO 65 JJ=1,NY
013200           Y2=(JJ-1)*RDZC
013220           Y1=Y2-RDZC
013240           Y3=Y2+RDZC
013260           B422=-(Y3+Y1)
013280           B522=Y3*Y1
013300           B423=-(Y2+Y1)
013320           B523=Y2*Y1
013340           B421=-(Y2+Y3)
013360           B521=Y2*Y3
013380           DO 85 II=1,NX
013400           X2=(II-1)*RDZD
013420           X1=X2-RDZD
013440           X3=X2+RDZD
```

```
013460           B222=-(X3+X1)
013480           B322=X3*X1
013500           B212=-(X3+X2)
013520           B312=X3*X2
013540           B232=-(X1+X2)
013560           B332=X1*X2
013580           D(II,JJ,5)=B122*(F22(X1,Y1)+F22(X3,Y3)-F22(X1,Y3)-F22(X3,Y1))
013600           D(II,JJ,4)=B112*(F12(X1,Y1)+F12(X3,Y3)-F12(X1,Y3)-F12(X3,Y1))
013620           D(II,JJ,6)=B132*(F32(X1,Y1)+F32(X3,Y3)-F32(X1,Y3)-F32(X3,Y1))
013640           D(II,JJ,8)=B123*(F23(X1,Y1)+F23(X3,Y3)-F23(X1,Y3)-F23(X3,Y1))
013660           D(II,JJ,7)=B113*(F13(X1,Y1)+F13(X3,Y3)-F13(X1,Y3)-F13(X3,Y1))
013680           D(II,JJ,9)=B133*(F33(X1,Y1)+F33(X3,Y3)-F33(X1,Y3)-F33(X3,Y1))
013700           D(II,JJ,2)=B121*(F21(X1,Y1)+F21(X3,Y3)-F21(X1,Y3)-F21(X3,Y1))
013720           D(II,JJ,1)=B111*(F11(X1,Y1)+F11(X3,Y3)-F11(X1,Y3)-F11(X3,Y1))
013740           D(II,JJ,3)=B131*(F31(X1,Y1)+F31(X3,Y3)-F31(X1,Y3)-F31(X3,Y1))
013760 85        CONTINUE
013780 65        CONTINUE
015200 C
015300 C      INITIAL FILM THICKNESS VISCOSITY AND DENSITY CALCULATION
015400 C
015500   10       CONTINUE
015600          CALL SA1(NX,NY,NHY,NXY,NXHY,XD,YD,D,W,S,PR,PHI)
015700           HNTH=DDC+HO
015800C        WRITE(4,3401) HMIN,NHSAVE,W(NCTR),H(NCTR)
015900C        WRITE(6,3401) HMIN,NHSAVE,W(NCTR),H(NCTR)
016000   3401    FORMAT(3X,' HMIN=',D14.5,' NHSAVE=',I6,' W(NCTR)=',D14.5,' H(NCTR)=',D14.5)
016100   312     CONTINUE
016200           DLW=W(NCTR)/DDC-1.0
016300           DLH=H(NCTR)-HMIN
016400           WRITE (6,300) NX,NY,NHY,MN,FP
016500           WRITE (4,300) NX,NY,NHY,MN,FP
016600 300       FORMAT(1X,'NX=',I5,' NY=',I5,' NHY=',I5, ' MN=',I5,' FP=',D10.5)
016700           WRITE (6,250)  ZD,ZC,XI,YI
016800           WRITE (4,250)  ZD,ZC,XI,YI
016900 250       FORMAT(1X,'ZD=',D10.4,' ZC=',D10.4,' XI=',D10.4,' YI=',D10.4,1X)
017000           WRITE(6,500) PHZMX,DLW,DLH,RX,RY,R
017100           WRITE(4,500) PHZMX,DLW,DLH,RX,RY,R
017200 500       FORMAT(1X,'PHZMX='D11.5,' DLW=',D11.5,' DLH=',D11.5,' RX=',D11.5,
                 ' RY=',D11.5,' R=',D11.5,)
017300           DO 50 JW=1,NHY
017400           IWP=(JW-1)*NX
017500           IE=IWP+1
017600           IS=IWP+NX
017700           PRINT 150,JW
017800           PRINT 200,(W(M),M=IE,IS)
017900           PRINT 200,(H(M),M=IE,IS)
018000           WRITE(6,150) JW
018100           WRITE(6,200)(W(M),M=IE,IS)
018200           WRITE(6,200)(H(M),M=IE,IS)
018300 50        CONTINUE
018400 150       FORMAT(/5X,'JW=',I5)
018500 200       FORMAT(/,10(1X,D12.5))
018600           STOP
018700           END
```

APPENDIX 4

COMPUTER PROGRAM LIST 3

PROGRAM NAME	UTILITY
SEHLI	Analyze the surface roughness effect on the EHL elliptical contacts.
SAI	Subprogram used to calculate the deformation under contact stresses.

```
000020 C          SEHLI
000100           IMPLICIT REAL*8(A-H,O-Z)
000200           REAL*4 XE(70)
000300           DIMENSION XD(150),YD(70),PR(5000)
000400           DIMENSION FF11(1800),FF22(1800)
000500           DIMENSION D(69,17,9)
000600           DIMENSION W(1600),H(1600),S(1600),GPR(3200)
000700           DIMENSION DENS(1800),VIS(1800),XMU(1800),PHI(1800)
000800           DIMENSION A(1800),B(1800),C(1800),DLZ(1800),XL(1800),XM(1800)
000900           DIMENSION PRLD(1800),DVLD(1800)
001000           DIMENSION ZPR(1800),PRSV(1800)
001100           COMMON B222,B322,B422,B522,B212,B312,B232,B332,B423,B523,B421,B521
001200           COMMON/AA/HO,PRX,HMIN,NHSAVE
001300           COMMON/BB/CF11,CF22
001400           NAMELIST /INPUT/HO,SMU,SMV,EP,FP,XLMD,GMM
001500           NAMELIST/OUTPUT/G,ALPHA,RBY,XK,PBAR,PCHECK,FBAR,FCHECK,STRS,HAMRK
001600           NAMELIST/FRICT/CFRI,CFRICK
001700           DATA PI/3.14159265359D0/
001800           DATA PIVAS,VISO,VISE/4858.7D0,4.11D-6,6.31D-9/
001900           DATA ELPHA,BETA/5.82744D-6,1.68348D-5/
002000           DATA Z/0.67D0/
002100           DATA ZZZ/0.13/
002200           DATA PHIMX/100.0D-10/
002300 C         ***   ***   ***
002400           DATA ROSM1,ROSM2,ROSM3,ROSM4,ROSM5/50.0,5.0,5.5,5.0,70.0/
002500           DATA ROSM/100.0/
002600           DATA OERR,ITER,TAU,ITSOR/500.0,0,0.0,0/
002700           DATA ORF/1.6D0/
002800           DATA DEL1,DEL2,DEL3/4.0D-4,0.05#D-2,0.3D-3/
002900           DATA DDEL,DDEL1/0.025D0,0.09D0/
003000           DATA ITMAX,NFITMX,INTAU/138,40,0/
003100 C
003200 C
003300 C
003400           DATA RX/1.11125D0/
003500           DATA RAY,RBY/1.11125D0,-1.1861150D0/
003600 C   ***
003700           DATA ZD,ZC/13.0D0,5.0D0/
003800           DATA NX,NHY/69,9/
003900           DATA XN,YM/4.0D0,1.6D0/
004000 C
004100           READ(5,INPUT)
004200           RY=1.0/((1.0/RAY)+(1.0/RBY))
004300           NXHY=NX*NHY
004400           NY=2*NHY-1
004500           NXY=NX*NY
004600           NXM1=NX-1
004700           HSMIN=6.4237D-6*RX
004800           SGM=HSMIN/XLMD
004900           CF11=3.0*((GMM-2.0)/(GMM+1.0))*SGM*SGM
005000           CF22=3.0*((1.0-2.0*GMM)/(1.0+GMM))*SGM*SGM
005100           CFDP=(3.0/(GMM+1.0))*SGM*SGM
005200 C
005300 C         CURVATURE SUM AND DIFFERENCE
```

```
005400 C
005500           PRX=1.0/RX
005600           PRY=1.0/RY
005700           RHO=PRX+PRY
005800           GAMMA=(PRX-PRY)/RHO
005900           ALPHA=PRX/PRY
006000           PAL=1.0/ALPHA
006100           PDAL=PAL*PAL
006200 C
006300 C         INITIAL GUESS FROM SIMPLIFY EQ
006400 C
006500           Q=PI/2.0-1.0
006600           FSS=PI/2.0+Q*DLOG(ALPHA)
006700           ESS=1.0+Q/ALPHA
006800           XKK=ALPHA**(2.0D0/PI)
006900 C
007000 C         ELLIPTIC INTEGRALS ES AND FS
007100 C
007200 C         XK=SQRT(2.0D0)
007300           XK=XKK
007400           ES=ESS
007500           FS=FSS
007600 C
007700 C         XK IS THE ELLIPTICITY PARAMATER
007800 C
007900           KITER=0
008000    1      KITER=KITER+1
008100           AK=SQRT(1.0D0-(1.0D0/(XK**2)))
008200           CALL CEL(FS,ES,AK,IER)
008300           XJK=SQRT((2.0*FS-ES*(1.0+GAMMA))/(ES*(1.0-GAMMA)))
008400           A9=XK-XJK
008500           XK=XJK
008600           IF(DABS(A9).GT.1.0D-8) GO TO 1
008700 C
008800 C         INITIAL SEMIMAJOR AND SEMIMINOR AXES OF CONTACT ELLIPSE
008900 C
009000 C         FP=WD*EP/(PRX*PRX)
009100           WD=FP*PRX*PRX/EP
009200           AX1=(6.0*XK*XK*ES*FP/(PI*EP*RHO))**(1.0/3.0)
009300           BX1=AX1/XK
009400 C
009500           PHZMX=1.5*FP/(EP*PI*AX1*BX1)
009600           DDC=PRX*FS*((((4.5*RHO)/ES)*(FP/(PI*EP*XK))**2)**(1.0/3.0)
009700           WRITE(6,1010) DDC,AX1,BX1
009800           WRITE(4,1010) DDC,AX1,BX1
009900  1010     FORMAT(1X,'DDC= ',D12.5,' AX1=',D12.5,' BX1=',D12.5)
010000 C         PDXK=1.0/(XK*XK)
010100 C         PXK=1.0/XK
010200 C
010300 C         NODAL STRUCTURE
010400 C
010500           DZD=1.0/ZD
010600           DZC=1.0/ZC
010700           RDZD=BX1*DZD
```

```
010800           RDZC=AX1*DZC
010900           RZD=1.0/RDZD
011000           RZC=1.0/RDZC
011100           HDZD=0.5*DZD
011200           HDZC=0.5*DZC
011300           XD(1)=HDZD
011400           YD(1)=0.0
011500 C         RXD(1)=XD(1)*BX1
011600 C         RYD(1)=YD(1)*AX1
011700           DO 5 I=2,NX
011800           XD(I)=XD(I-1)+DZD
011900 C         RXD(I)=XD(I)*BX1
012000 5         CONTINUE
012100           DO 6 I=2,NY
012200           YD(I)=YD(I-1)+DZC
012300 C         RYD(I)=YD(I)*AX1
012400 6         CONTINUE
012500           T3=0.5*PRX*BX1*BX1
012600           T2=0.5*PRY*AX1*AX1
012700           Z1=0.5*ZD
012800           Z2=0.5*ZC/XK
012900           Z3=Z1*Z1
013000           Z4=Z2*Z2
013100 C
013200 C      DIMENSIONLESS PARAMETER GROUPING
013300 C
013400        V=SQRT(SMU**2+SMV**2)
013500        THETA=ATAN(SMV/SMU)
013600        U=VISO*PRX*V/EP
013700        PHEE=1./(1.+(2.*PRY)/(3.*PRX))
013800        Q1=VISE/VISO
013900        Q2=EP/19608.5268
014000        Q5=ELPHA*EP
014100        Q6=BETA*EP
014200        G=EP/PIVAS
014300           NCGF1=52
014400           NCIR=NXHY-NX+NCGF1
014500           WRITE(6,INPUT)
014600 C
014700 C         CURVATURE AND HERTZIAN PRESSURE
014800 C
014900           DO 8 J=1,NHY
015000           JP=(J-1)*NX
015100           DO 9 I=1,NX
015200           N=I+JP
015300           S20=(YD(J)-YM)**2
015400           S21=(XD(I)-XN)**2
015500           S51=S20+S21
015600           S(N)=T2*S20+T3*S21
015700           ECIR=1.0-S51
015800           IF (ECIR.LE.0.0) GO TO 7
015900           PR(N)=PHZMX*ECIR**0.5
016000           PRSV(N)=PR(N)
016100           GO TO 9
```

```
016200  7        PR(N)=0.0D0
016300           PRSV(N)=PR(N)
016400  9        CONTINUE
016500  8        CONTINUE
016600 C
016700 C         INFLUENCE COEFFICIENT
016800 C
016900           RZE=RZD
017000           RZDE=RZD/2.0
017100           B122=RZD*RZE*RZC*RZC
017200           B112=-RZD*RZDE*RZC*RZC
017300           B132=-RZDE*RZE*RZC*RZC
017400           B123=-B122/2.0
017500           B113=-B112/2.0
017600           B133=-B132/2.0
017700           B121=B123
017800           B111=B113
017900           B131=B133
018000           DO 65 JJ=1,NY
018100           Y2=(JJ-1)*RDZC
018200           Y1=Y2-RDZC
018300           Y3=Y2+RDZC
018400           B422=-(Y3+Y1)
018500           B522=Y3*Y1
018600           B423=-(Y2+Y1)
018700           B523=Y2*Y1
018800           B421=-(Y2+Y3)
018900           B521=Y2*Y3
019000           DO 85 II=1,NX
019100           X2=(II-1)*RDZD
019200           X1=X2-RDZD
019300           X3=X2+RDZD
019400           B222=-(X3+X1)
019500           B322=X3*X1
019600           B212=-(X3+X2)
019700           B312=X3*X2
019800           B232=-(X1+X2)
019900           B332=X1*X2
020000           D(II,JJ,5)=B122*(F22(X1,Y1)+F22(X3,Y3)-F22(X1,Y3)-F22(X3,Y1))
020100           D(II,JJ,4)=B112*(F12(X1,Y1)+F12(X3,Y3)-F12(X1,Y3)-F12(X3,Y1))
020200           D(II,JJ,6)=B132*(F32(X1,Y1)+F32(X3,Y3)-F32(X1,Y3)-F32(X3,Y1))
020300           D(II,JJ,8)=B123*(F23(X1,Y1)+F23(X3,Y3)-F23(X1,Y3)-F23(X3,Y1))
020400           D(II,JJ,7)=B113*(F13(X1,Y1)+F13(X3,Y3)-F13(X1,Y3)-F13(X3,Y1))
020500           D(II,JJ,9)=B133*(F33(X1,Y1)+F33(X3,Y3)-F33(X1,Y3)-F33(X3,Y1))
020600           D(II,JJ,2)=B121*(F21(X1,Y1)+F21(X3,Y3)-F21(X1,Y3)-F21(X3,Y1))
020700           D(II,JJ,1)=B111*(F11(X1,Y1)+F11(X3,Y3)-F11(X1,Y3)-F11(X3,Y1))
020800           D(II,JJ,3)=B131*(F31(X1,Y1)+F31(X3,Y3)-F31(X1,Y3)-F31(X3,Y1))
020900 85        CONTINUE
021000 65        CONTINUE
021100           IF(MST.NE.1) GO TO 10
021200         READ (9) (PR(N),N=1,NXHY)
021300         READ (9) H001,(H(N),N=1,NXHY)
021400 C         GO TO 99
021500           DO 318 I=1,NXHY
```

```
021600           PR(I)=PR(I)*SQRT(H0/H001)
021700           PRSV(I)=PR(I)
021800  318      H(I)=H0-H001+H(I)
021900 C
022000 C      INITIAL FILM THICKNESS VISCOSITY AND DENSITY CALCULATION
022100 C
022200  10       CONTINUE
022300         CALL SAI(NX,NY,NHY,NXY,NXHY,XD,YD,D,H,W,S,PR,PHI,FF11,FF22)
022700  3401     FORMAT(3X,' HMIN=',D14.5,' NHSAVE=',I6,' HNTH=',D14.5,' H(NCTR)=',D14.5)
022800         DO 21 N=1,NXHY
022900         DENS(N)=1.+(Q5*PR(N))/(1.+Q6*PR(N))
023000 C          DENS(N)=1.0
023100         VIS(N)=Q1**(1.-(1.+Q2*PR(N))**Z)
023200         XMU(N)=DENS(N)/VIS(N)
023300 21      CONTINUE
023400 C
023500 C      RELAXATION COEFFICIENTS A,B,C,D,L,AND M
023600 C
023700           NFITER=0
023800  11       NFITER=NFITER+1
023900           OERR=5.0
024000           ITER=0
024100 22      ITER=ITER+1
024200         DO 24 J=2,NHY
024300           JP=(J-1)*NX
024400         DO 23 I=2,NXM1
024500         N=I+JP
024600         N1=N+1
024700         N2=N-1
024800         N3=N+NX
024900         N4=N-NX
025000         IF (J.EQ.NHY) N3=N4
025100         Y1=XMU(N1)*FF11(N1)
025200         Y2=XMU(N2)*FF11(N2)
025300         Y3=XMU(N3)*FF22(N3)
025400         Y4=XMU(N4)*FF22(N4)
025500         Y5=H(N1)
025600         Y6=H(N2)
025700         Y7=H(N)
025800         Y8=H(N3)
025900         Y9=H(N4)
026000         Y10=Y1*DSQRT(Y5)
026100         Y11=Y2*DSQRT(Y6)
026200         Y12=Y3*DSQRT(Y8)
026300         Y13=Y4*DSQRT(Y9)
026400           A(N)=Z3*(3.*Y1+Y2)
026500           B(N)=Z4*(Y3+3.*Y4)
026600           C(N)=Z3*(Y1+3.*Y2)
026700           DLZ(N)=Z4*(3.*Y3+Y4)
026800           XL1=4.*(Z3*(Y1+Y2)+Z4*(Y3+Y4))
026900           XL2=1.5/(Y7*1.5)
027000           XL3=Z3*(Y10*(3.*Y5-4.*Y7+Y6)+Y11*(Y5-4.*Y7+3.*Y6))
027100           XL4=Z4*(Y12*(3.*Y8-4.*Y7+Y9)+Y13*(Y8-4.*Y7+3.*Y9))
027200           XL(N)=XL1+XL2*(XL3+XL4)
```

```
027300          XM1=12.*U*BX1*PRX/(Y7**1.5)
027400          XM2=(Y5*DENS(N1)-Y6*DENS(N2))*COS(THETA)
027500          XM3=(Y8*DENS(N3)-Y9*DENS(N4))*SIN(THETA)
027600          XM(N)=XM1*(Z1*XM2+Z2*XM3)
027700 23     CONTINUE
027800 24     CONTINUE
027900 C
028000 C      RELAXATION FORMULA
028100 C
028200  20      CONTINUE
028300          ITSOR=0
028400 25        ITSOR=ITSOR+1
028500          STDN=0.0
028600          SERR=0.0
028700          SUM1=0.0
028800          MSUM9=0
028900        DO  30 J=2,NHY
029000          JP=(J-1)*NX
029100        MEND=0
029200        DO  29 I=2,NXM1
029300        MN=I+JP
029400        MNA=MN+1
029500        MNB=MN-1
029600        MNC=MN+NX
029700        MND=MN-NX
029800        IF(J.EQ.NHY) MNC=MND
029900        ZPR(MN)=PHI(MN)-ORF*(PHI(MN)+(XM(MN)-A(MN)*PHI(MNA)-B(MN)*PHI(MND)
              -C(MN)*PHI(MNB)-DLZ(MN)*PHI(MNC))/XL(MN))
030000          IF(ZPR(MN).LT.PHIMX) GO TO 26
030100          MSUM9=MSUM9+1
030200          ZPR(MN)=PHIMX
030300 26     CONTINUE
030400        IF (ZPR(MN).LE.0.) GO TO  27
030500          Y18=(ZPR(MN)-PHI(MN))/ZPR(MN)
030600 C        SUM1=SUM1+DABS(Y18)
030700          STDN=STDN+DABS(ZPR(MN))
030800          SERR=SERR+DABS(ZPR(MN)-PHI(MN))
030900        GO TO  28
031000 27     ZPR(MN)=0.0D0
031100          STDN=STDN+DABS(ZPR(MN))
031200          SERR=SERR+DABS(ZPR(MN)-PHI(MN))
031300        MEND=MEND+1
031400        IF (MEND .EQ. 1) XE(J)=XD(I)
031500 28     PHI(MN)=ZPR(MN)
031600 29     CONTINUE
031700 30     CONTINUE
031800          SERR=SERR/STDN
031900        IF (SERR.GT.DEL1) GO TO  25
032000 C      IF (SUM1.GT.DDEL1) GO TO  25
032100 31     CONTINUE
032200 C
032300 C       FILM THICKNESS   VISCOSITY AND DENSITY ITERATION
032400 C
032500 311  CONTINUE
032600        PRMX=.1D-13
```

```
032700           ROSM=ROSM1
032800           TDN=0.0
032900           ERR1=0.0
033000           SUM2=0.0
033100           DO 54 J=2,NHY
033200           JP=(J-1)*NX
033300           DO 54 I=2,NXM1
033400           N=I+JP
033500           A(N)=PHI(N)/(H(N)**1.5)
033600           DLZ(N)=A(N)-PR(N)
033700           TDN=TDN+DABS(A(N))
033800           ERR1=ERR1+DABS(DLZ(N))
033900    54     CONTINUE
034000           ERR=ERR1/TDN
034100           WRITE(4,3000) ITER,ERR,OERR,INTAU
034200           WRITE(6,3000) ITER,ERR,OERR,INTAU
034300  3000     FORMAT(1X,'ITER=',I5,'  ERR=',D14.5,'  OERR=',D14.5,'  INTAU=',I5)
034400 C         IF(ERR.LE.0.05) ROSM=ROSM2
034500 C         IF(ERR.GE.0.5) ROSM=ROSM3
034600 C         IF(ERR.GE.1.0) ROSM=ROSM4
034700 C         IF(INTAU.LT.3.AND.ERR.GE.1.125*OERR) GO TO 411
034800           OERR=ERR
034900 C         OROSM=ROSM
035000 C         INTAU=0
035100 C         DO 414 J=2,NHY
035200 C         JP=(J-1)*NX
035300 C         DO 415 I=2,NXM1
035400 C         N=I+JP
035500 C         DVLD(N)=DLZ(N)
035600 C         PRLD(N)=PR(N)
035700 C415      CONTINUE
035800 C414      CONTINUE
035900 C         GO TO 312
036000 C411      INTAU=INTAU+1
036100 C         ROSM=OROSM*2.0
036200 C         IF(ERR.GE.3.0*OERR) ROSM=OROSM*4.0
036300 C         IF(ERR.GE.5.0*OERR) ROSM=OROSM*6.0
036400 C         OROSM=ROSM
036500 C         DO 416 J=2,NHY
036600 C         JP=(J-1)*NX
036700 C         DO 417 I=2,NXM1
036800 C         N=I+JP
036900 C         DLZ(N)=DVLD(N)
037000 C         PR(N)=PRLD(N)
037100 C417      CONTINUE
037200 C416      CONTINUE
037300   312    CONTINUE
037400         DO 315 J=2,NHY
037500            JP=(J-1)*NX
037600            NEND=0
037700         DO 316 I=2,NXM1
037800         N=I+JP
037900            PR(N)=(PHI(N)/(H(N)**1.5)+(ROSM-1.0)*PRSV(N))/ROSM
038000            PRSV(N)=PR(N)
```

```
038100       IF(PR(N).LT.PRMX) GO TO 33
038200       PRMX=PR(N)
038300       NPSAVE=N
038400  33      CONTINUE
038500          IF(PR(N) .GT. 0.12780D0) PR(N)=0.12780D0
038600       DENSN=1.+(Q5*PR(N))/(1.+Q6*PR(N))
038700 C        DENSN=1.0
038800       VISN=Q1**(1.-(1.+Q2*PR(N))**Z)
038900       XMUN=DENSN/VISN
039000       Y99=(XMUN-XMU(N))/XMUN
039100       SUM2=SUM2+DABS(Y99)
039200       DENS(N)=DENSN
039300       VIS(N)=VISN
039400 316    XMU(N)=XMUN
039500 315    CONTINUE
039600       VSMX=Q1**(1.-(1.+Q2*PRMX)**Z)
039700       WRITE (4,480) ITSOR,SERR,SUM1
039800       WRITE (6,480) ITSOR,SERR,SUM1
039900 480    FORMAT(5X,'ITSOR=',I8,6X,' SERR=',D14.5,' SUM1=',D14.5)
040000          WRITE(4,3200) ROSM,PRMX,VSMX,NPSAVE
040100          WRITE(6,3200) ROSM,PRMX,VSMX,NPSAVE
040200  3200    FORMAT(5X,'  ROSM=',D14.5,' PRMX=',D14.5,' VSMX=',D14.5,' NPSAVE=',I6)
040300        CALL SAI(NX,NY,NHY,NXY,NXHY,XD,YD,D,H,W,S,PR,PHI,FF11,FF22)
040400  4       WRITE(4,3400) HMIN,NHSAVE
040500          WRITE(6,3400) HMIN,NHSAVE
040600  3400    FORMAT(5X,' HMIN=',D14.5,' NHSAVE=',I6)
040700       WRITE(4,810) SUM2
040800       WRITE(6,810) SUM2
040900  810   FORMAT(6X ,5HSUM2=,D16.5)
041000       WRITE (10) (PR(N),N=1,NXHY)
041100       WRITE (10) HO,(H(N),N=1,NXHY)
041200       REWIND 10
041300          IF(ITER.NE.0.AND.ERR.LT.DEL2) GO TO 32
041400       IF(ITER.GT.ITMAX) GO TO 32
041500       GO TO 22
041600 C
041700 C      APPLIED NORMAL LOAD
041800 C
041900 32   CONTINUE
042000          QU4=0.0
042100          PSUM=0.0
042200          DO 37 I=2,NXM1
042300          QU1=2.0
042400          QU3=0.0
042500          IM=I/2
042600          IBM=IM+IM
042700          IF(IBM.NE.I) QU1=1.0D0
042800          DO 36 J=2,NY
042900          N=I+(J-1)*NX
043000          PSUM=PSUM+PR(N)
043100  36      QU3=QU3+PR(N)
043200  37      QU4=QU4+QU3*QU1
043300          FBAR=2.*EP*AX1*BX1*QU4/(3.*ZC*ZD)
043400          FCHECK=1.*EP*AX1*BX1*PSUM/(ZC*ZD)
```

```
043500           PBAR=FBAR*PRX*PRX/EP
043600           PCHECK=FCHECK*PRX*PRX/EP
043700           WRITE(6,2400) NFITER,FBAR,FCHECK
043800           WRITE(4,2400) NFITER,FBAR,FCHECK
043900  2400     FORMAT(1X,' NFITER=',I3,' FBAR=',D14.6,' FCHECK=',D14.6)
044000 C
044100 C
044200 C
044300           AX=(6.0*XK*XK*ES*FBAR/(PI*EP*RHO))**(1.0/3.0)
044400           BX=AX/XK
044500           CINLT=XD(NCGF1)/BX
044600           COULT=(XD(NX)-XD(NCGF1))/BX
044700           CSIDE=YD(NHY)/AX
044800           WRITE(6,1200) AX,BX,CINLT,COULT,CSIDE,AX1,BX1
044900  1200   FORMAT(1X,'AX=',D12.5,' BX=',D12.5,' CINLT=',D12.5,
                COULT=',D12.5,' CSIDE=',D12.5,'AX1=',D12.5,'BX1=',D12.5)
045000           SUM3=DABS((FP-FBAR)/FP)
045100           IF(SUM3.LE.DEL3.OR.NFITER.GT.NFITMX) GO TO 12
045200           IF(ERR.LT.0.030) ITMAX=60
045300           IF(ERR.LT.0.010.AND.NFITMX.LT.40) NFITMX=1+NFITMX
045400 C         IF(SUM3.LT.1.0D-3) DEL2=0.6*DEL2
045500           IF(ITER.GT.132) ROSM1=ROSM1+20.0
045600           IF(ITER.LE.5) XJENN=0.3D0
045700           IF(ITER.GT.5) XJENN=0.4D0
045800           IF(ITER.GT.10) XJENN=0.6D0
045900           IF(ITER.GT.25) XJENN=0.9D0
046000           HO=HO*(XJENN+(1.0-XJENN)*(FP/FBAR)**2ZZ)
046100           WRITE(6,4400) HO
046200           WRITE(4,4400) HO
046300  4400     FORMAT(1X,'HO=',D14.6)
046400  19       CONTINUE
046500           DO 440 J=1,NHY
046600           JP=(J-1)*NX
046700           DO 441 I=1,NX
046800           N=I+JP
046900           H(N)=HO+PRX*(S(N)+W(N))
047000  441      PHI(N)=PR(N)*(H(N)**1.5)
047100  440      CONTINUE
047200           GO TO 11
047300  12       CONTINUE
047400           STRS=1.5*FBAR/(PI*AX*BX)
047500           HAMRK=3.63*U**0.68*G**0.49*PBAR**(-0.073)*(1.0-DEXP(-0.68*XK))
047600         HMHO=2.69*U**0.67*G**0.53*PBAR**(-0.067)*(1.0-0.61*DEXP(-0.73*XK))
047700 C
047800 C          FRICTION FORCE
047900 C
048000  99       CONTINUE
048100           DO 450 J=1,NHY
048200           JP=(J-1)*NX
048300           DO 452 I=2,NXM1
048400           N=I+JP
048500  452      GPR(N)=(H(N)+CFDP/H(N))*(PR(N+1)-PR(N-1))
048600  450      CONTINUE
048700           GSUM=0.0
048800           DO 451 J=1,NHY
```

```
048900           N=(J-1)*NX+1
049000           N1=(J-1)*NX+NX
049100           GPR(N)=(H(N)+CFDP/H(N))*(-3.0*PR(N)+4.0*PR(N+1)-PR(N+2))
049200           GPR(N1)=0.0
049300  451      CONTINUE
049400           NHYM1=NHY-1
049500           DO 465 J=1,NHYM1
049600           JQR=(NHY+J-1)*NX
049700           JQ=(NHY-J-1)*NX
049800           DO 465 I=1,NX
049900           M1=I+JQR
050000           M2=I+JQ
050100           GPR(M1)=GPR(M2)
050200  465        CONTINUE
050300           QU4=0.0
050400           PSUM=0.0
050500           DO 460 I=1,NXM1
050600           QU1=2.0
050700           QU3=0.0
050800           QU2=1.0
050900           IM=I/2
051000           IBM=IM+IM
051100           IF(IBM.NE.I) QU1=1.0D0
051200           IF(I.EQ.1) QU2=0.5
051300           DO 461 J=1,NY
051400           N=I+(J-1)*NX
051500           QV1=1.0
051600           IF(J.EQ.1.OR.J.EQ.NY) QV1=0.5
051700           PSUM=PSUM+GPR(N)*QV1*QU2
051800  461       QU3=QU3+GPR(N)*QV1
051900  460       QU4=QU4+QU3*QU1*QU2
052000           CFRI=AX1*BX1*EP*RX*RX*DZC*QU4/(FP*3.0*2.0)
052100           CFRICK=AX1*BX1*EP*RX*RX*DZC*PSUM/(FP*2.0*2.0)
052200           WRITE(6,1015) HMHO,H(NCTR),PR(NCTR)
052300           WRITE(4,1015) HMHO,H(NCTR),PR(NCTR)
052400  1015     FORMAT(1X,'HMHO=',D12.5,' H(NCTR)=',D12.5, ' PR(NCTR)=', D12.5)
052500 C
052600 C          OUTPUT
052700 C
052800        WRITE (6,OUTPUT)
052900           WRITE(6,FRICT)
053000           WRITE(4,FRICT)
053100 C          GO TO 63
053200 39      CONTINUE
053300           ICT=NXHY-NX+1
053400        WRITE(6,1750) (PR(N),N=ICT,NXHY)
053500 1750   FORMAT(1H ,2HPR/30(1H,10D13.5/))
053600        WRITE(6,1850) (H(N),N=ICT,NXHY)
053700 1850   FORMAT (1H ,1HH/30(1H ,10D13.5/))
053800        WRITE(6,1950) (PHI(N),N=ICT,NXHY)
053900 1950   FORMAT(1H ,3HPHI/30(1H ,10D13.5/))
054000        WRITE(6,2050) (S(N),N=ICT,NXHY)
054100 2050   FORMAT (1H ,1HS/30(1H ,10D13.5/))
054200        WRITE(6,2150) (DENS(N),N=ICT,NXHY)
```

```
      2150  FORMAT(1H ,7HDENSITY/30(1H ,10D13.5/))
            WRITE(6,2250) (VIS(N),N=ICT,NXHY)
      2250  FORMAT(1H.,9HVISCOSITY/30(1H ,10D13.5/))
               WRITE(6,2350) (XE(N),N=1,NHY)
       2350    FORMAT(1X,'XE'/20(1X,10D13.5/))
      43    CONTINUE
            WRITE(6,1700) (PR(N),N=1,NXHY)
      1700  FORMAT(1H ,2HPR/50(1H,10D13.5/))
            WRITE(6,1900) (H(N),N=1,NXHY)
      1900  FORMAT (1H ,1HH/50(1H ,10D13.5/))
            WRITE(6,1800) (PHI(N),N=1,NXHY)
      1800  FORMAT(1H ,3HPHI/50(1H ,10D13.5/))
      C     WRITE(6,2000) (S(N),N=1,NXHY)
      2000  FORMAT (1H ,1HS/50(1H ,10D13.5/))
      C     WRITE(6,2100) (DENS(N),N=1,NXHY)
      2100  FORMAT(1H ,7HDENSITY/50(1H ,10D13.5/))
            WRITE(6,2200) (VIS(N),N=1,NXHY)
      2200  FORMAT(1H ,9HVISCOSITY/50(1H ,10D13.5/))
      C
      53    CONTINUE
               WRITE(8) NX,NHY,NXHY,(PR(N),N=1,NXHY),(XD(N),N=1,NX),(YD(N),N=1,NHY),PRMX
               NCGF2=NCGF1+NZON2
               WRITE(8)NXY,NCGF1,NCGF2,JZON,(H(N),N=1,NXHY),RX,RY,AX,BX
       63   CONTINUE
            STOP
            END
```

```
0000020 C       ASHRI
0000100       SUBROUTINE SAI(NX,NY,NHY,NXY,NXHY,XD,YD,D,H,W,S,PR,PHI,FF11,FF22)
0000200         IMPLICIT REAL*8(A-H,O-Z)
0000300         DIMENSION D(NX,NY,9)
0000400         DIMENSION PR(NXY),PHI(NXHY),H(NXHY),W(NXHY),S(NXHY)
0000420         DIMENSION FF11(NXHY),FF22(NXHY)
0000500         DIMENSION XD(NX),YD(NY)
0000600         COMMON/AA/HO,PRX,HMIN,NHSAVE
0000620         COMMON/BB/CF11,CF22
0000700         DATA PI/3.14159265359D0/
0000800         NHYM1=NHY-1
0000900         DO 5 J=1,NHYM1
0001000         JQR=(NHY+J-1)*NX
0001100         JQ=(NHY-J-1)*NX
0001200         DO 5 I=1,NX
0001300         M1=I+JQR
0001400         M2=I+JQ
0001500         PR(M1)=PR(M2)
0001600  5      CONTINUE
0001700         DO 10 J=2,NY,2
0001800         JP=(J-1)*NX
0001900         DO 20 I=2,NX,2
0002000         N=I+JP
0002100 C       IF(PR(N).EQ.0.0) GO TO 20
0002200         N12=N-1
0002300         N32=N+1
0002400         N11=N12-NX
0002500         N21=N11+1
0002600         N31=N11+2
0002700         N13=N12+NX
0002800         N23=N13+1
0002900         N33=N13+2
0003000         DO 30 JW=1,NHY
0003100         JWP=(JW-1)*NX
0003200         JD=J-JW
0003300         JN=IABS(JD)+1
0003400         DO 40 IW=1,NX
0003500         M=IW+JWP
0003600         PW=W(M)
0003700         ID=I-IW
0003800         IN=IABS(ID)+1
0003900         IF(ID.GE.0.AND.JD.GE.0) GO TO 102
0004000         IF(ID.LT.0.AND.JD.LT.0) GO TO 103
0004100         IF(ID.GE.0.AND.JD.LT.0) GO TO 104
0004200                   GO TO 105
0004300  102    K12=N12
0004400         K32=N32
0004500         K23=N23
0004600         K13=N13
0004700         K33=N33
0004800         K21=N21
0004900         K11=N11
0005000         K31=N31
0005100                   GO TO 101
```

```
005200  103     K12=N32
005300          K32=N12
005400          K23=N21
005500          K13=N31
005600          K33=N11
005700          K21=N23
005800          K11=N33
005900          K31=N13
006000                  GO TO 101
006100  104     K12=N12
006200          K32=N32
006300          K23=N21
006400          K13=N11
006500          K33=N31
006600          K21=N23
006700          K11=N13
006800          K31=N33
006900                  GO TO 101
007000  102     K12=N32
007100          K32=N12
007200          K23=N23
007300          K13=N33
007400          K33=N13
007500          K21=N21
007600          K11=N31
007700          K31=N11
007800
007900  101     CONTINUE
008000          W22=D(IN,JN,5)*PR(N  )
008100          W12=D(IN,JN,4)*PR(K12)
008200          W32=D(IN,JN,6)*PR(K32)
008300          W23=D(IN,JN,8)*PR(K23)
008400          W13=D(IN,JN,7)*PR(K13)
008500          W33=D(IN,JN,9)*PR(K33)
008600          W21=D(IN,JN,2)*PR(K21)
008700          W11=D(IN,JN,1)*PR(K11)
008800          W31=D(IN,JN,3)*PR(K31)
008900          W(M)=(W22+W12+W32+W23+W13+W33+W21+W11+W31)+PW
009000  60      CONTINUE
009100  30      CONTINUE
009200  20      CONTINUE
009300  10      CONTINUE
009400  C
009500  C       FILM THICKNESS
009600  C
009700          HMIN=1.0
009800          DCFT=1.0/(60.0*PI)
009900          DO 55 J=1,NHY
010000          JP=(J-1)*NX
010100          DO 55 I=1,NX
010200          N=JP+I
010300          W(N)=DCFT*W(N)
010400          H(N)=HO+(S(N)+W(N))*PRX
010420          PDH=1.0/(H(N)*H(N))
```

```
:10440           FF11(N)=1.0+CF11*PDH
:10460           FF22(N)=1.0+CF22*PDH
:10500           IF(H(N).GT.HMIN) GO TO 51
:10600           HMIN=H(N)
:10700           NHSAVE=N
:10800    51     PHI(N)=PR(N)*(H(N)**1.5)
:10900    55     CONTINUE
:11000 C         WRITE(4,400) NHSAVE,HMIN
:11100 C         WRITE(6,400) NHSAVE,HMIN
:11200 C400      FORMAT(1X,'NHSAVE=',I10,'    HMIN=',D16.5)
:11300           RETURN
:11400           END
```

1. Report No.	2. Government Accession No.	3. Recipient's Catalog No.
NASA TM-87120		

4. Title and Subtitle	5. Report Date
Lubrication of Nonconformal Contacts	September 1985
	6. Performing Organization Code: 505-33-62

7. Author(s)	8. Performing Organization Report No.
Yeau-Ren Jeng	E-2728
	10. Work Unit No.

9. Performing Organization Name and Address	11. Contract or Grant No.
National Aeronautics and Space Administration Lewis Research Center Cleveland, Ohio 44135	
	13. Type of Report and Period Covered: Technical Memorandum
12. Sponsoring Agency Name and Address	14. Sponsoring Agency Code
National Aeronautics and Space Administration Washington, D.C. 20546	

15. Supplementary Notes

NASA Resident Research Associate from Case Western Reserve University (work performed under NASA Grant NCC 3-30).
This report was a dissertation submitted to the Faculty of Case Western Reserve University in partial fulfillment of the requirements for the degree of Doctor of Philosophy in January 1986.

16. Abstract

Minimum film thickness results for piezoviscous-rigid regime of lubrication are developed for a compressible Newtonian fluid with Roelands viscosity. The results provide a basis for the analysis and design of a wide range of machine elements operating in the piezoviscous-rigid regime of lubrication. A new numerical method of calculating elastic deformation in contact stresses is developed using a biquadratic polynomial to approximate the pressure distribution on the whole domain analyzed. The deformation of every node is expressed as a linear combination of the nodal pressures whose coefficients can be combined into an influence coefficient matrix. This approach has the advantages of improved numerical accuracy, less computing time and smaller storage size required for influence matrix. The ideal elastohydrodynamic lubrication is extended to real bearing systems in order to gain an understanding of failure mechanisms in machine elements. The improved elastic deformation calculation is successfully incorporated into the EHL numerical scheme. Using this revised numerical technique and the flow factor model developed by Patir and Cheng (1978) the surface roughness effects on the elastohydrodynamic lubrication of point contact is considered. Conditions typical of an EHL contact in the piezoviscous-elastic regime entrained in pure rolling are investigated. Results are compared with the smooth surface solutions. Experiments are conducted to study the transient EHL effects in instrument ball bearings. Results indicate a subregime of elastohydrodynamic lubrication called parched. A system is parched if oil films outside the Hertz contacts are so thin they do not flow under service accelerations.

17. Key Words (Suggested by Author(s))	18. Distribution Statement
Nonconformal contacts; Piezoviscous; Surface roughness	Unclassified - unlimited STAR Category 34

19. Security Classif. (of this report)	20. Security Classif. (of this page)	21. No. of pages	22. Price*
Unclassified	Unclassified		

*For sale by the National Technical Information Service, Springfield, Virginia 22161